E.O. Paton Electric Welding Institute of the National Academy of Sciences of Ukraine

International Scientific-Technical and Production Journal

The Paton WELDING JOURNAL

May/June **2017**
No. 5/6

Published since 2000

English translation of the monthly «Avtomaticheskaya Svarka» (Automatic Welding) journal published in Russian since 1948

Address
E.O. Paton Electric Welding Institute,
International Association «Welding»
11 Kazimir Malevich Str. (former Bozhenko Str.),
03680, Kiev, Ukraine
Tel.: (38044) 200 60 16, 200 82 77
Fax: (38044) 200 82 77, 200 81 45
E-mail: journal@paton.kiev.ua
www.patonpublishinghouse.com

State Registration Certificate
KV 4790 of 09.01.2001
ISSN 0957-798X

Subscriptions
$348, 12 issues per year,
air postage and packaging included.
Back issues available.

CONTENTS

doi.org/10.15407/tpwj2017.05–06.01

THE MAIN TENDENCIES OF DEVELOPMENT OF AUTOMATION AND ROBOTIZATION IN WELDING ENGINEERING (Review)

A.A. MAZUR, O.K. MAKOVETSKAYA and **S.V. PUSTOVOJT**
E.O. Paton Electric Welding Institute, NASU
11 Kazimir Malevich Str., 03680, Kiev, Ukraine. E-mail: office@paton.kiev.ua

The paper represents arranged economical-statistical information on development of automation and robotization in welding engineering. Currently, the main peculiarity of the world economy is application of advanced automated (robotic) systems. Decrease of expenses for re-equipment of enterprises due to cost reduction of robots, computer numerical controllers, automation hardware and software promotes investment in automation of commercial production. 14 Ref., 4 Tables, 8 Figures.

Keywords: *welding, automation, robotization, welding robots*

Currently, the main peculiarity of the world economy is transfer from era of industrial automation to ever kind application of advanced automated/robotic systems in manufacture. Wide implementation of information and computer technologies have changed a concept of automation of modern production and formed a potential for its global growth. The market of automation means and technologies has become attractive in terms of direct investments all over the world. An average annual sales growth at the world market of production automation in course of last 10 years made around 6.6 %; in 2015 volume of sales exceeded 185 bln USD and following the forecast [1] will reach 352 bln USD till 2024.

The main reason of investment attractiveness for commercial production automation became significant decrease of expenses on enterprise re-equipment. Cost reduction of robots, computer numerical controllers, automation hardware (probes, processors) and software resulted in cut down of payoff period of technological equipment and investments. An average price of a robot in 2015 has dropped by 30 % in comparison with 2000. Data on spot welding robot price can be presented as an example. Based on data of Boston Research Company (BSG) its price has reduced by 27 %, on average from 182 thou USD to 133 thou USD (in comparison with 2005), and till 2025 its decrease will make 22 % more. Drop of hardware and software price is expected in the near decade and can make more than 20 %.

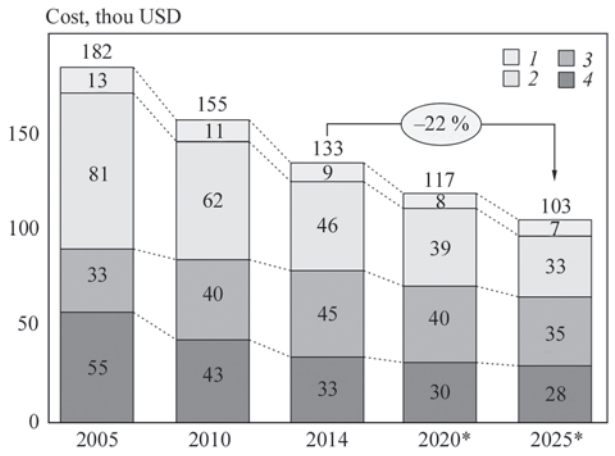

Figure 1. Dynamics of change of cost structure of a system for typical spot welding robot in motor car construction industry of the USA (* — prediction): *1* — project management; *2* — system engineering; *3* — peripheral devices; *4* — robot

Dynamics of change of a cost structure of standard robot for resistance spot welding in motor car construction, according to data [2, 3], is given in Figure 1 [3]. Decrease of expenses on management of projects on robot implementation in production and reduction of system engineering cost due to advantages of offline programming are expected in a period till 2025. Removal of the safety barriers and probes results in cut down of expenses on peripheral devices. Insignificant fall of robot price (including software) can take place since it approaches to material expenses and production volume in the motor car industry is already high.

At the same time, according to the prediction, productivity of the robotic systems will annually rise approximately by 5 %. Currently, robots perform more than 10 % of all manufacturing operations and in 2025 more than 40 % of all manufacturing operations in industry will be performed by robots.

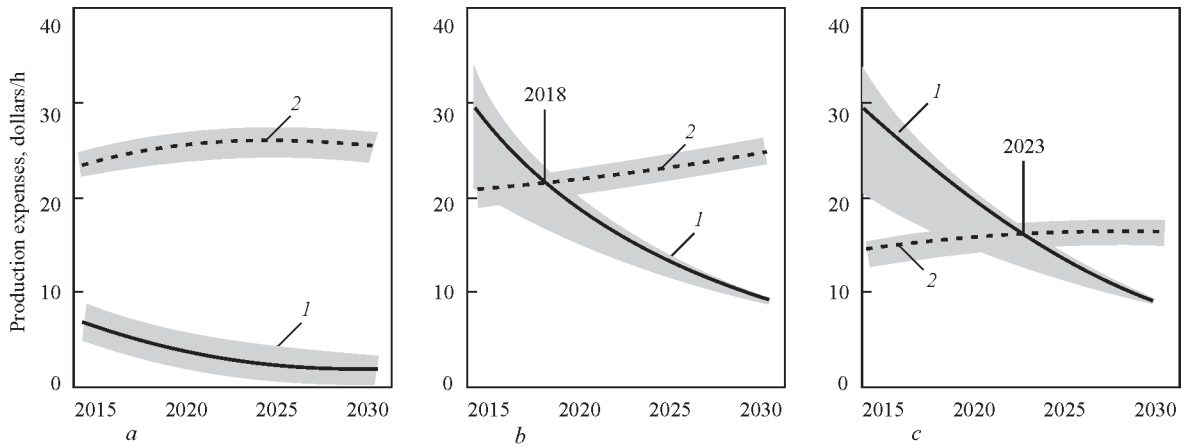

Figure 2. Comparison of production expenses in application of robots (*1*) and worker labor (*2*) in series of branches of USA industry: *a* — motor car construction; *b* — electric equipment; *c* — furniture production

Steady reduction of robotics price makes it more attractive for small and medium-sized enterprises and opens new possibilities of their wide application, thus in turn allows increasing labor productivity in many activity spheres.

Labor shortage on the world labor market is also a strong reason for implementation of robotics in industry. Based on data of the American Welding Society shortage of welders in the USA in 2020 will make around 290 thou workers and these working places will be replaced by robots. In accordance with the report «Future of automation» from ARK Invest approximately half of the working places in the USA will be automated and robotized till 2035. The report notes that automation promotes 103 % increase of additional labor cost per one dollar release and add 12 trn USD to real total GDP. Increased productivity being provided by automation will have large effect on economic growth, moreover real GDP per one worker in the USA will double from 113 thou USD in 2013 to 236 thou USD in 2035 or at an annual rate by 3.4 % [3, 4].

The data, presented in Figure 2 [3], show that robotics is already economically viable alternative to human labor in many branches of USA industry.

Modern market becomes more and more dynamic. Decrease of product life cycle, necessity in quick change of output product line, consideration of individual needs and wishes of customer during product manufacture is the key to success in a global scale competition. All this requires rapid adjustment, high accuracy and coordination in the production line and it is difficult to fulfill using workers labor. Production automation makes it possible as well as determines growth of a demand in versatile and programmable automated equipment. One of the solutions for these problems was development of new generation robotics being collaborative and directed on joint work of robot and human. They have already started replacing the generation of «isolated» robots.

Present investigations show that joint work of robot and man is 80 % more productive than their individual work. Cobots (co-robots) are the new robots designed by pioneers of the market (Baxter from Rethink Robotics, Universal Robot) and world leaders such as ABB and KUKA. Cobots' developers have proved that virtually any modern robot can be transformed in a certified cobot, completely safe for human. It is only necessary to reset its control system and teach it to «listen to» new sensors.

The Universal Robots sold the first in the world cobot, as they were nicknamed, in 2008. It happened long before a term for this new class of robots started being widely used. Today this is the most rapidly growing segment of the world robotics market, which based of analytics' forecast will annually rise by 50 % and it is expected that in 2020 its volume will reach 3 bln USD [5].

An industrial robots (IR) demand shows the most dynamic growth in a segment of automation means, which in a structure of world automation market makes around 4 % and 17 % account for them in a structure of world market of automation means. Industrial robots perform technological operations quicker and more accurate than human, provide increase of productivity and decrease of total production expenses in the countries with developing as well as advanced economies countries.

Table 1 [6] shows a dynamics of development of world automation market in 2011–2015.

Growth of sales income in the robotics segment for more than 40 % exceeds the average growth of sales income in the segment of automaton means and by 15 % the average growth of income at whole automation market.

Based on data of the International Federation of Robotics (IFR) the average annual increase of IR

Table 1. Dynamics of growth of income from sales of main product segments at the world market of automation means 2011–2015, %

Sales income	2011	2012	2013	2014	2015
Automation means, total including:	5.9	4.3	5.3	5.3	5.5
robots	6.6	8.3	8.6	7.5	7.5
«machine vision» devices	6.6	3.7	7.1	6.2	6.7
sensors	5.6	3.6	3.6	4.2	4.2
relay and switches	5.5	3.5	3.6	4.2	4.3
movement devices	4.9	1.5	3.7	4.3	4.4
others	6.5	6.0	6.0	6.0	6.0

sales at the world market in 2010–2015 made 16 % and average annual IR sales rose up to 183 thou units. Increase of sales by almost 60 % indicates significant growth of IR demand and investments all over the world. Total worth of IR market in 2015 in relation to previous year increased by 9 % and reached the new maximum, namely 11.1 bln USD, and taking into account software and hardware it made 35 bln USD (+15.5 %).

The world park of IR in 2015 exceeded 1664 thou units, but virtual number of acting IR park is probably significantly higher, since practice shows that the most of IR can be successfully operated after expiration of their standard service life (12–15 years). IFR forecasts that the world park of IR in 2019 will make 2.6 mln units, which is 1 mln more than in 2015.

Table 2 gives data on quantitative volume of annual sales and IR park in the world and main regions in 2010, 2014 and 2015 as well as evaluation for 2016 [7].

In the last six years application of IR trebled mainly due to Asia countries. Asian region market is the largest, fast developing market, which makes more than a half of world market. The world leaders are China, Republic of Korea, Japan as well as the USA and Germany, their total portion makes more than 75 % of the world market.

In 2015 IR sales in the Asian region grew by 20 % and made 156 thou units. China is the leader in sales growth at regional as well as world market. In 2015 the volume of IR realization in China reached 68.6 thou units that made 44 % of all sales volume in the Asian region. In accordance with data from China Robot Industry Alliance (CRIA) China has essentially increased own IR production. Volume of sales of Chinese production IR rose by 29 % at internal market in 2015 and made around 20.4 thou units, and in comparison with 2013 production increased for more than 2 times. Figure 3 shows dynamics of sales of national and foreign production IR in China [8].

In 2015 growth of IR sales continued in other countries of Asian region, i.e. Republic of Korea (+55 %; 38.3 thou units), Japan (+20 %; 35.0 thou units), Taiwan (+4 %; 7.2 thou units) and others.

Volumes of IR sales in European market in 2015 rose by 10 %, at that its main segments are Germany (20.1 thou units), Italy (6.7 thou units) and Spain (3.8 thou units). North America is also important regional IR market. Sales volumes in the USA grew by

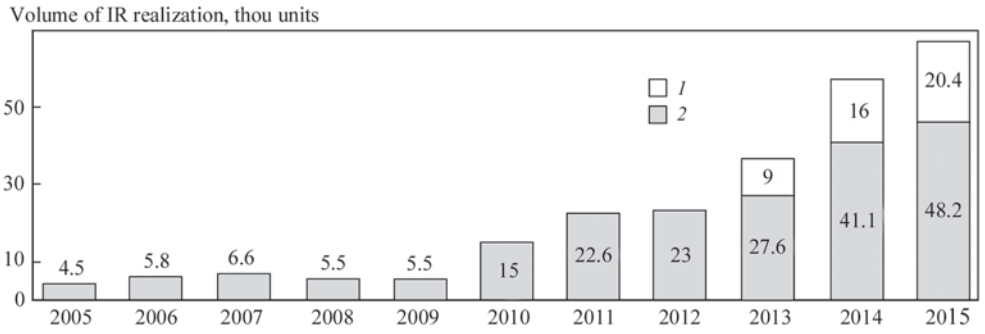

Figure 3. Dynamics of realization of IR of national (*1*) and foreign (*2*) production in China

Table 2. Number of annual sales of IR and general park of IR of all types and designations in world regions in 2010–2016, units

Region	Annual sales of IR				IR park			
	2010	2014	2015	2016 (estimation)	2010	2014	2015	2016 (estimation)
Total in the world, including:	120585	220571	253748	290000	1059162	1467900	1664000	1824000
America	17114	32616	38134	40200	179785	249500	272000	281000
Asia (including Australia)	69833	134444	160558	190200	520831	777100	1417000	908500
Europe	30741	45559	50073	54200	352142	411500	519000	431700
Africa	259	428	348	400	2232	4200	4500	4900

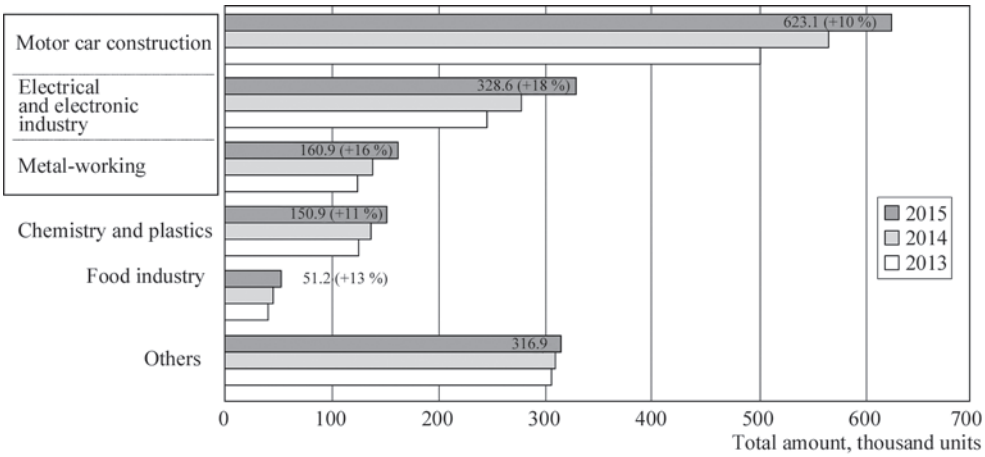

Figure 4. Number of annually installed IR in branches having the highest IR application, units

3 % and made 27.5 thou units, whereas that in Mexico increased two times and made 5.5 thou units.

In total more than 70 % of all IR sales accounts for motor car construction, electric and metal-working industry. The main consumer of IR and the main driving force for development of modern robotics is the motor car industry, portion of which makes more than 40 % of all IR sales in the world. 97.5 thou robots were installed in this branch in 2015 that is a new record for the last five years.

Significant increase of IR consumption can also be observed in electric/electron industry in manufacture of computers, medical, precision and optical instruments, telecommunications equipment and other products. In 2015 IR sales volumes in this branch increased by 41 % and reached a new peak of 64.6 thou units. Substantial growth of IR sales (+39 %) in 2015 is also noted in metal-working industry.

Number of professions successfully mastered by robots continuously grows every year. According to IFR data in the beginning of 2013 robots were already used motor car construction in a process cycle for more than 80 % of all operations, whereas in the beginning of XXI century this index made 45 % [7].

Figure 4 [9] shows data on annual installation of IR in the world in the main branches using them during 2013–2015. Figure 5 [10] presents dynamics of change of IR sales portion in motor car construction in 2005–2015.

Despite significant growth of IR market, the average level of commercial production automation in the world remains sufficiently low. In 2015 the average world index of robots density (number of IR per 10 thou employed in commercial production) made 55 units. An IR density index shows that Republic of Korea, Japan and Germany refer to the countries, commercial production of which has the highest level of automation. This index in 2015 made 478 units in Republic of Korea, 314 units in Japan and 292 units in Germany for 10 thou employed in industry.

Substantial lag in the level of robotization of branches of general machine building in comparison with motor car construction is observed. In industrially advanced countries the level of robotization of general machine building is 7–8 times lower than in motor car construction, and 19 times in BRIC countries. This is an impetus and potential for development of robotics market in industrially advanced countries as well as developing economy countries. Figure 6 [9]

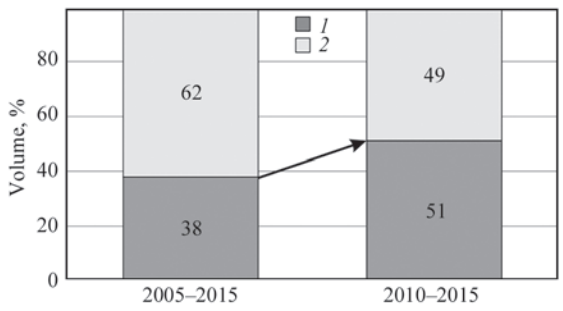

Figure 5. Dynamics of change of IR structure in motor car construction (*1*) and other branches of machine building (*2*), %

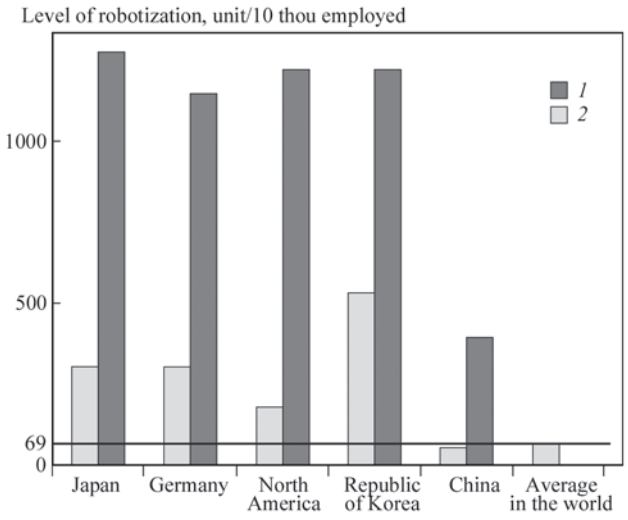

Figure 6. Density of IR in motor car construction (*1*) and branches of general machine building (*2*) in 2015

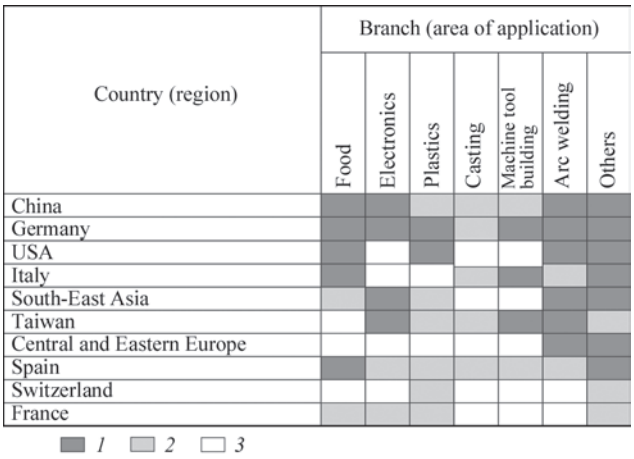

Figure 7. Evaluation of level of robotization in branches of general machine building in regional section on quantitative volume of IR annual sales: *1* —high (more than 300 units); *2* — medium (150–300 units); *3* — low (less than 150 units)

presents data of the level of robotization in motor car construction of Japan, Germany, USA and series of other world countries [7, 9].

Motor car construction in comparison with other branches of industry is the most automated branch. Motor car construction enterprises with the highest level of robotization are located in Japan, Republic of Korea, Germany and USA. High level of robotics is in electron industry of Japan and Republic of Korea.

Experts of KUKA Company based on IFR data and IR sales volume in 2013, has evaluated the level of robotization of general machine building branches in ten countries/regions of the world, where 80 % of the world market of general machine building are concentrated. Figure 7 shows the results of carried analysis [11, 12].

Data show (see Figure 7) that there is a significant potential for IR market growth in the most branches of general machine building of industrially advanced countries as well as developing economy countries.

The highest demand at the world IR market has robots for material treatment, their park makes 38 % of all world IR park and includes robots for casting, heat treatment, stamping/forging.

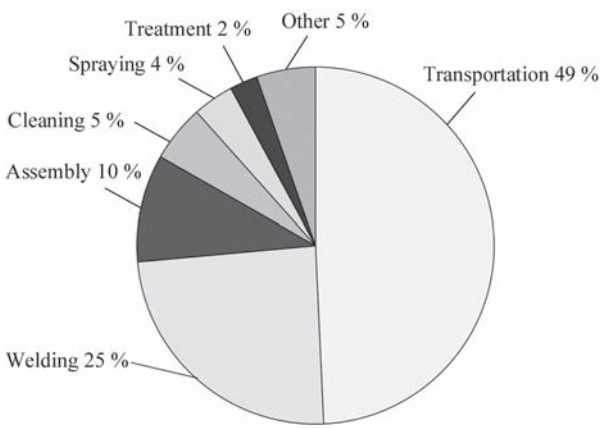

Figure 8. Structure of IR sales on types of technological operations for 2015

Robots for assembly make around 10 % , that for coating deposition is 4 % and special processes (laser and plasma cutting, water jet cutting etc.) 2 % of the world IR park (Figure 8 [7]).

In scope of global research of robotics market BSG Company predicts 10.4 % growth of annual average rate till 2025. Among them 10.1 % of annual growth of robot sales in production comes for welding, assembly, painting, loading-unloading operations and other types of work. Volume of sales will increase from 5.8 bln USD (in 2010) to 24.4 bln USD (in 2025). Thus, this robotics segment, regardless lower growth rate, will keep larger portion of robotics market. Around 8.1 % of annual sales growth accounts for the robots used in military purposes, first of all UAV, military exoskeletons, underwater vehicles and ground transport vehicles. Their sales volume will rise to 16.5 bln USD till 2025. For example, in Russia portion of military robots makes about 50 % of all IR park [3].

Estimation of IFR and series of analytical companies shows that welding robots makes 25–30 % of the world IR park or about 500 thou units. They mainly include robots for arc and spot welding. Portion of robots for arc and spot welding makes around 50 % in quantitative and monetary terms in the structure of world market of welding robots.

A structure of welding robots market in the regions significantly differs. The robots for spot welding dominate at the European and American markets (about 70 %) and arc welding robots (60–70 %) prevail at the Asian countries markets.

Volume of sales of the welding robots at the world market rises almost by 50 % from 33 to more than 59 thou units during 2008–2015. Countries of North America (23 %), China (21 %), Europe (18 %) and Japan occupy the main portion of the market (more than 70 %).

World market of welding engineering in 2016 reached 24.2 bln USD. It is expected that the market will rise by 5.6 % every year within the next five years. A segment of robotized welding equipment in the structure of this market makes about 12 % (2.8 bln USD), at that it is supposed that its average annual growth will make about 7 %.

Countries of Asian region cover almost 60 % (China — 21 %), that of Europe is 18 % and North America makes 23 % in the regional structure of sales of world market of welding robots. Portion of welding robots in the sales structure at national IR markets varies from 20 % in Malaysia to 62 % in India. In China this index in 2015 made 36 %, in Brazil 38 % and 24 % in Russia.

Table 3. World market of welding robots in 2015

Country	Robots for arc welding		Robots for spot welding		Total	
	pcs	%	pcs	%	pcs	%
Europe	3400	32.1	7200	67.9	10600	17.9
Russia and CIS	330	60.0	220	40.0	550	0.9
China	7600	61.8	4700	38.2	12300	20.7
Korea	3000	61.9	1850	38.1	4850	8.2
Japan	3520	56.6	2700	43.4	6220	10.5
Taiwan	780	75.7	250	24.3	1030	1.7
India	810	40.3	1200	59.7	2010	3.4
ASEAN	2550	54.3	2150	45.7	4700	7.9
the Near East	260	47.3	290	52.7	550	0.9
Africa	270	54.0	230	46.0	500	0.8
Oceania	320	49.2	330	50.8	650	1.1
South America	4800	34.8	9000	65.2	13800	23.3
Central and South America						
America	770	50.7	750	49.3	1520	2.6
Total	28410	47.9	30870	52.1	59280	100.0

Source: The Japan Welding News for the World.

According to data of the Japan Welding News publication more than 59 thou welding robots were installed in the world in 2015, among them 52 % are the robots for resistance welding and 48 % for arc welding. Table 3 shows data of the welding robots market in 2015 [13].

The world market of welding robots is flourishing and demonstrates continuous growth in the recent years. This process is significantly promoted by high rate of growth of motor car construction in China and India. An exceptional demand for welding robots is observed in general machine building.

A bias of world commercial production in the Asian region promoted decrease of prices for welding robots in short-term and long-term perspectives. This also allowed reducing payback time of robotization of welding processes and promotes rise of welding robots application at small and medium-sized enterprises.

The modern welding robots are equipped with tracking (machine vision) systems. It allowed performing continuous monitoring and control of welding parameters. Integration of 3D visual control systems in robotic complexes for arc welding has got a widespread use.

Significant growth of income is predicted in a long-term perspective in a sector of arc welding robots, since they get more and more application in general machine building branches, where manual and mechanized arc welding is far more often replaced by robotic welding.

Today keeping profitability under conditions of price reduction for welding robots is a serious problem for IR manufacturers all over the world. Price becomes the main criterion for the clients in selection of welding robots since they try to decrease capital input. Robotics suppliers should have tighter contact with the developers of systems for automation of industrial processes and production in whole and create individual solutions in accordance with the requirements of end users.

In order to increase compatibility of the different components taking part in technological process of welding, the manufacturers of welding robots try to set a partnership with the suppliers of power sources and other welding equipment.

Today the flexible and adjustable robots, which are good for mixed and multipurpose production lines [13], are in more and more demand.

Continuous work on improvement and development of brand new IR designs allowed significantly amending technical-economical indices of IR currently proposed at the market. Table 4 shows an example of comparison of some technical-economical indices in IR designed by KUKA Company [11, 14].

In the conclusion it should be noted that commercial robots today are the key element for revolutionary transformations of production. IRs fulfil the functions, which have already exceeded the bounds of performance of repetitive tasks.

Table 4. Comparison of IR technical-economical indices from KUKA company, % (indices of 1980 are taken for 100 %)

Index	2000	2010 (Quantee series)
Primary cost of production	30	20
Weight	50	40
Number of parts	30	20
Time of assembly	20	15
Maintenance expenses	30	30
Productivity	200	300

New generation of IR differs by such purely «human» features and capabilities as brain, dexterity, memory, learnability and object identification. Reduction of sizes, rise of speedwork, decrease of IR price, on the one hand, and necessity in increase of quality, productivity and flexibility of manufacture have become the main factors of growth of robotics demand and expansion of its application range.

Robotics allow preforming a revolutionary change of process of commercial production, promote complex solution of the problems of quality improvement and rise of productivity, saving of physical, power and human resources at new technological level.

The present day application of robots is frequently the single correct variant to survive under competitive conditions of large-series as well as small and medium-sized enterprises. Application of commercial robots is not an exclusive right of only large industrial corporations and large-series groups of companies.

Today reasonable price and flexibility of design of robotic technological complexes allow using such equipment for organizing production of commercial flow lines as well as small and medium-sized enterprises.

1. (2016) RBC Global Assist Management. Global megatrends: Automation in emerging markets. *http*://www.rbcgam.us
2. (2016) Industrial automation market — Global industry analysis, size, share, growth, trends and forecast 2016–2024. *http*://www.prnewswire.com
3. (2015) The Boston Consulting Group Inc. The robotics revolution/the net great leap in manufacturing. *http*://www.bcg.com
4. ARK Invest. The future automation. White paper. *http*://www.ark-invest.com
5. *Universal* robots and… the cobots. *http*://www.universalrobots.com
6. (2012) Global industrial automation. Credit Suisse. *Global Equity Research*, **14**, 102.
7. (2016) International Federation of Robotics. *World Robotics 2016 Industrial Robots*.
8. Roehricht, K. (2016) Study on emerging markets, with special focus on Asia. *http*://www.eu-robotics.net
9. Heagele, M. (2016) *An outlook for robots (in industry and service)*. Fraunhofer Stuttgart, IPA.
10. Robots. *https*:www.macquarieresearch.com/ideas/api/static/file/publications/730/3318/Robots230916e254524.pdf
11. Mohnen, P. (2012) KUKA AG German Corporate Conference Company Presentation. *KUKA AG*, January 21.
12. (2015) Hello future. *KUKA, Annual report*.
13. (2016) World demand for welding robots. *The Japan Welding News for the World*, 20(77), 9.
14. Spitzauer, A. (2012) *KUKA AG Company Presentation*. September.

Received 14.04.2017

doi.org/10.15407/tpwj2017.05–06.02

INTELLECTUALIZATION OF PROCESSES FOR CONTROL OF ARC WELDING PARAMETERS

A.E. KOROTYNSKY and **M.I. SKOPYUK**
E.O. Paton Electric Welding Institute, NASU
11 Kazimir Malevich Str., 03680, Kiev, Ukraine. E-mail: office@paton.kiev.ua

Intellectualization is a tendency of current stage of technology development. In a greater degree it refers to welding equipment, where one of the important issues is intellectualization of control of main parameters in the arc processes. Present work considers the issues of design of multifunctional transducers, designs of which are unified according to IEEE 1451.4 standard. The systems of measurement equations are given. They allow controlling welding parameters with minimum systematic errors in real time mode. 12 Ref., 1 Table, 4 Figures.

Keywords: *smart transducers, multifunctional transducers, measurement equation, welding parameters, error*

General approach in design of smart transducers (ST) was proposed by Brignell J. and Dorey A. in 1983 [1]. A sensing element (SE) of such a transducer is connected to controlled circuit using a switch (S), which is controlled by imbedded microprocessor (MP). The latter in accordance with selected algorithms and developed programs controls all measurement procedures as well as sets the modes of internal self-control. It can be control of ambient temperature, tracking of voltage of zero drift in analogue systems etc. Different ST architectures are described in details in work [2].

General information system development, which is considered as one of the elements of public life intellectualization, has affected development of sensor devices. If before the results of measurement were processed almost manually, then current stage of development of microprocessor equipment allows carrying all processing (scaling, calibration, noise suppression etc.) using a microprocessor block, which is connected to the sensing element (SE) of sensor. Such devices are called smart sensors [3, 4]. At that a series of additional requirements is made to them. Modern sensor, in addition to SE, shall contain means for signal processing, switching means, independent power supply, user's interface, facilities for protection from environment effect, aids which allow identifying sensor itself as well as point of its positioning(data take off place).

Current tendencies of design of the measurement systems are directed on development of smart sensors, which are integrated in a single crystal. Such sensors can contain whole smart multivariate (multi-channel) measuring systems (lab-on-chip) [5].

Engineer-researchers and designers, in order to develop necessary for customer sensor devices, work at reduction of their cost, size and levels of consumption; improvement of metrological parameters (sensitivity, accuracy, linearity etc.); standardization of communication process via interface buses or wireless systems; unification of manufacture and operation via standardization.

The first real step in a direction of global «intellectualization» of the transducers can be the International standard IEEE 1451.4, which sets the main requirements to primary measuring converters.

The Institute of Electrical and Electronics Engineers (IEEE) developed IEEE 1451.4 standard [6] as one of the elements of IEEE 1451 complex protocol. One of the aims of IEEE 1451.4 standard is simplification of sensor connection to measuring devices, facilities of signals processing and computer networks. The standard determines a set of interfaces and software structure as well as defines the main procedures of information exchange.

A block of IEEE 1451.4 standards regulates application of already existing analogue measuring converters of physical values as a part of computerized measuring analyzers. According to the standard each applied measuring converter shall have the Transducer Electronic Data Sheet (TEDS).

IEEE 1451.4 standard determines the procedures for table description of a sensor for electronic data sheet (TEDS), which in addition to baseline information (type of sensor, serial number, installation point etc.) can include the tables for calibration and linearization. A block diagram of TEDS application in smart sensors and sensor systems is shown in Figure 1.

Transducer interface contains a traditional analogue channel and not expensive serial digital channel, which provides access to TEDS structure. IEEE 1451.4 describes a mechanism of the analogue trans-

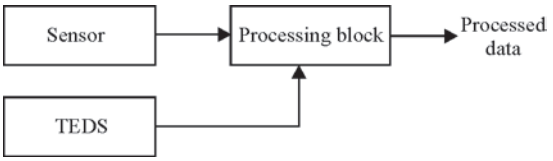

Figure 1. Scheme of TEDS application in smart sensors and sensor systems

ducers supporting an operation mode with self-description and communication protocol on serial channel. Presence of the analogue interface determines a necessity in providing compatibility of earlier manufactured and installed transducers with Plug&Play technology.

The main peculiarity of the proposed approach is application of TEDS technology for practical fulfillment of functioning algorithms in different type transducers, designed for welding process control. Further ST development taking into account the requirements of described standard has followed the way of development of multifunctional reconfigurable structures [7]. Besides, it was directed on synthesis of the algorithms of their functioning, which could consider specifics of their operation in specific environment, for example in welding arc zone, which generates large number of destabilizing factors. This work in particular is dedicated to the analysis of measurement algorithms using smart multifunctional transducers.

It is well known fact that earlier a transducer was usually considered as a measuring device, which can perform selective processing of some parameter $x_1(t)$, acting at so-called negentropy input [8]. All other inputs (they are usually called entropy) $x_2(t)$, $x_3(t)$, ... $x_n(t)$ are determined by destabilizing factors acting in a control zone. Electromagnetic noises, developed by welding and technological equipment, own electric and magnetic noises, thermal fields, ionizing emissions etc. can be referred to them. Development and improvement of sensor equipment moved in a direction of development of such solutions, which eliminate or significantly reduce effect of indicated factors on final results of the measurement.

The results of first researches, related with development of multifunctional transducers (MFT) [9, 10] appeared at the end of the 1980th. In them part of the entropy inputs was transformed in negentropy ones. This significantly increased volume and reliability of received information in regards with several parameters of the investigated process.

Analytical problem of analysis and synthesis of MFT is formed in the following way. It is assumed that controlled functions $x_2(t)$, ... $x_k(t)$ are known in the main equation, which functionally describes some parameter $x_1(t)$ being measured. Earlier they were not taken into account that resulted in additional measurement error. Respectively, we come to a system of k-equations, solution of which gives the desired result on each j-parameter.

Metrological capabilities of MFT, related with extraction of information on some input parameters acting in some concentrated space, make it greatly perspective tool for scientific and technological researches. Development of computer measurement methods [11] in combination with MFT allow substantially raising their metrological and dynamic characteristics by realizing the algorithms of mutual correction of the parameters being processed.

Figure 2, *a* shows schematic image of MFT. Its SE is capable to receive some set of input parameters $\{x_1, x_2, ... x_n\} = X_j$. Moreover, they can have different physical nature, for example, the input actions for resistance strain gage can be deformations, temperatures and vibrations. Set of inputs X_j is assigned with set of output parameters $\{y_1, y_2, ... y_n\} = Y_j$. Functional relationship between them is described by set of transition factors $k_1, k_2, ... k_n\} = K_j$. Figure 2, *b* shows «classical» transducer being sensitive to variation of one parameter x_1, other inputs $x_2 - x_n$ (marked by broken line) are entropic for it and being characterized by disturbance effect. Adder ($\sum$), used in the transducer, at the inputs of which act all output SE signals, realizes an algorithm of selection of controlled parameter x_1.

It is well known [8] that quasilinear transformation operator for such one-parameter transducer is described by an expression:

$$Z(t) = k_1 x_1 f_1(x_1, x_2, ... x_n) + \\ + b_1 \varphi_1(x_2, x_3, ... x_n) + \psi_1(x_1, x_2, ... x_n), \quad (1)$$

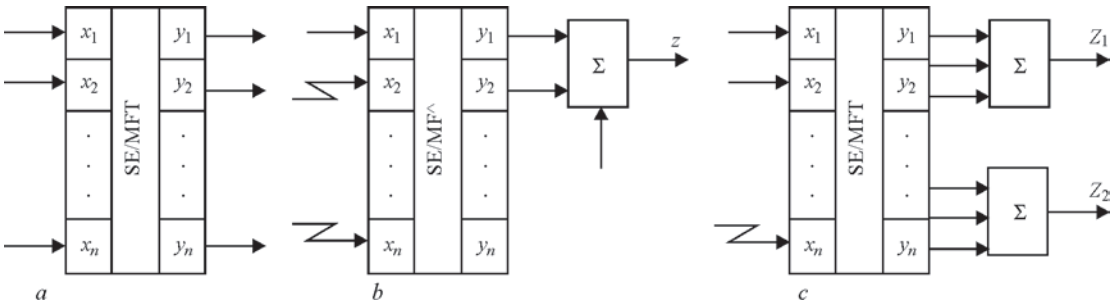

Figure 2. Schematic presentation of MFT (*a*), variant of classical transducer with one (SE) (*b*) and variant of two-parameter transducer (*c*)

where $Z(t)$ is the response function (output measuring signal); k_1 is the transition factor on controlled parameter; f_1 is the influence function taking into account effect of x_1 parameter and disturbances; φ_1 is the function taking into account effect of disturbances at the initial signal level; b_1 is the additive constituent of output signal; ψ_1 is the function of destabilizing factors considering non-linearity of transducer output characteristic.

Respectively, for two-parameter MFT, scheme of which is given in Figure 2, *c*, a system of quasilinear operators can be written in form of equations:

$$\begin{aligned} Z_1(t) &= k_1 x_1 f_1(x_1, x_2, \dots x_n) + \\ &+ b_1 \varphi_1\{x_2, x_3, \dots x_n) + \psi_1(x_1, x_2, \dots x_n), \\ Z_2(t) &= k_2 x_2 f_2(x_1, x_2, \dots x_n) + \\ &+ b_2 \varphi_2\{x_2, x_3, \dots x_n) + \psi_2(x_1, x_2, \dots x_n). \end{aligned} \quad (2)$$

Simultaneous solution of these equations allows finding the values of required parameters x_1 and x_2, information about which is set by one SE. And, respectively, three-parameter MFT is determined by a system of equations:

$$\begin{aligned} Z_1(t) &= k_1 x_1 f_1(x_1, x_2, \dots x_n) + \\ &+ b_1 \varphi_1\{x_2, x_3, \dots x_n) + \psi_1(x_1, x_2, \dots x_n), \\ Z_2(t) &= k_2 x_2 f_2(x_1, x_2, \dots x_n) + \\ &+ b_2 \varphi_2\{x_2, x_3, \dots x_n) + \psi_2(x_1, x_2, \dots x_n), \\ Z_3(t) &= k_3 x_3 f_3(x_1, x_2, \dots x_n) + \\ &+ b_3 \varphi_3\{x_2, x_3, \dots x_n) + \psi_3(x_1, x_2, \dots x_n). \end{aligned} \quad (3)$$

Thus, it follows from mentioned above that the expression for general member of system of n-equations, describing *n*-parametric MFT, should have form:

$$\begin{aligned} Z_n(t) &= k_n x_n f_n(x_1, x_2, \dots x_n) + \\ &+ b_n \varphi_n\{x_2, x_3, \dots x_n) + \psi_n(x_1, x_2, \dots x_n). \end{aligned} \quad (4)$$

It is easy to see that expression (4) is an analytical presentation of principle of MFT multidimensional selectivity. As it follows from given equations (1)–(4), mutual consideration of joint effect of all acting factors requires information on such large number of initial data, that solution of MFT design problem in general form looses practical relevance. Therefore, further presentation will only deal with specific types of transducers, peculiarities of tracing selection of parameters being measured.

TEDS technology provides formation of transducer electronic data sheet (TEDS) which is inserted directly in a device chip. Using it the transducer communicates its parameters to connected data collection system.

Thus, a quasilinear operator of any of used transducer, presented in form of polynomials (1)–(4), is fed into a reprogrammable memory (RM) for further application in all measuring procedures. Such approach, to significant extent, promotes rise of MFT metrological parameters.

As an example let's consider a problem of MFT development, which can simultaneously control two information parameters (deformation and intensity of acoustic emission) in pipeline assemblies testing. Currently, the procedure used for this is based on measurement of acoustic-emission radiation in the part subjected to deformation effect. However, the results of identification of these changes are not always single-value. Work [12] shows that the deformation approach gives more efficient estimations of vibration parameters.

Developed MFT, design scheme of which is given in Figure 3, joins indicated procedures of vibromeasurements. TsTS-21 piezoceramics is used in the transducer as SE. It interprets mechanical oscillations in the controlled part in a wide frequency range. Frequency selection of information parameters was used for division of deformation signals $\varepsilon(t)$ and signals of acoustic emission intensity N_{AE}. Two channels can be outlined in MFT structure, namely high-frequency used for N_{AE} registration and low-frequency for $\varepsilon(t)$ measurement. The functional blocks are identical, i.e. band filters (BF), linear amplitude detectors (LAD) and corresponding voltage converters (VC). The peculiarity is the working frequency range. In the first case it is Δf = 450–900 kHz, in the second case Δf = = 560–8500 Hz. $\varepsilon(t)$ channel is additionally equipped with converter of damping logarithmic decrement (CDLD), input of which is connected to LAD2. Such spread of working frequencies provides high accuracy of decoupling of channels for measurement of indicated parameters.

Since method of signal processing in N_{AE} path does not require special explanations (preliminary ampli-

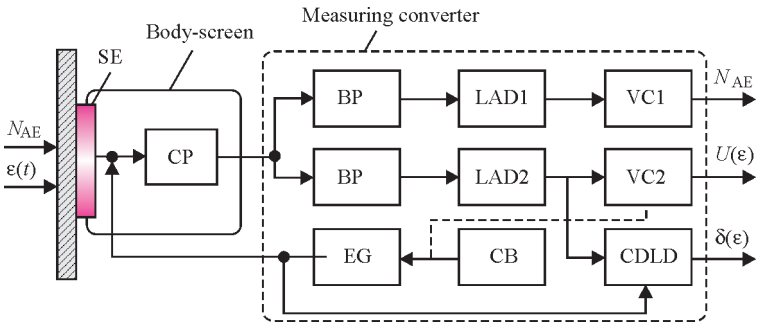

Figure 3. MFT design scheme

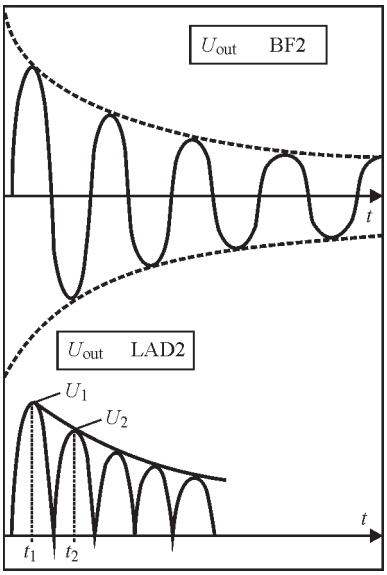

Figure 4. Diagram of work of DLD gage

fication in CP block, filtration, amplitude detection and registration in VC1), then let's elaborate on description of operation of deformation measurement path. It is based on a principle of measurement of static forces, caused by deformation of the part being controlled. At that, sine voltage, frequency of which corresponds to resonance frequency of piezoelement, is supplied to SE coating using excitation generator (EG) synchronized with control block (CB). Transformation function of CB output signal is significantly simplified:

$$U(t) = U_m \exp(-ht)\sin\omega t, \quad (5)$$

where h is the parameter determining a level of SE deformation; ω is the frequency of damped oscillations.

Synchronous integration of obtain signal with the help of VC2 allows forming output voltage as a deformation function: $U(\varepsilon) = f(h)$. Inverse dependence of $h = F[U(\varepsilon)]$ type can be used for transducer calibration.

Described scheme of MFT, as it follows from Figure 4, allows determining such an important characteristic of oscillating systems as damping logarithmic decrement (DLD):

$$d = \ln\left[U(t_1)/U(t_2)\right] = h(t_2 - t_1), \quad (6)$$

where $U(t_1)$, $U(t_2)$ are the instantaneous values of voltage registered by DLD converter in corresponding moments of time t_1, t_2.

It is necessary to note that this MFT has aperture time during which it does not perceive measurement information. This time is determined by EG oscillation period and makes ≤0.5 ms, and their $F_{EG} \geq 1$ Hz. In pauses the signals can be regenerated with necessary accuracy, corresponding to approximating function.

MFT is good to present by classification formula, taking into account their structural imaging. It looks like:

$$\text{MFT: } \{p_i/q_j/N(A_n/D_m)\},$$

where p_i is the number of controlled parameters; q_j is the number of used SE; N is the number of analogue (A_n) and discrete (D_m) output signals.

Respectively, two-parameter transducer with one SE and two output analogue signals, shown in Figure 1, *c*, can be set by the formula: $\{p_2/q_1/N(A_2)\}$.

E.O. Paton Electric Welding Institute of the NASU applicable to specific tasks of technological control has developed a series of MFT, characteristics of which are given in the Table. The Table also includes the following designations, namely SE–PC — piezoceramics type TsTS-21; STC — semi-con-

MFT characteristics

Designation	Function	Classification formula	Transducers' specification		
			SE type	Measuring transducer	Form of output signal
MFT of welding current and reactor temperature*	Fitting-out of welding equipment	$p_2/q_1/N(A_2)$	PC (TsTS-21)	IC/CVC	NAV/NAV
MFT of temperature and AE intensity*	Investigation of samples	$p_2/q_1/N(A_1D_1)$	PC (TsTS-21)	CVC/BF	NAV/NS
MFT of temperature and volumetric consumption of shielding gases	Fitting-out of welding equipment	$p_2/q_1/N(A_2)$	STC (Fonon-3)	CMC	NAV
MFT of bending value of AE intensity*	Technological tests	$p_2/q_1/N(A_1D_1)$	PC (TsTS-21)	PC/BF	NAV/NS
MFT of movement rate and welding torch position*	Fitting-out of welding equipment	$p_2/q_2/N(A_1D_1)$	FEC/R	TPC/SC	NS/NAV
MFT of welding deformations, temperature and AE intensity	Technological tests	$p_4/q_1/N(D_3)$	SGC	ACB/TNC/BF	NS/NAV
MFT of temperature, conductivity and dielectric constant of flux	Investigation of fluxes	$p_3/q_1/N(A_1D_2)$	CC	TNC/ACB	NAV/NS

*Results on MFT development were presented for the first time by the authors at the International Seminar of Poland Institute of Welding (Gliwice) in 1997.

ducting thermal electric converter Fonon-3; FEC — photoelectric converter; R — resistor transducer, SGC — strain-gauge converter.

The procedure of primary measurement conversion in given MFT is carried out using the following devices, namely IC — integrating converter; CVC — capacity-voltage converter; BF — band filter; CMC-calorimetric converter; PC — pressure converter; TPC — time-pulse converter; SC — scaling converter; ACB — alternating current bridge and thermal noise gage converter (TNC). The output signals of all indicated converters are rated in a way to correspond the requirements of input channels of computer hardware interfaces.

In the conclusion it should be noted that application of smart MFT in welding equipment allows significant expansion of volumes of received information relatively to technological processes, realized with their help. It is particularly important to note the possibility of mutual correction of received measuring signals at simultaneous control of several parameters of investigated process. As a result it allows significantly increasing measurement accuracy, and, respectively, quality of produced welded joints.

1. Brignell, J.E., Dorey, A.P. (1983) Sensor for microprocessor-based application. *J. Phys*., 952–958.
2. Dzhekon, R.G. (2008) *Advanced transducers*. Moscow: Tekhnosfera, 398.
3. Randy, F. (2002) *Understanding smart sensors*. 2nd Ed. Artech House Publishers, 412.
4. Vojtovich, I.D., Korsunsky, V.M. (2007) *Smart transducers*. Kiev: V.M. Glushkov Institute of Cybernetics.
5. *Gerard C.M.* Meijer (2008) *Smart sensor systems*. John Wiley&Sons, Ltd, 404.
6. *IEEE Std 1451.4–2004*: Standard for a smart transducer interface for sensors and actuators-mixed-mode communication protocols and transducer electronic data sheet (TEDS) formats. IEEE Standards Association, Piscataway, USA.
7. Marchenko, I.O. (2015*) System of design of multifunctional reconfigurable smart transducers*: Syn. of Thesis for Cand. of Techn. Sci. Degree. Novosibirsk.
8. Osadchy, E.P. (1979) *Design of transducers for measuring of mechanical values*. Moscow: Mashinostroenie.
9. Vasiliev, V.A., Chernov, P.S. (2012) *Smart transducers, their networks and information systems*. In: Proc. of Int. Sci.-Techn. Conf. (3–7 December, 2012, Moscow, Russia), 119–122.
10. Drozhzhin, A.I., Shchetinin, A.A., Sedykh, N.K. et al. (1977) Small-size transducers of temperature and deformation. *Pribory i Tekhnika Eksperimenta*, **5**, 216–218.
11. Alejnikov, A.F. (1988) *Measuring systems with multifunctional transducers*: Syn. of Thesis for Cand. of Techn. Sci. Degree. Novosibirsk.
12. Ovchninnikov, I.N. (1986) Procedure of testing under complex vibration loading. *Zavod. Laboratoriya*, **2**, 69–73.

Received 19.04.2017

doi.org/10.15407/tpwj2017.05–06.03

SOME PROBLEMS OF ROBOTIZATION OF GAS-SHIELDED CONSUMABLE ELECTRODE ARC WELDING

G.A. TSYBULKIN
E.O. Paton Electric Welding Institute, NASU
11 Kazimir Malevich Str., 03680, Kiev, Ukraine. E-mail: office@paton.kiev.ua

Robotization of gas-shielded consumable electrode arc welding provokes a series of problems. They are caused by necessity to equip welding robots with special sensing devices, which could communicate information on real process of arc welding to control system in very complicated for observation conditions. This work considers the possibilities of practical application of arc sensors, which in contrast to other sensing devices do not need special protection from light and heat flows, spattering of molten metal and intensive emission of fumes in measurement zone itself. Given are analytical relationships for numerical evaluation of welding tool deviation from joint line on the results of current measurements coming from the arc sensor. These relationships can be used for construction of algorithms of automatic correction of welding tool movement directly in process of arc welding. 29 Ref., 3 Figures.

Keywords: *robotization of arc welding, consumable electrode, electric-arc adaptive systems*

Application of robots for resistance spot welding started back in the 70th of the last century by «General Motors» Company in manufacture of automotive bodies [1] and with time got a widespread use in all countries with advanced economies. It was possible due to the fact that resistance spot welding operation can be easily robotized.

Situation with arc welding was completely different. Its performance using the robot with fixed program control requires very high accuracy of welded parts manufacture and assembly, which will keep constant form, area of groove preparation, gap between the parts being welded and their spatial position. However, these rigid requirements are not always fulfilled under real conditions of welding production. Therefore, deviations of a welding tool being moved on real welded joints by robot at previously set program are unavoidable. When indicated deviations come out of allowance limits, welded joint quality can become unacceptably low. There can be another reasons of mismatch of required and program set movement trajectory of welding tool, for example, temperature deformations of the thin parts in process of welding such called magnetic blowing etc.

Necessary quality of welded joint under conditions of not completely determined and partially varying «technological medium» is provided using adaptive control, which is realized as control of a welding robot in a function from controlled parameters of this medium. Adaptive welding robots are capable to «adjust» to varying arc welding conditions and, in particular, change spatial position of welded joints. However, realizing the adaptive control requires the welding robot to be equipped with special sensing devices (probes) which will provide control system with information on real current position of electrode tip relative to welded joint line.

The problem of sensor fitting-out of welding robot is still relevant. The matter is that gas-shielded consumable arc welding is accompanied by powerful light, electromagnetic and heat radiation, spattering of molten metal, intensive emission of fumes and dust directly in measurement zone. Functioning reliability of optical, inductive or acoustic sensing devices is not high under such conditions. In this connection, following from many publications [2–20], particular attention is given to electric arc sensors, i.e. sensors in which welding arc itself is an information source. They are called Arc Sensors in the literature. Intense interest to them is caused also by the fact that determination of electrode tip position relative to welded joint line is carried out directly in welding point at complete absence of any measurement devices close to it. However, arc sensors are capable to function only under specific conditions.

Aim of this work is to consider the conditions of application of the arc sensors in the systems of adaptive control of welding robots and get analytical relationships for evaluation of consumable electrode tip deviation from joint line of parts being welded on the results of current measurements coming from the arc sensor.

Conditions of application of arc sensors. One of the main conditions lies in the fact that cross-section line of the surfaces being welded $F = F(y)$ has an extreme nature (Figure 1) and the extremum itself was on the axial line of welded joint. Majority of welded

joints fulfill this condition according to works [21, 22]. Fillet, tee, lap as well as butt joints with V-groove can be referred to them.

One more indispensable condition is permissibility (from point of view of welding technology) of electrode oscillations across welded joint line directly in welding process. According to work [22] application of transverse oscillations in majority of cases is quite permissible and even results in positive effect, i.e. weld width rises, penetration depth reduces, weld metal overheating and its chemical inhomogeneity reduce. Therefore, arc welding in the most of the cases is performed using transverse oscillations following technical reasons.

And finally, it is important that frequency of transverse oscillations does not come in a frequency band, where welding current oscillations caused by another reasons, for example, voltage fluctuations on welding current source input or globular metal transfer can be present. Fulfillment of these conditions can transform the arc in a source of information on current state of electrode tip relative to welded joint line and become a sort of sensing element of some virtual sensing device [23].

Thus, presence of extremal characteristic in the control object and application of search oscillations as a mean for receiving information on virtual position of the system relative to extremum are as it is well known [24–27] the main indices showing attachment of the system with the arc sensors in feedback circuit to a class of adaptive systems of extremal type. A series of sufficiently effective methods of extremum searching were developed in theory of extremal control, the complete understanding on which can be found in special literature, for example, in work [24]. Two methods, i.e. difference method and method of modulating action are the most appropriate according to work [20] for solution of the tasks of welded joint line tracking.

Herein, we in short words will describe only the difference method. The idea of difference (or, as it is sometimes called, differential) method lies in the following. A trajectory of movement of welding tool in a working space of welding robot is set in a form of «zigzag» curve $y = y(x)$, having symmetrical location relative to axial line, which ideally should match the axial line of welded joint. Value of $F = F(y)$ function is measured in the process of movement on curve $y = y(x)$ in its left and right extreme points and calculate the difference ΔF of measured values. If axial line of $y = y(x)$ curve matches the axial line of welded joint, then difference ΔF will equal zero. Variation of this difference from zero directly indicates deviation of axial curve line $y = y(x)$ from desired line. A signal corresponding to ΔF difference is used for correction of current position of welding tool.

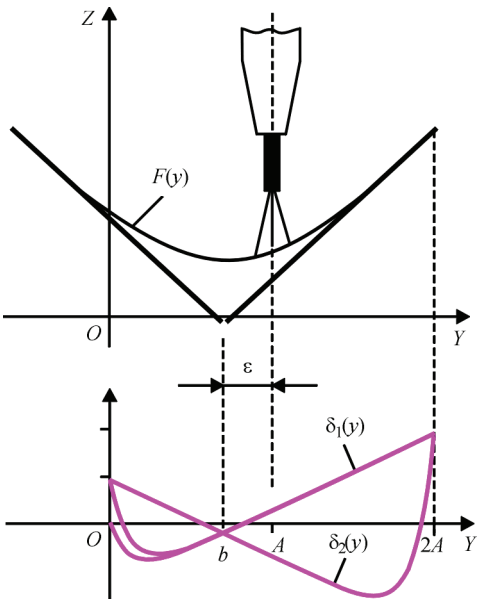

Figure 1. Scheme of movement of welding tool across joint line of welded being parts and diagrams of $\delta_1 = \delta_1(y)$ and $\delta_2 = \delta_2(y)$ functions

Construction of electric arc adaptive system based on difference method requires only welding current probe i. Measurement of welding current i or its deviation $\delta = i - i_n$ from nominal value i_n is carried out in the extreme points of torch transverse oscillations. The task is to find the analytical relationships, which based on measurement results, allow getting current numerical evaluation of side deviation $\varepsilon(t)$ of medium position of oscillating electrode from the welded joint line.

Numerical evaluations of ε (*t*) deviation. Let's assume that the welding tool in process of welding is moved across the fillet joint line (along axis Y in Figure 1) from point O to some point $2A$ and back with constant speed v_y = const. At that it is supposed that a rate of torch movement along axis X (directed up on normal to drawing plane) is preserved constant. i.e. v_x = const.

Line $F = F(y)$, following work [7], is approximated by parabola

$$F(y) = a(y-b)^2 + c, \qquad (1)$$

where a, b, c are the positive coefficients, characterizing form and position of curve $F(y)$ in coordinate system OYZ.

It is assumed that these coefficients in small interval of time $\theta = 2A/v_y$ do not vary significantly. The distance between point b and point A (Figure 1) being equal:

$$\varepsilon = A - b, \qquad (2)$$

characterizes desired deviation of middle position of the torch from joint line of elements being welded.

The relationship between the functions $\delta(y) = i(y) - i_n$ and $F(y)$ according to work [20] can be described by differential equation

$$\frac{d\delta}{dy}+\frac{1}{v_y T_w}\delta=\frac{1}{MT_w}\frac{dF}{dy}, \quad (3)$$

where

$$T_w=\frac{R_w}{EM}.$$

where M is the parameter characterizing electric, thermal and physical and geometry properties of consumable electrode; E is the intensity of electric field in arc column; R_w is the total resistance of welding circuit, and dF/dy is the slope of curve in current point of welding.

Using equation (3) and taking into account (1) and (2), write down separately two equations, corresponding to movement of electrode from point O to point $2A$ and back:

$$\left.\begin{aligned}\frac{d\delta_1}{dy}+\frac{1}{v_y T_w}\delta_1&=\frac{2a}{M\ T_w}(y-b),\\ \frac{d\delta_2}{dy}\quad+\frac{1}{v_y T_w}\delta_2&=\frac{2a}{MT_w}(2A-y-b).\end{aligned}\right\} \quad (4)$$

In these equations the deviation of welding current, appearing in movement of the torch from point O to point $2A$, is presented through $\delta_1=\delta_1(y)$ and deviation of welding current in torch movement in back direction $2A \rightarrow O$ through $\delta_2=\delta_2(y)$

Solutions of equations (4) have the following form

$$\delta_1(y)=\frac{2av_y}{M}(y-b-v_y T_w)+C_1\exp\left(-\frac{y}{v_y T_w}\right), \quad (5)$$

$$\delta_2(y)=-\frac{2av_y}{M}(2A-y-b+v_y T_w)+ +C_2\exp\left(-\frac{2A-y}{v_y T_w}\right), \quad (6)$$

where C_1 and C_2 are some constants. Since we are interested in deviations of welding current only in the extreme points of transverse oscillation of the electrode, then, the following relationships taking into account (2) are received assuming in equation (5) $y = 2A$ and in (6) $y = 0$ and introducing designations $\delta_R=\delta_1(2A)$, $\delta_L=\delta_2(0)$:

$$\left.\begin{aligned}\delta_R&=\frac{2av_y}{M}(A-v_y T_w+\varepsilon),\\ \delta_L&=\frac{2av_y}{M}(A-v_y T_w-\varepsilon).\end{aligned}\right\} \quad (7)$$

From here

$$\delta_R-\delta_L=\frac{4av_y}{M}\varepsilon. \quad (8)$$

The latter equation shows that if coefficient value a was known in process of measurement of δ_R and δ_L together with values of parameters v_y and M, then sufficiently accurate evaluation could be received on $(\delta_R-\delta_L)$ difference

$$\varepsilon=(\delta_R-\delta_L)\frac{M}{4av_y} \quad (9)$$

of interesting for us lateral deviation of the welding torch from axial line of the welded joint. Such type of evaluation, namely $\varepsilon = K_1(\delta_R-\delta_L)$, where K_1 is some constant was used in works [3, 11, 12].

Unfortunately, coefficient a, included in formula (9), can be considered as one with small variation only in not large time interval. In process of arc welding due to non-stationary movement of free surface of liquid pool, a is changed in unpredictable way and virtually can not be identified at present moment. Respectively, evaluation ε, received based on $(\delta_R-\delta_L)$ difference, reflects real deviation, in the best variant with accuracy up to one sign.

The natural question arises, is it possible to eliminate effect of uncontrolled variations of parameter a on evaluation ε, received based on the results of δ_R and δ_L measurement. It appears that such a possibility really exists. In fact, if we consider sum of $(\delta_R+\delta_L)$, which according to equation (7) equals

$$\delta_R+\delta_L=\frac{4av_y}{M}(A-v_y T_w), \quad (10)$$

then it is difficult not to see that multiplier $4av_y/M$ in the right part of this expression, containing unknown coefficient a, is the same as in the right part of the expression (8). This fact, for the first time, was outlined in work [28].

Let's divide relationship (8) by (10) and write the results as

$$\varepsilon=\frac{\delta_R-\delta_L}{\delta_R+\delta_L}(A-v_y T_w). \quad (11)$$

Now coefficient a is not involved in (11). This means that lateral deviation ε, determined by this formula, is completely independent on this coefficient. Expression (11) in contrast to (9) includes only measured values δ_R, δ_L and earlier known values of parameters A, v_y and T_w. In other words, evaluation of lateral deviation, calculated on formula (11), has a robustness property in relation to current change of form of pool free surface.

Figure 2 presents the results of computer modelling of process of consumable arc welding with transverse oscillations of torch at constant lateral deviation $\varepsilon_0 = 1$ mm and at two different values of parameter a, i.e. $a = 0.1$ mm^{-1} and $a = 0.25$ mm^{-1}. The values of other parameters, used in modelling, are typical for robotic arc welding: $v_x = 5$ mm/s; $v_y = 12$ mm/s; $A = 3$ mm; voltage of welding current source $u = 30$ V; electrode feed rate $v_e = 45$ mm/s; $i = 145$ A; $E = 2$ V/mm; $M = 0.31$ mm (s·A); $L = 0.4$ mH; $R_w = 0.04$ Ohm.

It can be seen from Figure 2 that $\delta=\delta(t, a)$ to significant extend depends on coefficient a. Substituting the results of δ_R and δ_L measurements in formula (11):

$\delta_R = 19.96$ A, $\delta_L = 5.94$ A (at $a = 0.10$ mm^{-1}),
$\delta_R = 55.07$ A, $\delta_L = 17$ A (at $a = 0.25$ mm^{-1}),

the following is received

$$\varepsilon_1 = \frac{19.96 - 5.94}{19.96 + 5.94}(3 - 12 \cdot 0.1) = 0.97 \text{ mm}$$

(at $a = 0.10$ mm^{-1}),

$$\varepsilon_2 = \frac{55.17 - 16.80}{55.17 + 16.80}(3 - 12 \cdot 0.1) = 0.96 \text{ mm}$$

(at $a = 0.25$ mm^{-1}).

Comparison of ε_1 and ε_2 between themselves and with ε_0 proves that coefficient a does not have noticeable effect on the results of ε calculation on formula (11) and calculation values ε_1 and ε_2 virtually match the real ε_0 deviation. This means that evaluation of lateral deviation ε, made on formula (11), is sufficiently effective.

We are not going to give in this article the details of noise resistance of differential arc sensor. It should only be noted that in the cases when the noises at input of welding current probe are significant, i.e. when signal-to-noise relationship is not enough for guaranteed evaluation of ε, one of the most efficient methods of noise suppression, so called accumulation method can be used [29]. For this not one reading, but several should be taken and averaged in process of $\delta_R(t)$ and $\delta_L(t)$ measurement. At that useful signals as well as instantaneous values of noises are averaged, but relationship of signal-to-noise as a result of averaging, as it is shown in work [29], will be n times (n — number of readings) higher than in one-shot measurement. Thus, evaluation reliability significantly increased with storage method application.

As for time of measurement accumulation τ, then its selection is regulated with Kotelnikov theorem, according to which $\tau = n/v$ condition should be fulfilled, where v is the half of spectrum of measurement signal. It should be noted that if movement of welding torch across the welded joint line takes place without stops in the extreme points, then measurement accumulation should be started somewhere before welding torch coming the extreme point, i.e. at moment of time $t_m = 2A/v_y - \tau$. At that is assumed that the start of the time reading is the moment when welding torch is located in a previous extreme point.

Thus, lateral deviation ε can be calculated on the next formula using accumulation method

$$\varepsilon = \frac{\overline{\delta}_R - \overline{\delta}_L}{\overline{\delta}_R + \overline{\delta}_L}(A - v_y T_w), \qquad (12)$$

similar to formula (11), but which instead of instantaneous values $\delta_R(t)$ and $\delta_L(t)$ used average values $\overline{\delta}_R$, and $\overline{\delta}_L$ received as a result of accumulation of n readings and their averaging in time interval τ.

In the conclusion it should be noted that a task of welding robot adapting to varying conditions of arc welding can be only partially solved with the help of the arc sensors, since these sensors function only in process of arc welding. Obviously, that additional adapting means are necessary at «free» movement of welding tool from one welded joint to another. A solution of a difficulty can be recently discussed idea on development of multisensor systems.

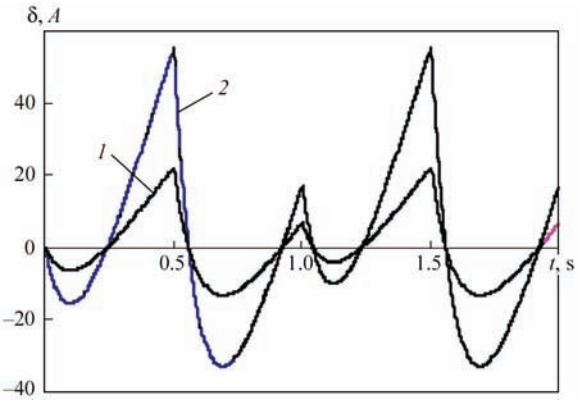

Figure 2. Curves of transition processes $\delta = \delta(t, a)$: *1* — at $a = 0.10$ mm^{-1}; *2* — at $a = 0.25$ mm^{-1}

In particular, the welding robot equipped with the sensing system, consisting of two devices, i.e. arc sensor and video camera, can be used for consumable electrode arc welding of fillet joints and joints with groove preparation. The video camera allows on-line evaluation of a difference of geometry characteristics of welded joint on the characteristics set by program. Based on this information the welding robot control system automatically corrects a welding tool movement program before arc welding start and at transfer from one welded joint to another. The video camera is not used in process of welding and current information on welding tool position relative to welded joint

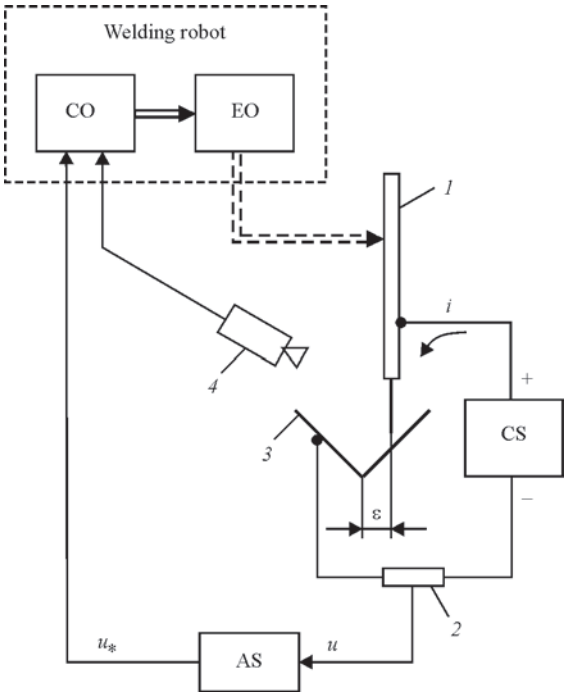

Figure 3. System for adaptive control of welding robot with two sensing devices in feedback circuit (see designations in the text)

line comes from other sensor. This information is used for correction of welding tool movement directly in process of arc welding.

Figure 3 shows one of the possible variants of system for adaptive control of welding robot with two sensor devices in feedback circuit, where the following designations are taken: CD — control device; ED — executive devices; CS — welding current source; AS — arc sensor; *1* — welding tool; *2* — current probe; *3* — part being welded; *4* — video camera. Signal $u = K_2 i$, where K_2 = const, comes to input of AS. Signal $u_* = u_*(u)$, corresponding the requirements of interface of specific welding robot, is formed at AS output. Evaluation of ε deviation, appearing in process of arc welding, is calculated in CD on formulae (11) or (12) and used for automatic correction of welding tool movement directly in process of arc welding. Correction of spatial position of welding tool before and after arc welding operation is carried out based on information coming from video camera *4*.

Conclusions

1. Application of robots for gas-shielded consumable electrode arc welding provokes a series of problems related with necessity to equip the robots with special sensing devices, which would provide a system for control of current information in course of welding process in very complicated for observation conditions.

2. Possibility was considered for partial solution of this problem using the arc sensing devices, which in contrast to optical, induction or acoustic sensors are not effected by light, electromagnetic or heat radiation, turbulent flows of gas, spattering of molten metal, intensive emission of fumes and dust directly in the measurement zone.

3. The formulae are given for numerical evaluation of the welding tool deviation from the joint line based on the results of current measurements coming from the arc sensor. These formulae can be used for construction of the algorithms of automatic correction of welding tool movement directly in arc welding process.

4. Application of the arc sensor together with the video sensor systems is perspective for widening the adapting capabilities of the welding robot.

1. Gettert, V., Gerden, G., Huettner, H. et al. (1988) *Welding operations*. Noscow: Mashinostroenie.
2. Ushio, M. (1991) Sensors in welding. *Transact. of JWRI*, 20(**2**), 157–163.
3. Cook, G.E. (1983) Robotic arc welding: Research in sensory feedback control. *IEEE Trans. Ind. Electron*, IE-30, **3**, 252–268.
4. Kisilevsky, F.N., Dolinenko, V.V. (1986) Determination of transverse displacement of torch relative to joint in welding with oscillations. *Informatsionnye Materialy SEV*, **1**, 37–41.
5. Fujimura, H., Joint, H. (1987) Joint tracking control sensor of GMAW. *Transact. of JWS*, 58(**1**), 32–40.
6. Tsybulkin, G.A., Timchenko, V.A., Vlasov, O.V. (1990) *Joint tracking device in arc welding*. USSR authors' cert. 1586873.
7. Yongyi, A., Li, Y. (1991) Arc sensor used in MIG/MAG weld tracking. *Transact. China Weld. Inst*., 12(**3**), 155–160.
8. Kim, I.W., Na, S.J. (1991) A study on an arc sensor for gas metal arc welding of horizontal fillets. *Welding Research Suppl*., **8**, 216–221.
9. Inoue, K., Zhang, J., Kang, M. (1991) Analysis of detection sensitivity of arc sensor in welding process. *Transact. of JWRI*, 20(**2**), 53–56.
10. Tsybulkin, G.A. (1992) *Joint tracking device*. USSR author's cert. 1706796.
11. Kim, I.W., Na, S.J. (1993) A self-organizing fuzzy control approach to arc sensor for weld joint tracking in gas metal arc welding of butt joints. *Welding Research Suppl*., **2**, 60–65.
12. Dilthey, U., Stein, L., Oster, M. (1996) Through-the-arc sensing – An universal and multipurpose sensor for arc welding automation. *Int. J. for the Joining of Materials*, 8(**1**), 6–12.
13. Sugitani, Y. (2000) Making best use of the arc sensor. *J. of JWS*, 69(**2**), 46–50.
14. Karpov, V.S., Panarin, V.M., Pomelov, D.S. (2000) Study of harmonic components of welding current in welding of various joints. *Svarochn. Proizvodstvo*, **8**, 3–7.
15. Kim, C.H., Na, S. J. (2001) Development of rotating GMA welding system and its application to arc sensor. In: *Proc. of 11th Int. Conf. on Computer Tech. in Welding* (Columbus, USA), 46–50.
16. Akulovich, L.M., Bukhovets, E.K., Stolovich, A.Yu. (2001) Arc tracking system of weld line. In: *Proc. of 2nd Int. Symp. on Welding and Related Technologies: World Experience and Achievements* (Minsk, Belarus, 2001), 136–137.
17. Dilthey, U., Gollnick, J., Paul, C. (2002) Erweiterung der Einsatzgebiete von Lichtbogensensoren. *Praktiker*, **5**, 164–168.
18. Savu, I.D. (2003) Building of the reference signal for the through-the-arc sensor systems function in two wires GMA welding. *Sudura*, **XIII**, 28–41.
19. Yoo, W.S. et al. (2006) End point detection of fillet weld using mechanized rotating arc sensor in GMAW. *Welding J*., **8**, 180–187.
20. Tsybulkin, G.A. (2011) *Arc sensor systems for welding robots*. Kiev: Stal.
21. Steklov, O.I. (1986) *Principles of welding production*. Moscow: Vysshaya Shkola.
22. (1974) *Technology of electric fusion welding of metals and alloys*. Ed. by B.E. Paton. Moscow: Mashinostroenie.
23. Tsybulkin, G.A. (2014) *Adaptive control in arc welding*. Kiev: Stal.
24. Kuntsevich, V.M. (1961) *Systems of extreme control*. Kiev: Gosizdat Tekhn. Literatury Ukr.SSR.
25. Krasovsky, A.A. (1963) *Dynamics of continuous self-regulated systems*. Moscow: Fizmatgiz.
26. Rastrigin, L.A. (1974) *Systems of extreme control*. Moscow: Nauka.
27. Chaki, F. (1975) *Modern control theory. Nonlinear, optimum and adaptive systems*. Moscow: Mir.
28. Tsybulkin, G.A. (1999) To evaluation of in-process electrode displacement from line of joint being welded. *Avtomatich. Svarka*, **12**, 53–54.
29. Kharkevich, A.A. (1965) *Noise control*. Moscow: Nauka.

Received 18.04.2017

doi.org/10.15407/tpwj2017.05–06.04

CONCEPT OF CREATION OF AN IMPROVED ARTIFICAL INTELLIGENCE SYSTEM AND COMPUTERIZED TRAINER FOR VIRTUAL WELDING

JUIHUEI YAO[1], **S.I. PELESHENKO**[1], **V.N. KORZHIK**[2], **V.Yu. KHASKIN**[2] and **V.V. KVASNITSKY**[3]
[1]ShenzhengWeihan Science and Technology Co., Ltd., A4 Building
1001 Xuan Ave., 518071, Shenzhen, Guangzhou, China
[2]E.O. Paton Electric Welding Institute, NASU
11 Kazimir Malevich Str., 03680, Kiev, Ukraine. E-mail: office@paton.kiev.ua
[3]NTUU «Igor Sikorsky KPI»
37 Pobedi Prosp., 03056, Kiev, Ukraine

One of the effective ways to solve the problem of shortage of highly qualified welders is application of virtual welding systems for their training. Such systems are based on artificial intelligence, used to develop a computerized trainer fitted with an interface adapted to learning objectives. Now already such systems enhance the training capabilities through increasing the number of modeled welding technologies and welding techniques. It can be anticipated that in the future they will help various institutions to significantly reduce the cost of training specialists. The objective of the work was creation of artificial intelligence for training welders, allowing development of a virtual system for real-time training in welding with functions of prediction and modeling of morphology, as well as intellectual evaluation of weld quality. Performance of work led to development of an artificial intelligence system for a network of welding trainers V60, having the following advantages: capability of modeling a realistic appearance and quality of weld; capability of modeling the stress-strain state of welded parts and temperature fields in real time; data base for modeling a large number of welding technologies and applied materials; capability of modeling 3D printing processes; availability of a system for virtual testing and analysis of welded part quality; certification system; entertainment module; access to expert department and high cost-effectiveness. It was found that the quality of welding process simulation by virtual trainer depends on the graphic component speed and it is the higher, the higher the level of taking into account the thermal impact of welding source on heating of the sample being welded and the arising stress-strain state. 13 Ref., 1 Table, 10 Figures.

Keywords: *welding trainer, manual arc welding, nonconsumable arc welding, consumable arc welding, artificial intelligence, virtual welding*

As noted by leading welding specialists from different countries of the world, the issues of training and improving the qualifications of welders should be given constant attention [1]. Another important point is correct organization of welding operations and compliance with relevant labour protection standards in industrial enterprises. In recent years work in these areas has been insufficient, either in Ukraine, or in other countries of the world, including China. This led to reduction of the number of trained welders, as well as a drop in the interest of such workers in finding a job in their specialty. So, vice-president of one of the companies, located in the zone of Yangtze river delta, notes: «We are facing a serious challenge. We cannot find highly-qualified welders, who would agree to work for 280000 Yuan ($40000) a year». There is a catastrophic shortage of highly-qualified welders in the city of Wuhan (PRC).

Different attempts are made in China to try to solve the problem of shortage of highly-qualified welders. So, in order to implement the project of construction of high-speed railways, the Chinese government sent the best Chinese welders to advanced training courses in Germany. The expenses for such training reached 1 mln Euros. The usual practice for China is training welders at courses within the country. But in this case also dozens of millions are spent. This problem, however, is not only economic in its nature. The social aspect of the problem includes the prejudices associated with this profession. This involves beliefs about the low social status associated with the profession, poor labour conditions and low salary. All this leads to unwillingness of young people to study the welding trade. Technical problems that reduce the popularity of the profession include: high level of workplace contamination (aerosols, spatter, etc.) and professional risks. There are also problems, directly related to personnel training: complexity of implementation of educational process and assessment of trained specialists, use of large quantities of consumable welding materials and energy carriers, allocation of study time and equipment, etc.

One of the effective ways to solve the problem of shortage of highly-qualified welders is application of virtual welding systems for their training. Such systems use artificial intelligence, which is the base of computerized trainer, fitted with an interface adapted to training objectives. International Institute of Welding already began application of such systems for training welders [2]. Now already such systems enhance the training capabilities through increase of the number of modeled welding technologies and methods. It is anticipated that in the future they will help different organizations to significantly reduce the cost of specialist training.

The objective of this work is creation of artificial intelligence for training welders, which allows development of a virtual system for real-time welding training with the functions of prediction and modeling of the morphology, as well as intellectual evaluation of weld quality. The following tasks were addressed to achieve this goal:

1. Analysis of currently available virtual welding trainers, determination of their advantages and disadvantages.

2. Virtual real-time modeling of various processes of welding joints of different types for a certain range of welded materials, including modeling of weld pool, metal spattering from it, arising thermal fields, prediction of weld formation, as well as displaying the working parameters of welding processes and evaluation of weldment quality.

3. Development of user interface for use of virtual reality glasses (helmet), different kinds of welding tools and working platform with parts fastened to it.

4. Development and testing of virtual welding trainer with artificial intelligence system and comparison with currently available analogs.

Developments in the field of virtual welding systems have been conducted from the beginning of 1980s. Display trainer ETS, developed in 1981 at PWI together with G.E. Pukhov Institute of Modeling Problems in Power Engineering of the NAS of Ukraine, allowed for the first time evaluating in practice the prospects for application of information technologies in welder training [3] and was the prototype of a whole gamma of trainers, developed later on. In cooperation with PWI, development of welding training systems was carried on by SLV Halle (Germany) and, as the first European Institute, they proposed a welding trainer useful in training [4]. At the start of 2000s, two tendencies clearly stood out in the field of development and improvement of technical means for welding personnel training (welding trainers), namely development of purely virtual and semi-virtual systems [5]. The latter at that time were recognized as the closest to real welding processes, allowing effectively creating, perfecting and consolidating the required persistent psychomotor skills of welders. At present it is more correct to divide the available welding trainers into the following kinds:

Computerized. They are maximum close to real welding processes. They use low power electric arc, and have no the real weld, welder's motions are followed in the form of melting line on a metal plate, modes and their variation depending on welder's motion, are recorded by a computer program [6]. Trainers of this type include: TSDS-05M1 (PWI, Ukraine) [7], GSI SLV Welding Trainer (GSI SLV, Germany) [5], and Real Weld Trainer (Real Weld Systems, Inc. USA) [6].

Semi-virtual. They use virtual technologies for partial modeling of welding equipment and parts being welded. Physical models of welded parts are applied. This type of trainers is also called augmented reality trainers. They include Soldamatic Augmented Training (Seabery Soluciones, Spain) [8], and Miller Augmented Arc (USA).

Virtual. They use virtual technologies for modeling the environment, parts being welded, welding equipment, etc. Presence of physical objects is minimized. Examples of such trainers are The Lincoln Electric VRTEX 360 (USA) [9], 123 Certification ARC®+ (Canada), Fronius Virtual Welding (Fronius, Austria) [10], «Volzhanka-1» (Nyzhny Novgorod, RF) [11], and Weihan V60 (PRC).

Let us consider in greater detail the main of the above models, belonging to these three kinds of welding trainers.

PWI developed TSDS-06M1 trainer, belonging to computerized trainers [5]. Its main advantage is maximum closeness to real welding conditions through application of low amperage arc. This trainer, however, is designed only for coated-electrode manual arc welding (MMA) and inert-gas nonconsumable (tungsten) electrode manual welding (TIG) with and without filler wire feeding, as well as for inert/active gas consumable electrode welding (MIG/MAG). It has operational automatic feedback to training system in the form of speech signals. TSDS-06M1 model is one of the best in computerized welding trainer class. GSI SLV Welding Trainer (GSI SLV, Germany) is a development close to it [5]. Unlike TSDS-06M1 trainer, Soldamatic Augmented Reality Trainer allows using virtual welder's helmet to simulate the main welding technologies: MMA, TIG and MIG/MAG (inert/active gas consumable electrode manual welding) [8]. For complete simulation of welding processes it uses physical models of parts being welded (or their plastic simulation) with QR-code applied on their surface.

The welding process is simulated in Augmented Reality helmet display due to presence of QR-codes on the models of parts and welding torches. This trainer is one of the most popular in the world. It is used by such companies as Abicor Binzel, Miller, etc. Welding trainer VRTEX 360 of Lincoln Global, Inc. Company (USA) is designed similarly [9]. Unlike Soldamatic trainer, VRTEX 360 trainer is fitted with virtual welding helmet with individual focus adjustment in each of the eyepieces. Virtual Welding Trainer of Fronius Company can be regarded as virtual one to a greater degree [10]. It supports training both with application of physical models, and without them. Here, the welder should work standing. Welding trainer «Volzhanka-1» developed at Sormovskii Mechanical College (Nizhnii Novgorod, RF) is virtual in its pure form [11]. It is fitted with a helmet completely recreating virtual reality of three above-mentioned welding processes without the need for physical model application. Welder can work both sitting and standing.

In modern computerized trainers, reading and calculation of various welding parameters occur during welding at low-amperage welding current, through application of sensor cameras, computerized feedback systems and special software. This can be regarded as an essential drawback of the training system, as the welding process is not reproduced completely — there arises the need for application of consumables and specially equipped classrooms, capability of full adjustment of current is absent, real-time adjustment of gas flow rate, selection of these gases and their mixtures, selection of filler material type and composition, etc., become difficult. In virtual systems all that is available in full. Advantages of computerized systems are the capabilities of working with the welding torch under the conditions maximum close to real welding, familiarization with the welding arc, and training in its excitation. In their turn virtual systems provide the following advantages:

1. Monitoring of the process of each student training from teacher (instructor) computer-trainer or direct observation of student's progress in the display of the trainer, on which he is working.

2. Possibility for the teacher (instructor) to render assistance and correct the student's work in real time.

3. Optional capability is provided of online/offline monitoring and correction of the work directly by specialists of trainer developer-company, or leading welding specialists of international training and research institutions, with which the developer company has cooperation.

4. Access to the forum for discussing with instructors and specialists the questions of interest to students.

5. Lectures of leading welding specialists in online/offline mode.

6. The student receives visual and sound prompts from the system proper during welding.

7. Elimination of the risk of injury to students during training.

8. Capability of using several levels of training complexity; for instance three levels — beginner, advanced, professional. Welding parameters, materials and defined objectives vary, depending on the level of complexity. This helps the instructor in development and implementation of his own training plans.

9. Automatic evaluation of student performance by the system. After completion of each welding process/stage, the student and instructor obtain the calculations in the form of diagrams and graphs, which indicate second by second welding parameters, presence of defects, etc., that facilitates the work of the teacher (instructor).

The above advantages, as well as a larger number of developments of welding trainer models (for instance, [8–11]), is indicative of prevalence of the interest of leading world companies dealing with welding, in application of virtual and semi-virtual welding trainers, compared to computerized ones.

The main advantages of the considered virtual and semi-virtual welding trainers include:

- possibility of considerably reducing the training cost through saving materials of samples, power, gases and welding consumables;
- possibility of simulating the main welding processes in different positions in space;
- visual operative demonstration of welder's errors;
- recording all the welding process parameters with the capability of their repeated reproduction to better understand the influence of welder's actions on the quality of the obtained result.

Features of a particular welding trainer design are the level of allowing for thermal impact of the welding source on heating of the sample being welded and level of allowing for the arising stress-strain state (SSS). The higher these levels, the closer to reality are the results of virtual simulation of welding processes. Quality of welding process simulation in virtual environment directly depends on the engine, in which the graphic component is created. The disadvantages of the considered trainers include:

- limited number of modeled welding processes (usually MMA, TIG, and MIG/MAG);
- limited number of welding consumables and welded sample materials;
- application of individual approach in training, lack of use of network resources and remote access;

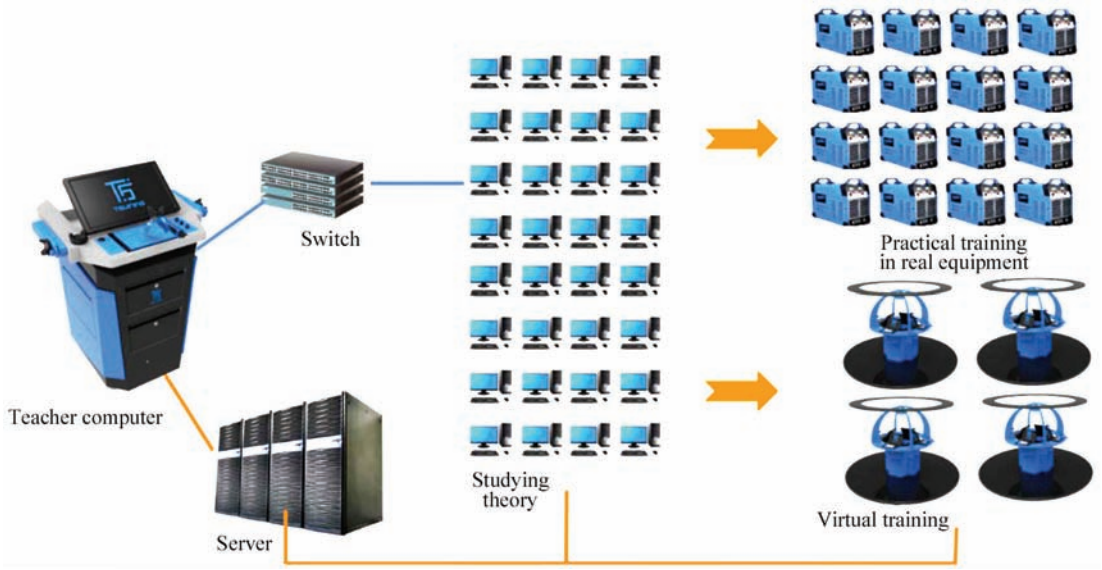

Figure 1. Concept of the complex for welding training, including real and virtual trainers

- no possibility of gaining real experience of conducting welding processes;
- incomplete application of virtual reality capabilities.

To eliminate the above drawbacks, and allow for the above features, it is rational to apply the following concept of development of welding training complex (Figure 1). Virtual training of a welder should be interspersed with real training, and should be based on deep study of the theory. Transition to welding practice is possible only after studying the theory and only under the conditions of continuous monitoring of the training process by the teacher. Such monitoring can be carried out both directly and in remote access mode that will provide one of feedback variants. Virtual welding trainers should be integrated into a single network, allowing students with good progress helping slow students that will ensure another feedback variant. Databases for modeling welding processes should be stored in remote servers and should be supplemented as far as possible with updated information about the used materials and processes. Individual virtual welding trainers should have the structure shown in Figure 2. For the first time we suggest adding an entertainment module alongside the teaching modules. As shown by practice, periodic short-term switching of students' attention from the object of instruction to entertainment object increases the efficiency of assimilation of knowledge.

Implementation of the proposed concept of welding training system requires realizing artificial intelligence common for its entire virtual part (Figure 3). It should consist of a database for modeling the studied welding processes, system of working with these data, system of dialogue mode for communication with the welder trainee and shell-program combining these three parts in a single whole.

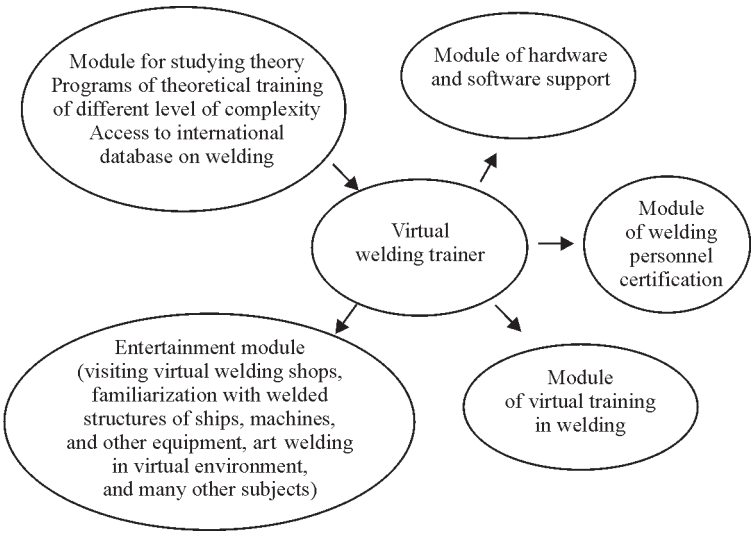

Figure 2. Welding trainer structure

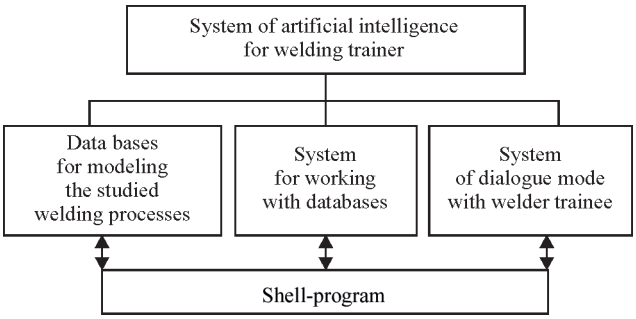

Figure 3. Structure of artificial intelligence for virtual welding trainer

One the objectives of artificial intelligence operation, is realization of feedback to teacher (instructor) computer during training. The instructor should be able to remotely give assignments in real time, adjust welding parameters and follow the process, either from his computer or directly in trainer displays. The welder trainee should be able to get advice in online mode both from the educational establishment experts, and from specialists of developer-company (in our case Weihan Science and Technology Company), including specialists of partner-institutions, among which are welding institutes and leading world companies.

Based on described approaches, Weihan Science and Technology Company (Shenzhen, PRC), using the experience of PWI and NTUU «Kiev Polytechnic Institute», developed virtual welding trainer Weihan V60 (Figure 4). Beginning of serial production of Weihan V60 model, belonging to Virtual welding Trainer Line, by Weihan Science and Technology Company, is planned for June, 2017.

When developing the concept of creation of Virtual Welding V60 system, the above-mentioned features were taken into account and characteristic drawbacks inherent to welding trainers, were eliminated as far as possible. So, to make the virtual trainer maximum close to reality, it uses real welding torches, on which

Figure 4. Virtual welding trainer V60: *1* — mobile platform; *2* — touch screen; *3* — virtual blank; *4* — bracket for welding simulation in different positions in space; *5* — virtual welding torch; *6* — box for storing virtual reality glasses (helmet); *7* — box for blanks; *8* — box for torches

Vive tracker controllers are installed, which serve as a marker for torch modeling in virtual reality (Figure 5). Such controllers allow following the position and displacement of welding torches in space. MMA torch is of a special modification. Its design and operating principle are similar to that of MMA torch in Augmented Arc Welding Simulator of Miller Company (USA) (Figure 6). To achieve maximum closeness to conditions of operation with a real electrode, this torch simulates its melting with shortening during welding. Application of virtual reality glasses or helmet HTC Vive of HTC Company (Korea), allows per-

Figure 5. Application of Vive tracker controller for modeling virtual welding torches based on real ones and tracing their movement in space: *a* — Vive tracker controller; *b* — real welding torches with controllers put on them

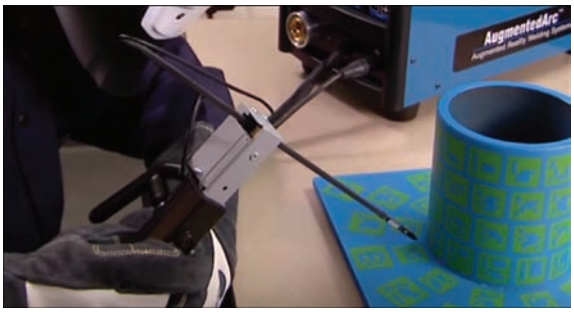

Figure 6. Virtual MMA torch simulating electrode melting with its shortening during welding

formance of virtual welding in any position on virtual sample (Figure 7), and additional bracket (position *4* in Figure 4) also allows using real physical samples. Virtual reality helmet HTC Vive is considered one of the best to date [12]. It allows simulation of characteristic sounds of welding processes. An additional accessory (Vive tracker controller) allows adding any new object to virtual reality. Note that modern technologies made virtual reality helmet a comparatively inexpensive and accessible accessory, application of

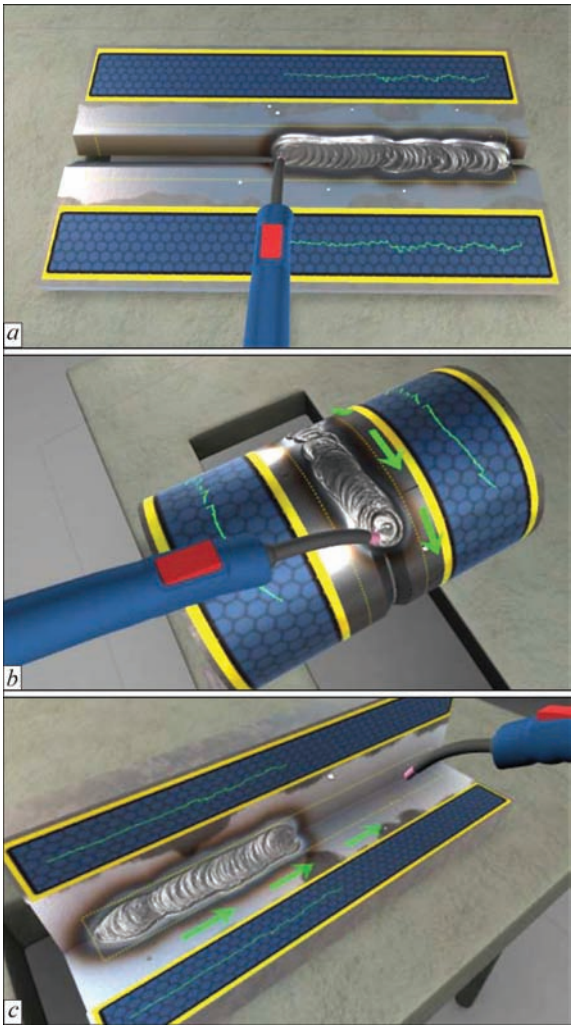

Figure 7. Virtual MIG/MAG welding in V60 trainer: *a* — butt weld in the downhand position; *b* — orbital welding of position butt weld; *c* — fillet weld

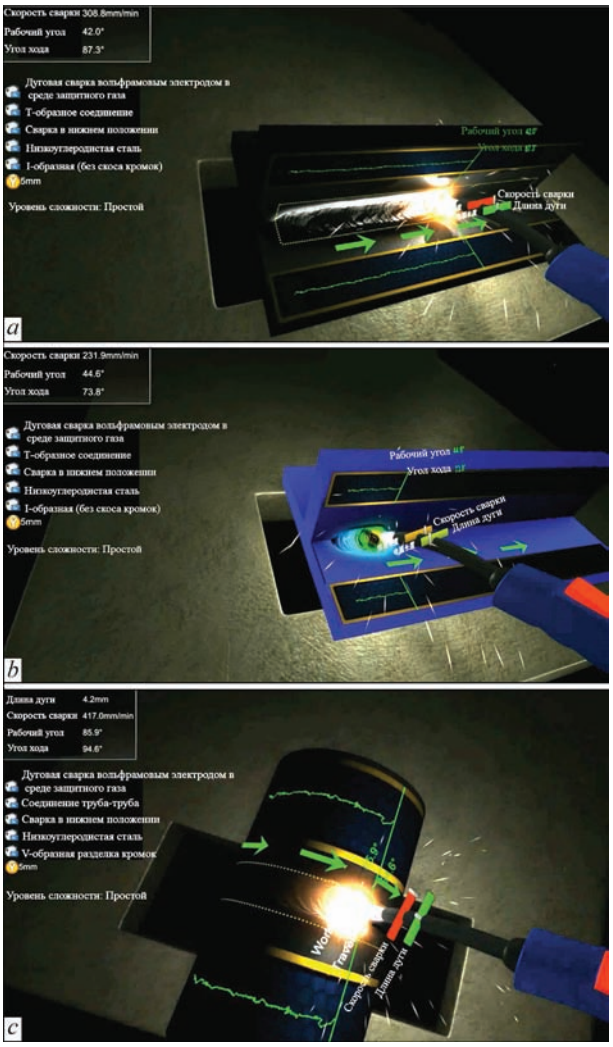

Figure 8. Displaying TIG welding process parameters in real time, allowing for dynamics of temperature fields and spattering from the pool in V60 trainer: *a*, *b* — tee joint; *c* — orbital welding of position butt weld

which is capable of improving the teaching process in any of the three types of welding trainers. Unity software, which is one of the best now, was used to achieve a high quality of welding process simulation in virtual environment in V60 trainer [13].

Modeling of the weld, weld pool, spattering from the pool and temperature fields is applied in V60 trainer (Figure 8). Working parameters of welding process, as well as the entire welding scene, is visualized in real time. All this gives a realistic picture of the weld, produced during virtual welding (Figure 9).

At present V60 trainer works with three main welding processes (MMA, TIG and MIG/MAG), but modeling of the processes of plasma and laser welding is actively pursued. Furtheron, it is also intended to model such hybrid welding processes as laser-MIG, plasma-MIG and laser-plasma.

It is intended to integrate virtual trainers V60 into training stations, each of four trainers (Figure 10). Stations in their turn are combined into classroom net-

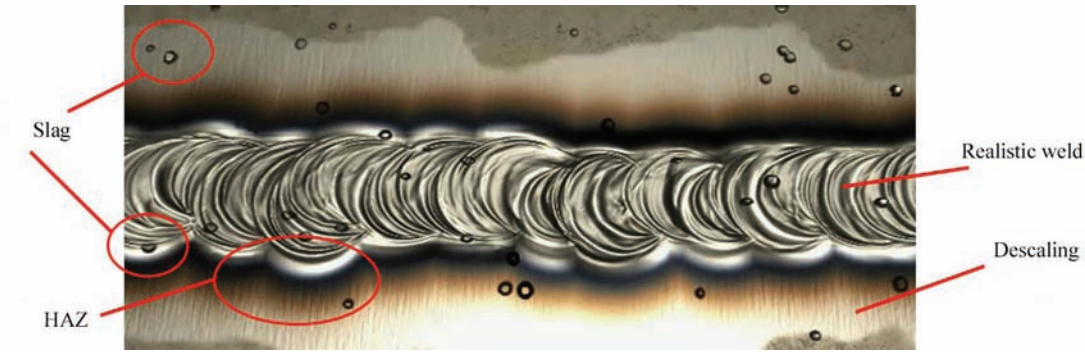

Figure 9. Displaying a realistic view of the weld produced during virtual welding in V60 trainer

work, allowing realization of «student-student», «student–teacher», «student–specialist-consultant» communication. Compared to existing analogs, developed system of artificial intelligence and training network of welding trainers V60 offers a number of additional advantages (Table). The following main advantages can be mentioned:

- modeling a realistic appearance and quality of the weld;
- modeling stress-strain state of welded parts; modeling temperature fields in real time;
- modeling a large number of welding technologies and applied materials, as well as 3D printing processes;
- virtual testing and analysis of welded part quality;
- certification system; entertainment module; access to expert department;
- high cost-effectiveness.

Figure 10. Design of virtual training station with four welding trainers V60

It should be separately noted that the applied in welding trainer Virtual Welding V60 database, concept and virtual software can be the basis for development of augmented reality helmet for welding. In such a helmet, the virtual picture of the welding process is superposed onto the real one. It allows the welder correcting the torch position and process speed directly during welding, so as to obtain the best result. Creation of an augmented reality helmet can be the next step in development of various welding technologies.

Advantages of the developed system of artificial intelligence and learning network of V60 welding trainers, compared to currently available analogs (differences from analogs are underlined) [3–11]

System of virtual training of welders			
Training module	**Certification module**	**Entertainment module**	**Hardware support module**
Study of theory Process animation visualization Lectures of leading welding experts Access to the most common data on welding	International certification system National certification system Certification system of nuclear welders	Virtual engineering Art welding Graffiti by welding Visiting virtual welding shops, automatic welding lines	Trainer working platform Optical following of displacement virtual Welding helmet Welding torches Touch-panel Host computer Projector Defect simulation
Virtual training module			
Part position in welding	**Welding materials**	**Welding technologies**	**Joint types**
Downhand position Overhead position Vertical position Horizontal position	Titanium and titanium alloy Magnesium and magnesium alloy Low-carbon steel Aluminium and aluminium alloy Stainless steel Copper and copper alloy Zinc-plated steel	Manual arc welding Consumable electrode welding TIG welding Laser welding Plasma welding Stud welding	Horizontal butt joint T-joint Pipe-pipe joint Pipe-plate joint Overlap joint of plates

Conclusions

1. An artificial intelligence system for welder training has been developed, which allows conducting real time virtual training with functions of prediction and modeling of the morphology, as well as intellectual assessment of weld quality.

2. Proceeding from analysis of available virtual welding trainers it was found that their main disadvantages are limited number of modeled welding processes (usually, MMA, TIG and MIG/MAG); limited quantity of welding consumables and materials of samples being welded; lack of application of network resources or remote access; no possibility of gaining real experience of conducting the welding processes; and incomplete use of virtual reality capabilities.

3. It is found that quality of welding processes simulation by virtual trainer depends on graphic component engine and is the higher, the higher the levels of allowing for thermal impact of welding source on heating of sample being welded and arising stress-strain state.

4. Developed artificial intelligence system for network of welding trainers V60 has the following advantages: capability of modeling a realistic appearance and quality of the weld; capability of real time modeling of stress-strain state of welded parts and temperature fields; database for modeling a greater number of welding technologies and applied materials; capability of modeling 3D-printing processes; availability of a system of virtual testing and analysis of welded part quality; certification system; entertainment module; access to expert department; and high cost-effectiveness.

1. Lipodaev, V.N. (2014) Problems of organizing of welding works in Ukraine. New technologies and equipment for high quality welding: Seminar. *Avtomatich. Svarka*, **1**, 68–71.
2. Paton, B.E., Korotynsky, A.E., Bogdanovsky, V.A. et al. (2010) Information technologies in training of welders and specialists of welding production: Current tendencies. *Svarka i Diagnostika*, **1**, 10–15.
3. Paton, B.E., Bogdanovsky, V.A., Vasiliev, V.V. et al. (1988) Electronic simulator systems in welding. *Avtomatich. Svarka*, **5**, 45–48.
4. *http*://www.svarkainfo.ru/rus/lib/blog/?year=2011-06&docId=1044: Application of welding simulators in training of welding specialists.
5. Keitel, S., Ahrens, C., Moll, H. (2014) Computer-based technologies and their influence on welding education. *The Paton Welding J*., **10**, 51–55.
6. (2014) IIW Commission XIV Workshop success: Showcasing latest international developments in welding training systems. *Australasian Welding J*., **59**, 18–22.
7. *http*://stc-paton.com/rus/services/simulator06: Training of personnel of welding production and certification of products of welding and related productions. Welding simulators for electric arc welding. Simulator TSDS-06M.
8. *http*://avtograph-oem.ru/press-center/news/prezentaciya_virtualnogo_trenazhera_svarwika_soldamatic: Presentation of virtual welding simulator Soldamatic.
9. *http*://www.lincolnelectric.com/ru-ru/equipment/trainingequipment/Documents/VRTEX_360_brochure_rus.pdf: Virtual welding simulator VRTEX 360.
10. *http*://tctena.ru/stati/virtual_welding: Welded joints in world of virtual education.
11. http://www.ruspromsoft.ru/solutions/education/weldingtrainer: Virtual welding simulator Volzhanka-1.
12. *https*://www.vive.com/ru/product: System of virtual reality Vive.
13. http://fb.ru/article/178300/igrovoy-dvijok-unity-d-porusski: Ilyushenko, H. Playing slide Unity. Unity 3D.

Received 19.04.2017

doi.org/10.15407/tpwj2017.05–06.05

ROBOTIC WELDING OF THIN-WALLED PARTS BY TOPTIG METHOD WITH WELDING MODE MONITORING SYSTEM

E. TURYK[1], **L. SZUBERT**[1], **S. DUDEK**[2] and **V. GROBOSZ**[1]
[1]Institute of Welding
ul. Bł. Czesława 16/18, 44-100, Gliwice, Poland. E-mail: is@is.gliwice.pl
[2]Pratt & Whitney
ul. Hetmańska 120, 35-078, Rzeszów, Poland

The process of robotic TOPTIG welding of thin-walled T-joints and butt joints of nickel alloy Inconel 718 was developed. The welding installation TOPTIG 220 DC provides a wide range of adjusting the parameters in the process of non-consumable electrode inert gas welding with mechanized filler wire feed and possibility of robotizing welding in the places with a limited access to the weld zone. Based on the results of investigations of robotic TOPTIG welding, the technological features of making T-joints and butt joints of thin-walled parts of Inconel 718 alloy were determined. The measuring system of the installation provides registration of technological parameters of welding process, signaling about deviations from the preset values, formation of database on welding technologies and the possibility of their viewing. The carried out certification showed that the developed welding technology meets the requirements of standards EN ISO 15614-1 and EN ISO 15613. 7 Ref., 1 Table, 7 Figures.

Keywords: *robotic welding, TOPTIG method, thin-walled parts, heat-resisant nickel alloy Inconel 718, TOPTIG welding process monitoring*

In application of manual argon arc welding of thin-walled parts, the quality of welded joint depends largely on qualification of welders. To solve this problem, it was suggested to use the TOPTIG robotic welding method with a mechanized filler wire feed at the angle of 20° to the axis of a tungsten electrode [1–3]. In this method the system of mechanized feeding of filler wire is integrated with a gas nozzle, which allows reducing the dimensions of torch and expanding the opportunities of its application. In particular, the new torch provides an access to the places where application of traditional TIG welding torch with mechanized feeding of filler wire is not possible (Figure 1).

Below, as an example, the experience of developing the technology of robotic TOPTIG welding of thin-walled parts of the nickel alloy Inconel 718 with a system for registration of welding process parameters is described.

Development of technology of TOPTIG welding of thin-walled parts. The technological investigations were carried out in the welding station equipped with the welding robot CLOOS ROMAT 310 of Carl Cloos Schweisstechnik GmbH production and the welding installation TOPTIG 220 DC of Air Liquide Welding production.

The welded butt and T-joints of specimens were produced in accordance with the standard EN ISO 15614-1 [4] and those of the model parts were made in accordance with the standard EN ISO 15613 [5]. For welding the alloy Inconel 718 [6], the welding

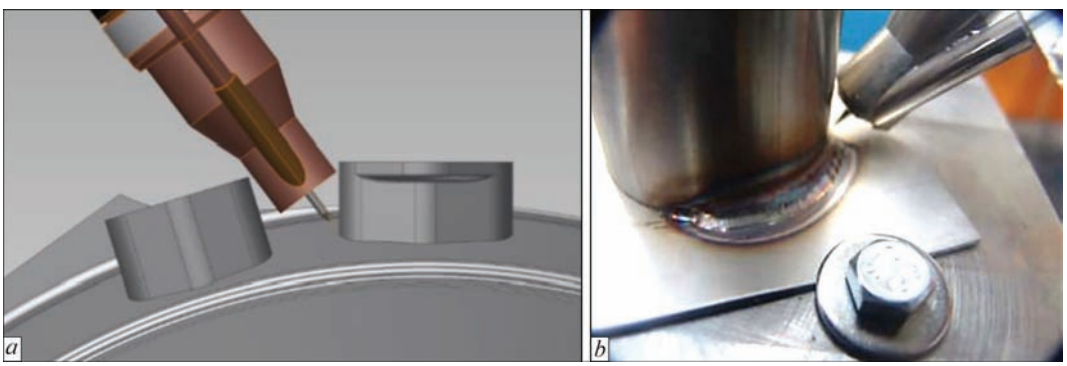

Figure 1. Scheme of TOPTIG welding torch arrangement between welded-on couplings (*a*) and fragment of weld of model element made by TOPTIG torch (*b*)

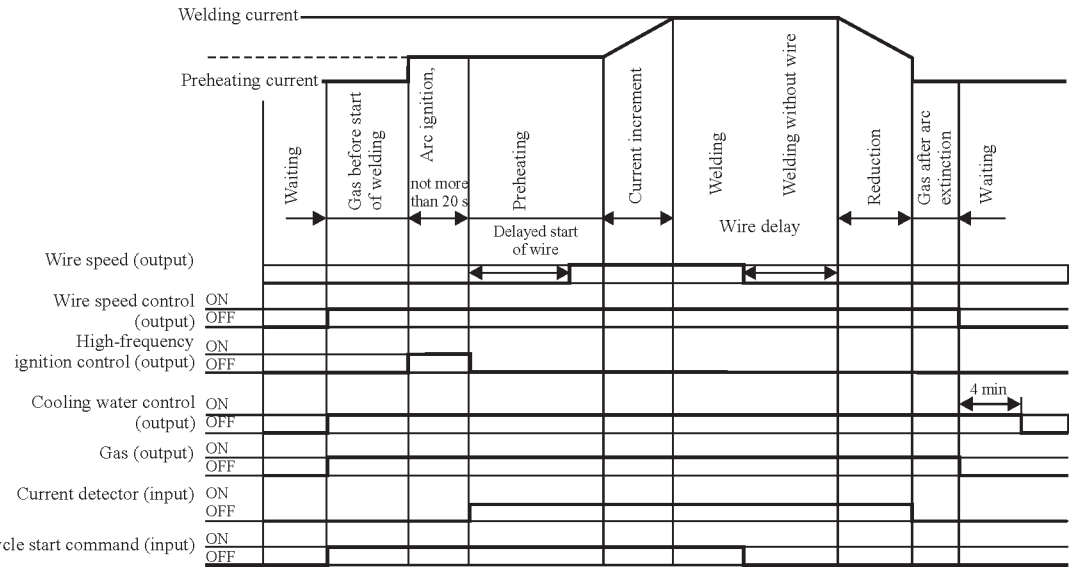

Figure 2. Time diagram of TOPTIG welding cycle [7]

wire NiFe19Cr19Nb5Mo3 of 1.0 mm diameter was used. As a shielding gas, high purity argon (ISO 14175-I1) of grade 4.8 (99.998 %) was used, and the consumption of argon was 15 l/min. The time diagram of TOPTIG welding cycle is shown in Figure 2.

When selecting the welding mode, it is necessary to take into account the peculiar features of the control system of the installation TOPTIG 220 DC, which provides the adjustment of pulsation of the wire feed speed and the possibility of synchronizing the wire feed with current pulses. Figure 3 shows oscillograms of welding current, arc voltage and wire feed speed in the TOPTIG welding process.

During the experiments the parameters of welding process were changed in a wide range and their influence on the course of the process and weld formation was evaluated. As a result of experiments, the modes of welding T-joints and butt joints were selected in the flat position, providing a stable process and the required quality of welded joints (Table). The macrostructure of welded joints is shown in Figure 4.

The carried out non-destructive testing and mechanical tests showed that the developed technology fully meets the requirements of the standards EN ISO 15614-1 and EN ISO 15613 on the welding process certification.

System for measuring and monitoring of parameters of the robotic TOPTIG welding process. Taking into account the high requirements specified to welded joints of the nickel alloy Inconel 718, it was decided to equip the serial robotic complex for TOPTIG welding with system for continuous monitoring of the welding process (Figure 5).

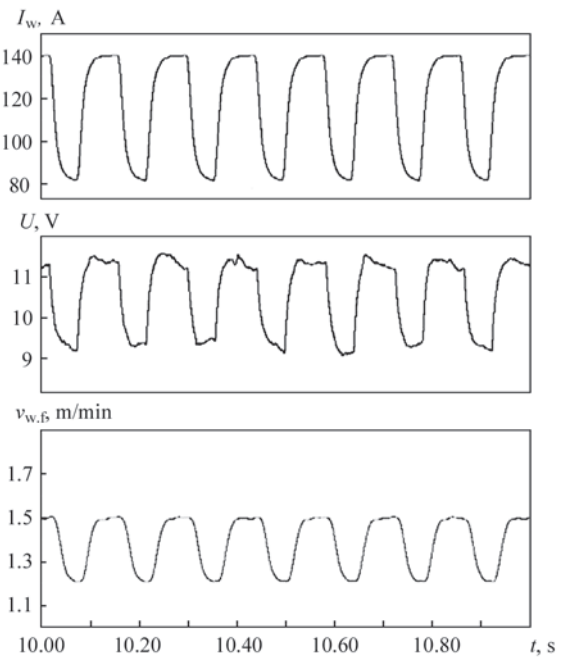

Figure 3. Oscillograms of current, arc voltage and wire feed speed during welding by the TOPTIG method

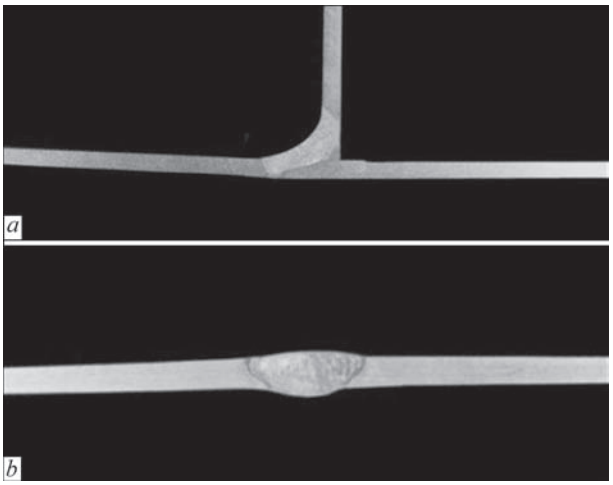

Figure 4. Macrostructure of T-joint (*a*) and butt joint (*b*) of 1.5 mm thickness, made by the TOPTIG method using welding parameters according to the Table

Range of adjustment of welding parameters in the installation TOPTIG 220 DC and the modes of welding the joints of 1.5 mm thick parts

Parameter	Adjustment range	T-joint	Butt joint
Time of gas supply before welding, s	0–10	1.0	1.0
Preheating current, A	5–220	100	70
Preheating time, s	0–10	1.4	1.4
Time of current increment before start of welding, s	0–10	0.5	0.5
Pulse current, A	5–220	140	130
Current in the pause between pulses, A	5–220	70	66
Pulse duty cycle, %	20–80	60	60
Pulse frequency, Hz	0.1–200	7	7
Welding speed, cm/min		26	29
Time of arc extinction, s	0–10	1.0	1.0
Time of stopping gas supply after the arc break, s	0–20	19	19
Initial delay of wire feed, s	0–10	1.0	1.0
Wire feed speed at the pulse, m/min	0–10	2.0	1.2
Wire feed speed in the interval (pause) between pulses, m/min	0–10	1.5	0.8
Delay in stopping the wire feed at the arc extinction, s	0–3	0.1	0.1

Based on the technical documentation of the equipment included in the robotic welding station and the results of carried out experiments, the parameters to be monitored, the method of interaction of the control systems of the welding equipment with the system of robot control were selected, and the locations for mounting the sensors of the monitoring system were determined.

The monitoring system was fully automated and its operation was synchronized with the operation of the control program of industrial robot, power source and TOPTIG welding head. When the welds (or their sections) are produced successively, the data on welding parameters are registered, processed, visualized and stored in the database.

The developed measuring system for monitoring the technological parameters of the TOPTIG welding process in the robotic station ensures the registration and recording of the following information in the database:

- welding current;
- arc voltage;
- consumption of argon supplied to the welding torch and for shielding the weld reverse side;
- purity of argon (analyzer signal of oxygen content in argon);
- welding speed (read from the robot program);
- wire feed speed;
- bar-codes: identification number of the part (welded unit), numbers of order, serial and reference numbers, numbers of welding operation (entered by the operator of the station using a bar-code scanner);
- name of welding program (read from the robot program);
- number of welding program (read from the TOPTIG installation by means of the robot control system);
- date and time of welding (it is read from the robot program);
- temperature of environment;
- relative humidity;
- dividing the weld into separate sections based on signals from the robot.

The computer program of measuring system is divided into several independent modules in the way to provide a preliminary determined functionality of the system. Figure 6 shows the main window of the module «OPERATOR», intended for the operator of the station. The program interacts with the module «REGISTRATOR», which sends the registered oscillograms of welding parameters in online mode.

In the program window several panels, including the diagram panels, information panel and signalization panels can be selected. Before the beginning of welding process the operator enters the data into the information panel (number of part, number of order, reference numbers, operation number) from the manufacturing plan of the workpiece to be welded using touch-screen or bar-code scanner. These data are attached to the oscillograms of welding parameters and

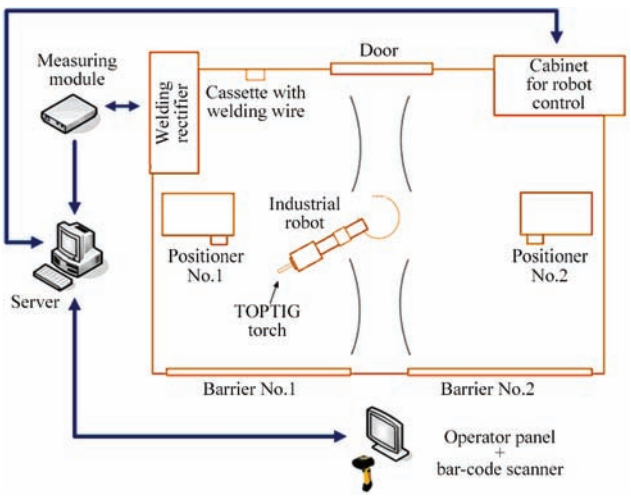

Figure 5. Layout of TOPTIG robotic welding station with system for monitoring the welding parameters

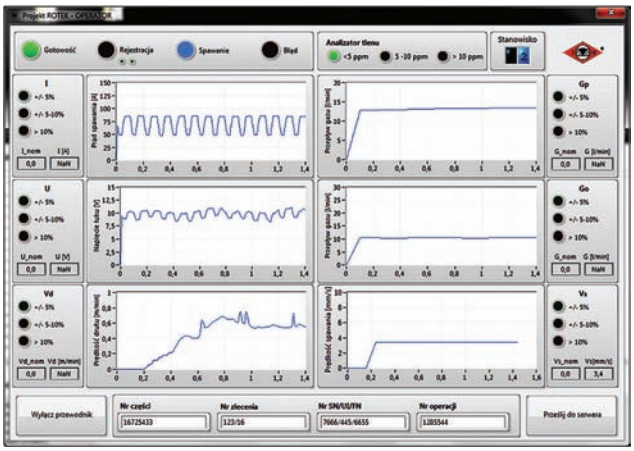

Figure 6. Graphical user interface of the software module «OPERATOR»

saved in the database. The signaling of violations of the preset welding mode is provided.

Figure 7 shows the main window of the module «VISUALIZER». The main task of this module is to view the archive data stored in the database. In this window, the following can be selected: diagram panel, which shows oscillograms of welding parameters; table of data records, in the strings of which the values of parameters for the next welds are stored; filter panel, with the help of which the subset of data based on certain parameters (e.g., number of part, number of order, serial number, operation number, number of robot program, date and time of the welding) can be selected. The program provides the ability to print the corresponding report according to the user's needs.

Conclusions

The welding installation TOPTIG 220 DC provides a wide range of adjusting the parameters in the process of welding by non-consumable electrode in inert gas with mechanized feeding of filler wire and the opportunity for robotizing welding in the places with a limited access to the weld zone. Based on the results of investigations of robotic TOPTIG welding, the technological features of making T-joints and butt joints of thin-walled parts of Inconel 718 alloy were determined. The carried out certification of the process showed that the developed welding technology meets the requirements of standards EN ISO 15614-1 and EN ISO 15613.

Figure 7. Graphical user Interface of the software module «VISUALIZER»

The replacement of manual TIG welding of thin-walled parts by robotic TOPTIG welding improved the operation conditions of welders and ensured the high quality of parts being welded. The developed measuring system provides registration of parameters of welding process, signaling about deviations from the preset welding parameters, formation of data bank on welding technologies and possibility of their viewing.

1. (2010) TOPTIG: Innovative process of non-consumable electrode welding. LLC Air Liquide Welding Ukraine. *Svarshchik*, **5**, 15–17.
2. (2009) Technologies of joining for aerospace industry. *Avtomatich. Svarka*, **8**, 3–4.
3. (2017) A new robot welding process for industry. Air Liquide Welding TOPTIG. *https*://www.oerlikon-welding.com
4. *EN ISO 15614-1*: Specification and qualification of welding procedures for metallic materials: Welding procedure test. Part 1: Arc and gas welding of steels and arc welding of nickel and nickel alloys.
5. *EN ISO 15613*: Specification and qualification of welding procedures for metallic materials: Qualification based on preproduction welding test.
6. (2017) High Performance Alloys, Inc.: Inconel 718 description. *www*.hpalloy.com/Alloys/descriptions/INCONEL 718.aspx.
7. (2014) TOPTIG DC safety instructions for operation and maintenance. Cat. Nº W000257751. *Air Liquide Welding*, **3**, 73.

Received 16.04.2017

doi.org/10.15407/tpwj2017.05–06.06

STABILIZATION OF WELDING CURRENT OF RESISTANCE SPOT WELDING MACHINES AT MAINS VOLTAGE FLUCTUATIONS

Yu.N. LANKIN, V.F. SEMIKIN and **E.N. BAJSHTRUK**
E.O. Paton Electric Welding Institute, NASU
11 Kazimir Malevich Str., 03680, Kiev, Ukraine. E-mail: office@paton.kiev.ua

The paper deals with the approaches to development of open-loop systems of welding current stabilization in resistance spot welding machines at mains voltage fluctuations. A microcontroller regulator of resistance welding is described, which provides automatic determination of the initial angle between full-phase current and voltage of the machine, as well as welding current stabilization at mains voltage fluctuations. System of angle determination and current stabilization is implemented as finite state machine with digital model of the object of control, presented in the tabulated form. This enabled application of a simple general purpose eight-bit microcontroller for the regulator. 7 Ref., 1 Figure.

Keywords: *stabilization, welding current, mains voltage, resistance welding*

Under production conditions, the process of resistance spot welding is exposed to numerous disturbances, leading to appearance of defective joints. The principal disturbances are as follows:

- mains voltage fluctuations;
- increase of electrode contact surface at their wear in operation;
- increase of impedance of machine welding circuit as a result of addition to it of considerable ferromagnetic masses in welding of large-sized parts;
- shunting of welding current and force applied to the electrodes, through earlier welded spots, located in immediate vicinity of welding point.

More or less considerable fluctuations of mains voltage are always found during resistance welding in reality, and, therefore, elimination of their influence on welded joint quality is required first of all. The adjustable variable in resistance welding usually is the effective value of welding current and much more seldom this is the interelectrode voltage or power, evolving in the welded spot.

To eliminate the influence of external disturbances, open-loop automatic control systems (ACS) with disturbance control, or closed-loop systems with negative feedback by adjustable variable, or combined ones are used. Historically, open-loop ACS with disturbance control were the first to be developed for resistance welding. They stabilize welding current only at mains fluctuations. Next came ACS with negative feedback, stabilizing welding current, irrespective of the kind of disturbance.

Open-loop ACS are simpler and more reliable than the closed-loop ones. Therefore, they have become the most widely accepted systems. Already the early, still ignitron welding current circuit breakers of PIT and PISh type (Electric Plant, Leningrad) with electronic valve control circuits provided automatic stabilization of welding transformer voltage at mains voltage fluctuations. Stabilization circuit was rather complicated and thorough adjustment was required at variations of resistance machine cos φ. Presence of a filter in control voltage circuit led to certain inertia of the stabilizer, so that short-term mains fluctuations could not be compensated at hard welding modes.

First transistor circuits for current control in resistance welding machines, developed at PWI in the 60s, provided practically inertialess stabilization of current at mains voltage fluctuations [1], stabilization of mean value of voltage in welding transformer at fluctuations of mains voltage and machine cos φ [2]. At the same time, the staff of the Institute of Cybernetics of AS of Ukr.SSR (V.N. Nikulin, V.I. Skurikhin), together with PWI, developed a completely digital system of program control of power evolved in the welding zone, with regulation by disturbances, namely by fluctuations of mains voltage, ohmic and reactive resistance of machine welding circuit [3, 4]. For the first time, general principles of construction of such devices were developed, a number of issues of designing digital control, measuring and converting devices for resistance welding machines controls were solved. The system was built as an automatic machine with finite number of internal states. All the states are presented in the form of tables, containing a matrix of reciprocal object model and measuring and computing matrix, from which the value of the angle of switching-on the contactor power valves is

read for each period of mains voltage, depending on set power value, mains voltage and load resistance. This system was ahead of its time for dozens of years. Digital systems of resistance welding control, usually being functionally inferior to it, were developed only after appearance of microcontrollers.

All the modern microcontroller regulators for resistance welding are fitted with the function of «parametric» stabilization of welding current at mains voltage fluctuations. Change of effective value of current of not more than ±3 % at mains voltage fluctuations of 0.9 to 1.05 of the nominal value is claimed. To ensure the accuracy of stabilization in some regulators, for instance, RKS-601, RKS-14, RKS-22, it is necessary to manually enter the value of machine power coefficient cos φ. Now, in the majority of regulators, for instance, RKM-511, RKM-812, RKM-1501, RKS-502, RKS-801(K155), RKS-807, RKS-901, automatic adjustment for power coefficient is performed. In the most perfect regulators RKM-802, RKM-804, RKM-805, RKM-806, KCU KS 02 a combined regulation principle is implemented. They simultaneously contain a closed-loop circuit of regulation by welding current deviation from set value and open-loop circuit for regulation by external disturbance (mains voltage).

Apparently, the most popular algorithm of current stabilization at mains voltage fluctuations for microprocessor regulators for resistance welding was developed by VNIIESO specialists [5]. According to it, current stabilization is performed in each half-period, starting from the second one, by setting angle α of thyristor switching-on in keeping with expression $\alpha = IU/b_1 - b_0/b_1$, where I is the set current value, referred to current of full-phase switching at nominal mains voltage; U is the measured mains voltage, referred to nominal voltage; b_0, b_1 are the parameters of regulation characteristic, represented by second degree polynomials of power factor of full-phase switching of welding circuit. Value of cos φ required for calculation of b_0 and b_1 is automatically determined in the first half-period by measured value of the angle of conduction λ at certain angle α_0, knowingly less than φ, from expression $\cos\varphi = C_0(\alpha_0) + C_1(\alpha_0)\lambda$, where $C_0(\alpha_0)$ is the second degree polynomial of α_0, $C_1(\alpha_0)$ is the third degree polynomial of α_0 [6].

Automatic determination of cos φ, used for current stabilization at mains voltage fluctuations, is even more necessary for automatic limitation of minimum angle of thyristor switching-on in all resistance welding regulators without exception. The point is that if thyristor switching-on angle is set less than angle α, welding contactor will conduct half-wave current of just one polarity, and welding transformer will go into emergency mode with DC bias. To satisfy condition $\alpha > \varphi$, it is more convenient to measure not cos φ, but φ [7]. In this work expression $\varphi = a_0 + a_1\lambda + a_2\alpha + a_3\alpha^2$ is used for φ, where a_1, a_2, a_3 are the constant coefficients.

In the above-described and the majority of other digital current regulators rather cumbersome analytical models of the object of control at mains voltage fluctuations are used, which require real-time mathematical calculations with floating point. They make unreasonably high requirements of regulator microcontroller capacity. In our opinion, it is the most rational to use digital automatic machines with finite number of internal states, presented in table form. Such automatic machines do not require mathematical calculations by complex formulas, thus allowing application of the simplest and least expensive microcontrollers for their realization.

A model of resistance welding regulator is realized in a simple eight–bit microcontroller PIC16F886. Regulator provides adjustment of the duration of standard set of welding cycle positions: compression, forging, current-pulse, pause from 1 up to 99 in mains periods, as well as assigning welding current I_{set} in the range of 25–90 % of full-phase current.

System of current stabilization at the change of mains voltage is designed as table-type finite state machine. Angle φ of full-phase current shift relative to voltage applied to resistance welding machine, is determined at current flowing in the first period of welding pulse. For this purpose sufficiently high fixed angle of thyristor switching-on $\alpha_0 = 0.7\pi$ is set, so that the corresponding current were definitely less that the set welding current. The φ value is determined by measured λ values from φ–λ table for α_0.

Seven tables of I_{nom} dependence on α, at nominal mains voltage U_{nom} are stored in regulator microcontroller memory for different φ values, for which cos φ is in the range of 0.2–0.8. From these tables α can be selected to obtain the assigned values of welding current. However, at mains voltage $U_m \neq U_{nom}$ another table should be used, which is calculated by expression $I_m(\alpha) = I_{nom}(\alpha)U_m/U_{nom}$. To reduce the used memory of microcontroller, just the minimum required part of this table is calculated for α, changing after $\Delta\alpha = \pi/200$ from α_1, for which $I_{nom}(\alpha_1) = I_{set}$, up to α_2, for which $I_m(\alpha_2) = I_{set}$. As here fast operations of program multiplication of single-byte numbers and bitwise shifts are used, calculations take small enough time even in low-capacity controllers. Thus, the angle of thyristor switching-on, required to obtain set current at nominal mains voltage, is corrected in accordance with fluctuations of mains voltage that provides current stabilization.

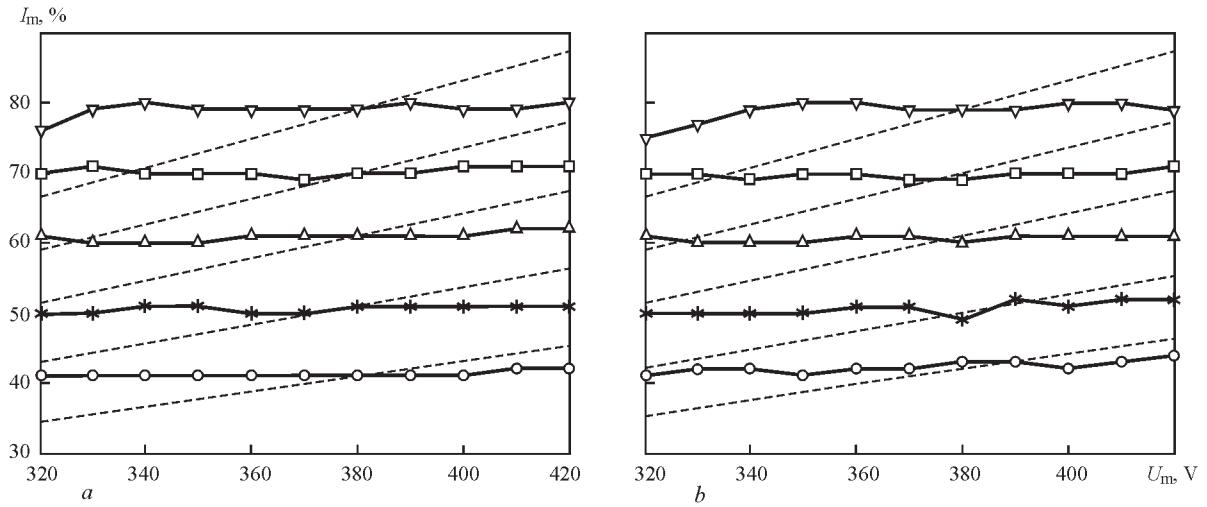

Static characteristics $I_m = f(U_m)$ at variation of mains voltage: *a* — $\varphi = 0.2\pi$; *b* — $\varphi = 0.35\pi$

The Figure gives experimental static characteristics of the regulator at mains voltage variation for different values of set current and load power factor. $I_m = f(U_m)$ dependencies in absence of stabilization are also shown here by a dashed line. From this Figure it follows that at mains voltage fluctuations from 320 to 420 V, effective value of current changes by not more than ±2 % of the set value. Only for current set at the level of 80 % of full-phase value, current stabilization is limited by minimum mains voltage of 325 V for $\varphi = 0.2\pi$ and 334 V for $\varphi = 0.35\pi$. This is related to the fact that for reliability minimum angle α was program limited to value $\varphi–\pi/18$.

1. Lankin, Yu.N. (1961) Control circuit of ignitron breaker with automatic stabilizing of current. *Avtomatich. Svarka*, **4**, 25–27.
2. Lankin, Yu.N., Masalov, Yu.A. (1972) *Control circuit of valve breaker*. USSR author's cert. 349523. Int. Cl. B 23k 11/24.
3. Nikulin, V.N. (1963) Program control systems with self-correction based on digital devices. *Avtomatich. Svarka*, **5**, 28–33.
4. Nikulin, V.N. (1967) *Development and investigation of program control system with self-correction for automation of resistance spot welding process*: Syn. of Thesis for Cand. of Techn. Sci. Degree. Kiev: PWI.
5. Akselrod, F.A., Ibragimov, U.U., Ioffe, Yu.E. et al. (1987) *Method of stabilizing of welding current in resistance welding with thyristor control*. USSR author's cert. 1355409. Int. Cl. B 23 K 11/24.
6. Akselrod, F.A., Ibragimov, U.U., Ioffe, Yu.E. et al. (1987) *Method of determination of power coefficient of full-phase current switching-on in resistance spot welding with single-phase current*. USSR author's cert. 1381358. Int. Cl. B 23 K 11/24.
7. Podola, N.V., Rudenko, P.M., Gavrish, V.S. et al. (1986) *Method of measuring of power coefficient of single-phase resistance welding machine*. USSR author's cert. 1310149. Int. Cl. B 23 K 11/24.

Received 26.04.2017

doi.org/10.15407/tpwj2017.05–06.07

COMPUTER SYSTEM FOR AUTOMATIC CONTROL OF ARC SURFACING PROCESSES USING ELECTRODE WIRES

I.A. RYABTSEV, V.G. SOLOVIOV, Yu.N. LANKIN and **A.A. BABINETS**
E.O. Paton Electric Welding Institute, NASU
11 Kazimir Malevich Str., 03680, Kiev, Ukraine. E-mail: office@paton.kiev.ua

A computer system for automatic control of processes of arc surfacing by electrode wires was developed. The use of a computer system in the appropriate surfacing equipment enables the operator to perform selection of arc surfacing method (under flux, with open arc or in shielding gases); selection of the type of electrode material, its grade and dimensions; to set, automatically maintain, control and record the set parameters of surfacing modes of a part, providing the necessary operational properties and geometric dimensions of deposited layers. With the accumulation of relevant databases on surfacing of parts of different purpose, dimensions and configuration, the use of the developed computer control system will significantly improve the efficiency of arc surfacing processes. 9 Ref., 4 Figures.

Keywords: *arc surfacing, automation of surfacing processes, surfacing technology, computer systems for surfacing control, surfacing power consumption*

The state-of-the-art of automation of surfacing processes assumes the creation of appropriate computer systems for presetting and control of the process parameters in a real time, analysis, processing and, if necessary, automatic correction of values of these parameters taking into account their influence on penetration depth, volume of base metal (VBM) in the deposited metal, as well as formation of deposited layers, their dimensions and quality.

The creation of effective means for automation of surfacing processes due to the development of methods for control and monitoring of the penetration of base metal and formation of deposited layers will allow significant improving the welded joint quality, operational properties of deposited metal and efficiency of surfacing works, as well as reducing the power intensity of surfacing processes.

For arc surfacing these systems, depending on the design, degree of wear and operational requirements for the deposited parts should provide:

- selection of arc surfacing method (under flux, with open arc or in shielding gases);
- selection of type of electrode material (solid or flux-cored wire, cold rolled or flux-cored strip), its grade and dimensions (diameter, cross-section);
- setting and automatic maintenance of the preset electrical and mechanical (surfacing speed, electrode wire stickout) parameters of surfacing modes, providing the necessary geometric dimensions of deposited layers;
- marking of random or deliberate deviations from the set surfacing modes;
- accumulation of relevant databases, recording and subsequent use of optimal modes for surfacing of specific parts.

The existing experience [1–3] shows that state-of-the-art of a computer technology can successfully solve these problems.

The main volume of information, used to evaluate different components of technological process of arc surfacing, is obtained as a result of analysis of signals of current I_s and voltage U_a. Other process parameters are as a rule less important.

To obtain the necessary information directly from the object under control (deposited part), visualization, registration of output data and processing of this information, different information and measuring systems (IMS) [4–9] are used.

Using the computer information and measuring system (CIMS) [3], developed at the E.O. Paton Electric Welding Institute, the authors of the article carried out systematic investigations of influence of electrical parameters of different methods of arc surfacing by flux-cored wire on stability of the process, penetration of base metal and formation of deposited layers [2]. CIMS provides control and registration of the following parameters of surfacing process:

- input of tasks for arc voltage U_{ap} and arc current I_{ap};
- actual values of arc voltage $U_a(t)$;
- actual values of arc current $I_a(t)$;
- mean values of arc voltage $\bar{U}_a$ and arc current $\bar{I}_a$ for the time of surfacing;

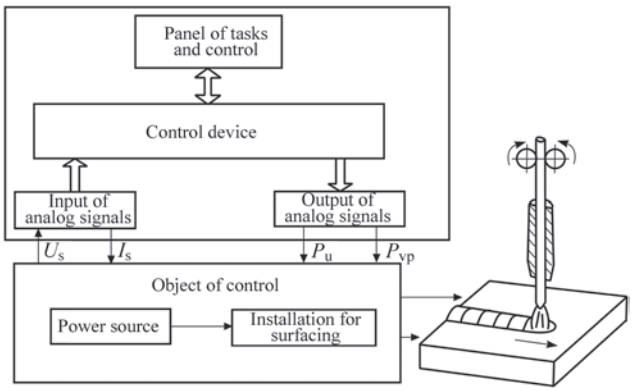

Figure 1. Block diagram of computer system for automatic control of arc surfacing (U_s, I_s — the values of actual voltage and current of surfacing; P_u, P_{vp} — the position of regulator of output voltage of current source and regulator of wire feed speed on the control panel)

- indication of working area of approximating functions (in the parameters of $\bar{U}_a$ and $\bar{I}_a$) which provide the accuracy of approximation by voltage ±1 V and current ±10 A.

As a result of investigations, a database on different methods and technologies of arc surfacing by flux-cored wires and their influence on penetration depth and VBM in the deposited metal as well as on sizes of the deposited beads was accumulated. On the basis of CIMS and accumulated database, a computer system for automatic control of arc surfacing technologies was developed.

A block diagram of the proposed computer control system is shown in Figure 1.

As is seen from the diagram, the task and control panel allows entering and controlling the modes data of the selected arc surfacing method for a particular part in the process of surfacing. These data are then automatically transferred to the control device of surfacing installation. From the control device, the analog signal is supplied directly to the surfacing installation and the power source. After switching on the process of surfacing of a particular part, the computer system installs a set mode by current and voltage for it. In the process of surfacing from the object under the control (surfacing installation and power source) a signal about actual values of surfacing current and voltage is supplied to the control device. In case of deviation of these values from the preset ones, the system performs their corresponding correction.

Depending on the specified task, the system enables the operator to solve different tasks when presetting the modes of automatic arc surfacing of a particular part. Thus, for example, if the operator enters the data on the method of arc surfacing, selected diameter of the electrode wire and surfacing modes into the computer system, then he receives data from the system about the possible dimensions of bead being

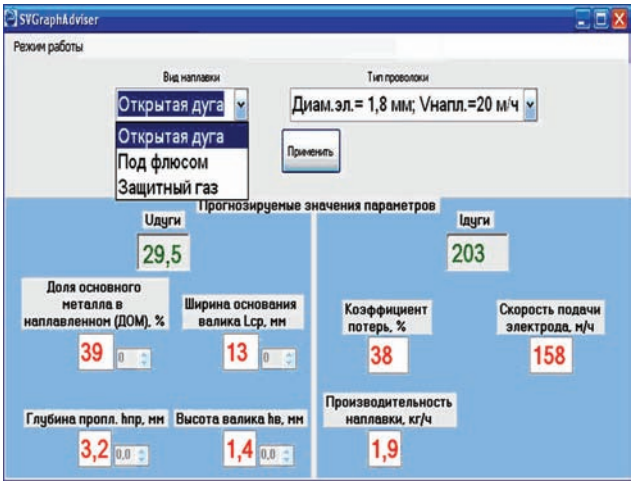

Figure 2. View of computer screen in selecting the surfacing method

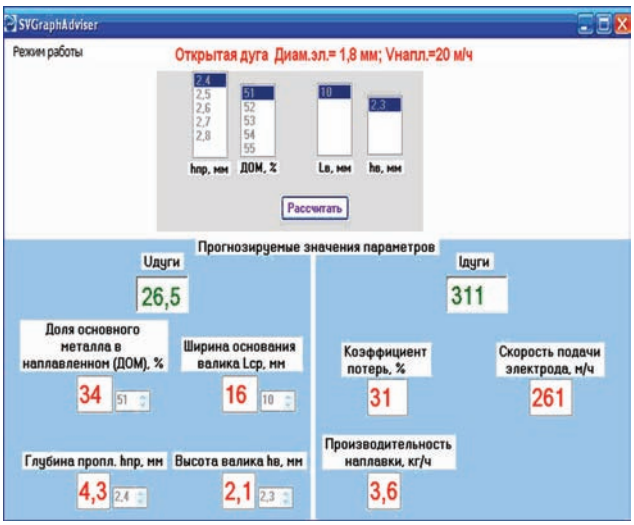

Figure 3. View of computer screen in selecting the electrode wire diameter

Figure 4. View of computer screen with preset modes of open arc surfacing by flux-cored wire of 1.8 mm diameter and predicted characteristics of surfacing process and geometric dimensions of deposited beads

deposited (width, height, penetration depth), VBM in deposited metal, surfacing efficiency, loss factor (Figures 2–4).

Or, on the contrary, if the operator enters the geometric characteristics of bead and VBM to the system, preset according to requirements of the drawing of a part to be deposited, then he receives data about electrical parameters of surfacing mode from the system, which will ensure the obtaining of such characteristics.

In the computer system, the order of priorities for setting parameters of melting bead was introduced. In particular, in the first case such parameters as «Type of surfacing» and «Diameter of flux-cored wire» (see Figures 2, 3) were taken as priority. Then, the surfacing modes are selected (see Figure 4). The list of values of selected parameters is limited within the range of «Admissibility of surfacing modes» from 0.85 to 1.0, which were selected from the results of experimental investigations and entered into the database. In the case of production needs, the «Admissibility of surfacing modes» can be extended to a minimum value of 0.25, but at the same time the deposited beads with a good formation should not be expected.

After calculation, the system provides predicted characteristics of surfacing process (loss factor and surfacing efficiency) and geometric dimensions of beads being deposited.

It should be noted that experience in developing a computer system for control of arc surfacing processes showed that when creating such systems, it is necessary to take into account the electrical characteristics of a specific surfacing installation and power source. The complex of these characteristics should include characteristics of welding source, electrical characteristics of connecting cables and electrical parameters of connections in the installation itself, including the resistance of contact of workpiece with the installation.

Conclusions

A computer system for automatic control of electrode wires arc surfacing processes was developed and tested in the laboratory conditions. Using a computer system in the appropriate surfacing equipment enables the surfacing operator to select the method of arc surfacing (under flux, with open arc or in shielding gases); to select the type of electrode material, its grade and dimensions; to preset, automatically maintain, control and record the set parameters of modes for surfacing of a particular part, providing the necessary geometric dimensions of deposited layers.

1. Demchenko, V.F., Kozlitina, S.S., Ryabtsev, I.A. (1998) Computer system for design of arc surfacing technologies. *Avtomatich. Svarka*, **11**, 61–66.
2. Lankin, Yu.N., Ryabtsev, I.A., Soloviov, V.G. et al. (2014) Effect of electric parameters of arc surfacing using flux-cored wire on process stability and base metal penetration. *The Paton Welding J.*, **9**, 25–29.
3. Ryabtsev, I.A., Lankin, Yu.N., Soloviov, V.G. et al. (2015) Computer information-and-measuring system for investigation of arc surfacing processes. *Ibid.*, **9**, 32–35.
4. Adolfsson, S., Babrami, A., Bolmsjo, G. et al. (1999) On-line quality monitoring in short-circuit gas metal arc welding. *Welding J.*, **2**, 59–73.
5. Koves, A., Golob, M. (2002) Fuzzy logic based quality monitoring in short-circuit gas metal arc welding. *IIW Doc. XII-1712–02*.
6. Wu, C.S., Polte, T., Rehffeldt, D.A. (2001) Fuzzy logic system for process monitoring and quality evaluation in GMAW. *Welding J.*, **2**, 33–38.
7. Pokhodnya, I.K., Milichenko, S.S., Gorpenyuk, V.N. et al. (1987) Influence of structure and coefficient of electrode coating mass of base type on stability of arc burning in welding. *Avtomatich. Svarka*, **8**, 32–35.
8. *Ye Feng* et al. On-line quality monitoring in robot arc welding process. *IIW Doc. 212-994–01*.
9. Pokhodnya, I.K., Farpenyuk, V.N., Milichenko, S.S. (1990) *Metallurgy of arc welding: Processes in arc and melting of electrodes*. Ed. by I.K. Pokhodnya. Kiev: Naukova Dumka.

Received 03.04.2017

doi.org/10.15407/tpwj2017.05–06.08

TECHNOLOGICAL ASPECTS OF THE ROBOTIC TOPTIG SURFACING OF BOILER STEEL TUBES USING ALLOY INCONEL 625

T. PFEIFER[1], **M. RÓŻAŃSKI**[1], **W. GROBOSZ**[1], **J. RYKAŁA**[1] and **I.A. RIABCEW**[2]
[1]Instytut Spawalnictwa w Gliwicach
Poland, 44–100. Gliwice, ul. Bl. Czeslawa 16–18. E-mail: is@is.gliwice.pl
[2]E.O. Paton Electric Welding Institute, NASU
11 Kazimir Malevich Str., 03680, Kiev, Ukraine. E-mail: office@paton.kiev.ua

The research aimed to develop technological parameters of the TOPTIG method-based surfacing (using alloy Inconel 625) of boiler tubes (Ø 45×5) made of steel 13CrMo4–5 ensuring the obtainment of the iron content on the overlay weld surface below 5 %. The research resulted in the development of sets of parameters enabling the obtainment of overlay welds characterised by very high quality and the minimum degree of the stirring of the overlay weld metal with the base material. The above named sets of parameters were utilised when making a number of overlay welds on tubes. The research involved macroscopic metallographic tests of overlay welds, the identification of the base material content in the overlay weld, the determination of the chemical composition of the overlay weld surface as well as the performance of microscopic metallographic tests and the microanalysis of the chemical composition. It was ascertained that the TOPTIG technology enabled the making of overlay welds characterised by very high quality and the minimum degree of the stirring of the overlay weld metal with the base material (only 3.28 %) and made it possible to obtain an iron content of 2.75 % on the overlay weld surface using forced cooling performed inside the tube. Surfacing without cooling led to a significantly higher base material content in the overlay weld (approximately 14 %), where the content of iron on the overlay weld surface amounted to 8.47 %. 13 Ref., 3 Tables, 8 Figures.

Keywords: *robotic surfacing, TOPTIG method, alloy Inconel 625, boiler tubes, waste incineration boilers, Fe content on the overlay weld surface*

Introduction. Power plants fed with fossil fuels and waste incineration plants used for power generation must satisfy strict requirements as regards power boiler components including furnaces, collectors, superheaters and pipings. The above-named requirements result from extreme working conditions of components exposed to abrasion and erosion. The incineration of waste in boilers results in the formation of flue gas containing aggressive chlorides and fluorides, the detrimental effect of which requires the use of appropriately effective protections from erosion and corrosion of e.g. tubes of heat exchangers and combustion chambers. Presently, the service life of such elements is increased by the surfacing of layers of nickel alloys, particularly having the composition of alloy Inconel 625, providing appropriate creep resistance at high temperature and corrosion resistance in the aggressive environment of fluorides and chlorides. Presently used surfacing methods include gas-shielded metal arc surfacing (using pulsed current and the low-energy CMT method), plasma–powder surfacing, laser surfacing and non-consumable electrode inert gas surfacing (TIG) [1–13].

One of the primary criteria to be satisfied by a surfaced coating is low iron content (maximum 5 % in the external zone), a thickness not exceeding 2.0÷2.5 mm as well as the lack of the microsegregation of alloying elements in the overlay weld. Iron content higher than that mentioned above reduces corrosion resistance, whereas an excessive thickness increases both the weight of structures and the costs of surfacing processes. In turn, the microsegregations of elements, particularly Nb and Mo, cause the formation of intermetallic phases decreasing the corrosion resistance of overlay welds [2, 3, 7, 8].

Technical reference publications contain information concerning the structure and properties of overlay welds made using gas-shielded metal arc surfacing, including the low-energy variant of CMT method [1–3]. The presented results indicate that, when welding using arc methods, the satisfaction of the above-presented requirements needs the making of a minimum of 2 layers, which extends the operating time and could lead to the formation of excessive stresses and strains of surfaced elements (length of surfaced tubes up to 12 m). The tests described in publication [1] re-

Table 1. Selected parameters and their designation

No.	Impulse current, A	Basic current, A	Filler metal wire feeding rate, m/min	Number of surfaced layers	Overlay weld designation on the tube
1	140	100	1.0	1	16/1
2	140	100	1.0	2	16/2
3	140	120	1.2	1	37/1
4	140	120	1.2	2	37/2
5	130	120	1.5	1	41/1
6	130	120	1.5	2	41/2
7	130	120	1.5	1	41/W/1
8	130	120	1.5	2	41/W/2

vealed that it was not possible to entirely eliminate the microsegregation of alloy components reducing the service life of the layers. It was ascertained that as a result of microsegregation occurring during the solidification of overlay welds, the cores of dendrites were richer in Ni, Fe and Cr, whereas the interdendritic areas were richer in Mo and Nb. During the solidification, the strongest segregation was that of niobium, less intense was that of molybdenum, whereas the segregation of chromium was the least intense. Individual research revealed that similar results were obtained using plasma-powder surfacing [10–13]. It appears that surfacing utilising the CMT and plasma–powder methods could be alternatively replaced by TIG surfacing: plasma surfacing with wire feeding and the surfacing utilising an innovative TIG method, i.e. TOPTIG (feeding the wire at an angle of approximately 20° in relation to the electrode), where the wire is fed either in a continuous or in a pulsed manner. This article presents the course and selected results of tests aimed at the determination of the effect of TOPTIG surfacing on the structure of overlay welds made of nickel alloy Inconel 625 applied on the base made of steel 13CrMo4-5.

Materials, test rig and testing methodology. The base material used in the tests had the form of seamless tubes (ø 45×5.0 mm) made of steel 13CrMo4–5 according to PN-EN 10216-2:2014-02 (15XM according to GOST4543-71). The technological tests involved the use of an OK Autrod NiCrMo–3 solid wire (Inconel 625) having a diameter of 1.0 mm (ESAB).

The technological tests of the surfacing process were performed using a station equipped with a ROMAT 310 robot (Cloos) and a TOPTIG 220DC machine (Air Liquide Welding).

The technological tests were initiated by the performance of a number of surfacing tests (simple overlay welds made on sheets) using various process parameters and aimed to identify the effect of basic current, impulse current and of a filler metal wire feeding rate on the quality, geometry and uniformity of overlay welds as well as on penetration depth. More than 60 various sets of parameters were tested. The further stage of research-related tests concerned with surfacing performed on tubes made of steel 13CrMo4–5 involved the use of parameters ensuring the obtainment of the highest quality and the lowest degree of the stirring of the overlay weld with the base. The most favourable parameters are presented in Table 1. The overlay welds were made on the tubes without cooling performed inside the tubes (items 1–6, Table 1). For comparative purposes, overlay welds were also made with the forced cooling performed inside the tube, where the cooling medium was water (items 7 and 8, Table 1).

After the overlay welds were made on the tubes, the latter were subjected to macroscopic metallographic tests and measurements enabling the calculation of the base material content in the overlay welds. The macroscopic metallographic photographs were used to determine the cross-sectional areas of excess overlay weld metal and of the partially melted base material as well as to identify the overlay weld height

Table 2. Overlay weld height (W), fusion area (F_w), overlay weld area (F_n) and the calculated content of the base material in the overlay weld (U_p)

Overlay weld geometry	Spec. 16/1	Spec. 16/2	Spec. 37/1	Spec. 37/2	Spec. 41/1	Spec. 41/2	Spec. 41/W/1	Spec. 41/W/2
U_p, %	13.78	11.04	13.11	8.40	14.24	7.52	5.67	3.28
F_w, mm^2	160.6	182.9	120.6	154.3	165.5	150.1	143.3	132.7
F_n, mm^2	1004.7	1474.6	799.6	1681.7	995.1	1844.6	1735.5	1662.6
H, mm	2.52	3.64	2.11	3.84	2.81	4.21	2.12	2.66

(*W*), penetration depth (*G*) and the base material content in the overlay weld. The above-named parameter was determined as the proportion of the area of penetration in the material to the area of the entire overlay weld. The overlay weld geometry measurements were performed using the Autodesk Inventor Professional 2016 software programme. The measurement results are presented in Table 2.

The subsequent stage of research involved the analysis of chemical composition of the overlay weld surface aimed to determine the content of iron as well as to measure hardness in the surfaced layer and in the HAZ. The analysis of the chemical composition was performed using spark source optical emission spectrometry and Q4 TASMAN spectrometer (Bruker). The hardness measurements (Vickers hardness test) were performed on the cross-sections of the overlay welds using a KB50BYZ-FA hardness tester (KB Prütechnik GmbH) and a load of *HV* 10.

The next stage involved microscopic metallographic tests, the microanalysis of the cross-sectional chemical composition and the determination of the surface distribution of chemical elements. The metallographic specimens were prepared by grinding utilising SiC papers having a granularity of 280–1200 followed by polishing involving the use of diamond pastes (3 and 1μm) and etching (3g $FeCl_3$, 10ml HCl, 90 ml C2H5OH). The determination of the overlay weld quality required the use

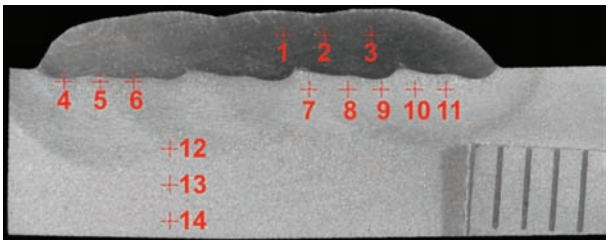

Figure 1. Arrangement of hardness measurement points in the overlay weld and HAZ

of an Olympus SZX9 stereoscopic microscope (SM) in the dark field at magnification of up to 500x. The microstructure was observed using a Hitachi S-3400N scanning electron microscope (SEM) and the SE (SecondaryElectrons) as well as the BSE observation techniques at magnification of up to 2000x.

The microanalysis of the chemical composition of the surfaced layers was performed using a Hitachi S-3400Nv scanning microscope provided with an energy dispersive spectrometer (EDS). The chemical composition tests were conducted using an accelerating voltage of 15keV. The analysis of the chemical composition of the overlay welds was supplemented with the analysis of changes in the chemical composition on the line perpendicular to the overlay weld and the surface distribution of chemical elements in the fusion area.

Test results. The calculated content of the base material in the overlay welds and the height of the overlay welds are presented in Table 2.

Table 3. Chemical composition of the overlay weld surface

Chemical composition, %	Specimen designation							
	16/1	16/2	37/1	37/2	41/1	41/2	41/W/1	41/W/2
C	0.035	0.026	0.041	0.024	0.030	0.020	0.019	0.019
Mn	0.167	0.073	0.236	0.056	0.143	0.033	0.088	0.08
Cr	19.74	20.92	18.74	20.62	20.13	20.51	21.70	21.09
Mo	8.020	8.401	7.399	8.181	7.975	7.988	6.871	8.248
Fe	10.20	4.542	14.77	3.98	8.470	4.290	3.467	2.755
Mg	0.0019	0.0017	0.0022	0.0020	0.0022	0.0023	0.0016	0.015
Nb	3.434	3.577	3.228	3.722	3.383	3.620	0.045	3.438
Ni	58.05	62.08	55.23	62.49	59.50	62.92	63.56	63.64

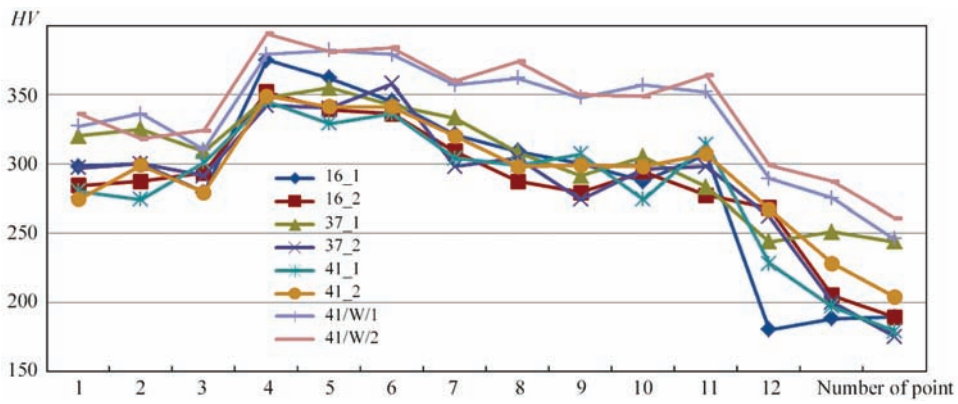

Figure 2. Graphic representation of selected hardness measurement points on the cross-section of overlay welds

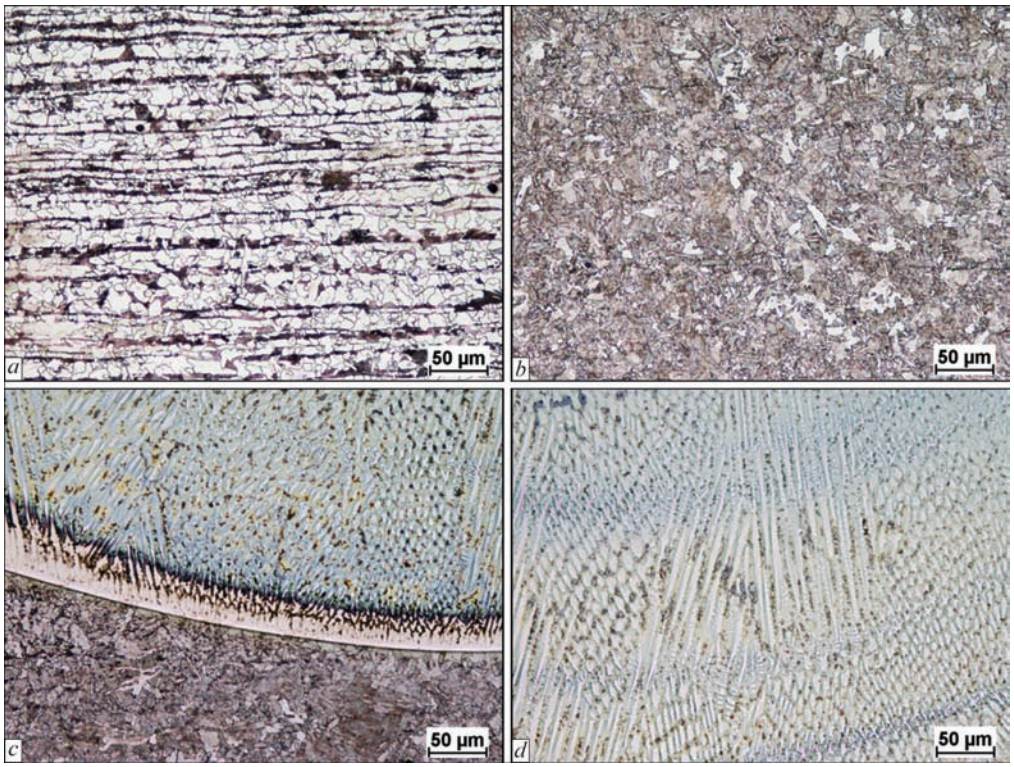

Figure 3. Microstructure of the overlay weld (item 7 of Table 1) made of alloy Inconel 625 on the tube made of steel 13CrMo4-5; ×200

The macroscopic metallographic tests revealed that the content of the base material in the overlay weld could be reduced by using two-layer surfacing or by performing forced cooling inside the tube.

The hardness tests were performed on the cross-section of the overlay welds in accordance with the scheme presented in Figure 1. Selected results are presented in the graphic form in Figure 2.

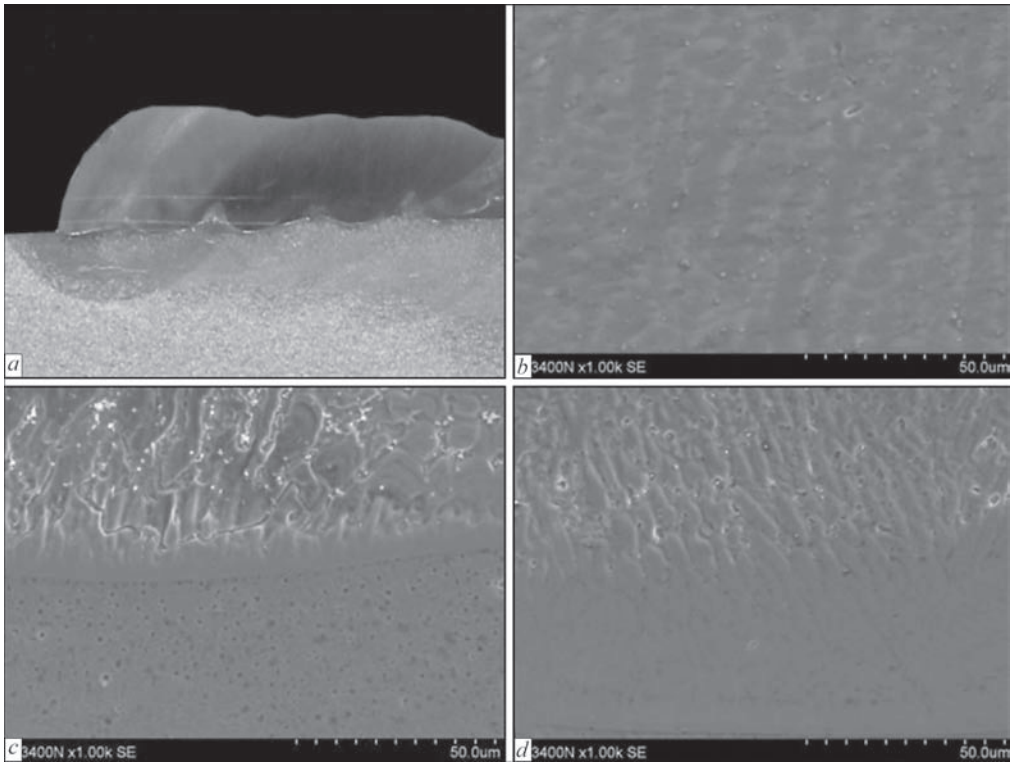

Figure 4. Structure of the overlay weld made of alloy Inconel 625 on the tube made of steel 13CrMo4–5, specimen of item 7 of Table 1: *a* — overlay weld macrostructure (SM); *b* — overlay weld structure, SEM, SE; ×1000; *c* — fusion line, SEM, SE; ×1000; *d* — fusion line with the visible zone enriched in chromium SEM, SE; ×2000

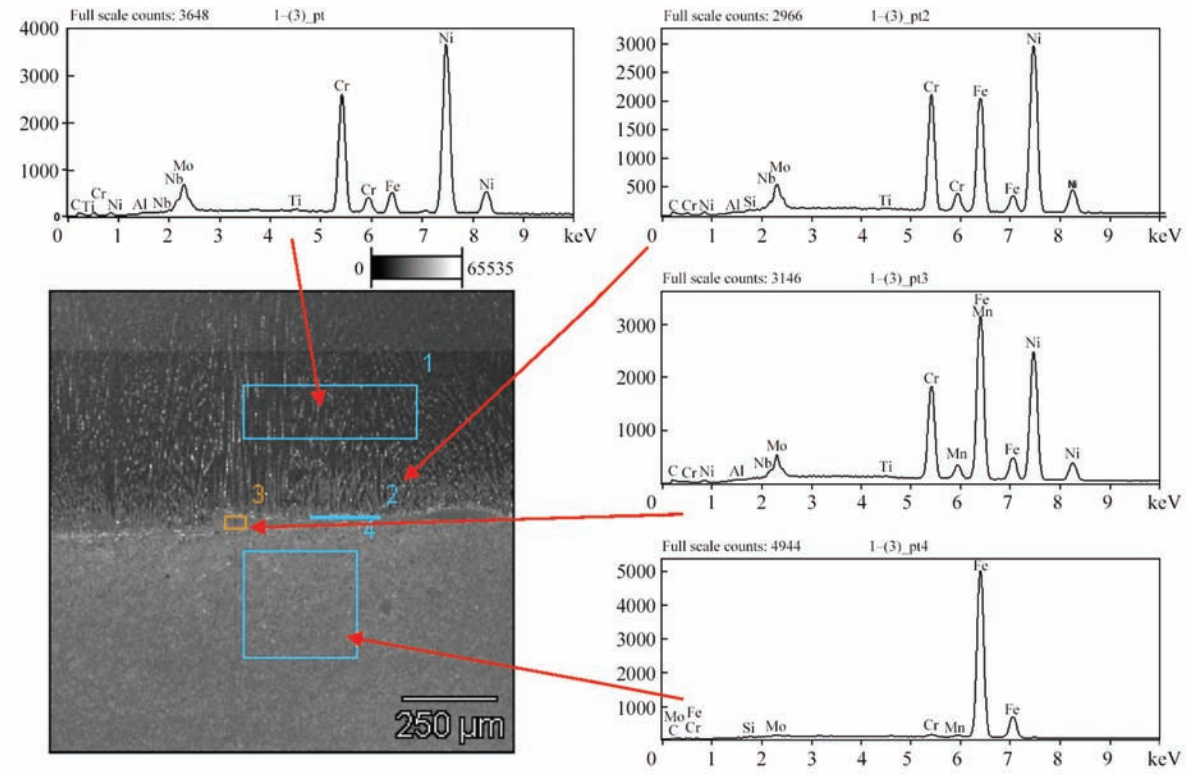

Weight,%	Al-K	Si-K	Ti-K	Cr-K	Mn-K	Fe-K	Ni-K	Nb-L	Mo-L
1-(3)_pt1	0.1	-	0.2	22.4	-	5.1	62.2	3.3	6.6
1-(3)_pt2	0.1	0.1	0.1	17.2	-	23.7	52.1	1.2	5.5
1-(3)_pt3	0.1	-	0.1	14.6	0.1	36.3	42.7	1.7	4.5
1-(3)_pt4	-	0.2	-	1.1	0.6	97.7	-	-	0.4
Atom %	**Al-K**	**Si-K**	**Ti-K**	**Cr-K**	**Mn-K**	**Fe-K**	**Ni-K**	**Nb-L**	**Mo-L**
1-(3)_pt1	0.3	-	0.3	25.4	-	5.4	62.4	2.1	4.1
1-(3)_pt2	0.2	0.2	0.1	19.2	-	24.6	51.6	0.8	3.3
1-(3)_pt3	0.2	-	0.1	16.2	0.2	37.6	42.0	1.0	2.7
1-(3)_pt4	-	0.5	-	1.1	0.6	97.5	-	-	0.2

Figure 5. Results of the chemical composition microanalysis (EDS) in the individual zones of the overlay weld; specimen of item 7 of Table 1

The chemical composition tests were performed on the overlay weld surface using spark source optical emission spectrometry. The tests aimed to determine the effect of surfacing conditions and parameters on the iron content of the overlay weld surface. The contents of selected chemical elements are presented in Table 3.

When analysing the chemical composition of the overlay weld metal it was ascertained that in terms of the two-layer overlay welds the content of iron on the overlay weld surface did not exceed 5 % in each case. However, it should be noted that the necessity of making another, i.e. the second, overlay weld significantly extends the production process. In cases of the one-layer overlay welds, made without the forced cooling of the tube, in each case the content of iron on the overlay weld surface exceeded 5 %, often reaching 10 %. In cases of the one and two-layer overlay welds made on the tubes cooled inside using flowing water, the content of iron on the overlay weld surface amounted to 3.46 % and 2.75 %, where the content of the base material in the overlay weld amounted to 5.67 % and 3.24 %, respectively.

The microscopic metallographic tests were performed in the base material area, HAZ, fusion line and in the one-layer overlay weld made using parameters of item 7 in Table 1. The tests involved the use of light and scanning electron microscopy. Figure 3 presents photographs made using the light microscope, whereas Figure 4 presents the microstructural photographs made using the scanning electron microscope. Figure 5 presents the results of the chemical composition microanalysis (EDS) in the individual zones, Figure 6 presents the linear distribution of chemical elements, whereas Figure 7 presents the surface distribution of chemical elements in the overlay weld fusion zone.

Analysis of test results. The tests aimed to determine the effect of TOPTIG surfacing conditions and parameters on the overlay weld geometry as well as on the content of the base material in the overlay weld

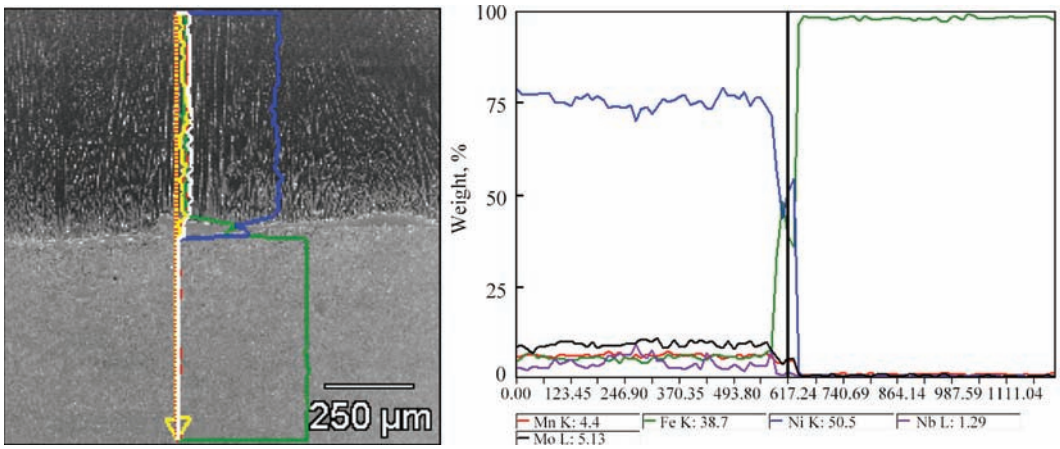

Figure 6. Linear distribution of chemical elements in the overlay weld fusion line in specimen 41/W/1 (item 7, Table 1)

and on the content of iron on the overlay weld surface. The tests also aimed at the identification of parameters, the use of which could ensure the obtainment of an iron content on the overlay weld surface not exceeding 5 %. The initial technological tests performed on sheets enabled the identification of parameters ensuring the obtainment of overlay welds characterised by very high quality and the base material content in the overlay weld not exceeding 15 %. The above-named parameters are presented in Table 1.

The macroscopic metallographic test results and the calculations identifying the base material content in the overlay weld revealed that in cases of one-layer overlay welds designated 16/1, 37/1 and 41/1 (items 1,3 and 5 of Table 1), the content of the base material in the overlay weld amounted to 13.78, 13.11 and 14.42 % respectively, whereas the iron content on the surface of the overlay welds amounted to 10.2, 14.47 and 8.47wt. %, respectively, and in each case exceeded the allowed limit value of 5 %. In cases of the two-layer overlay welds, the base material content in the overlay weld in specimens designated 16/2, 17/2 and 41/2 (items 2, 4 and 6 of Table 1) amounted to 11.04, 8.4 and 7,52 %, respectively, whereas the iron content on the surface of the overlay welds amounted to 4.54, 3.98 and 4.29wt. %, respectively. As can be seen above, in each case the condition limiting the allowed iron content in the overlay weld to 5 % was satisfied. However, it should be noted that the time required to make two-run overlay welds was unacceptable in terms of industrial applications. In addition, the reduction of the base material content in the overlay weld was obtained by increasing the volume of the filler metal, which, in turn, significantly increased the cost of surfacing. The foregoing inspired an attempted reduction of the degree of stirring of the overlay weld metal with the base material by using the forced cooling of the tube with water flowing during the process

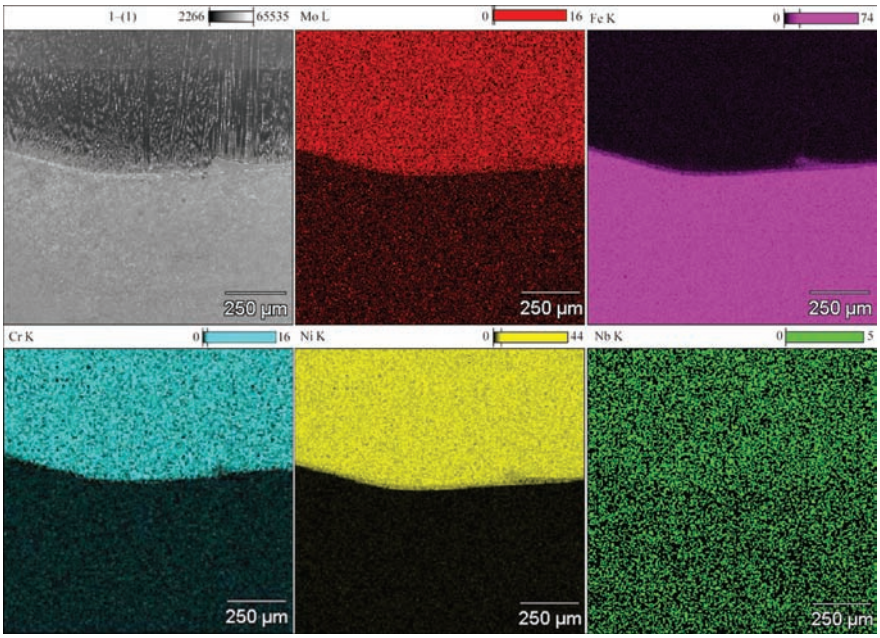

Figure 7. Surface distribution of chemical elements in the overlay weld fusion zone, specimen no. 41/W/1 (item 7, Table 1)

of surfacing. The subsequent tests involved the making of two overlay welds designated as 41/1 and 41/2 (items 7 and 8 of Table 1) subjected to macroscopic metallographic tests, measurements determining the base material content in the overlay weld and measurements of the chemical composition of the overlay weld surface. The base material content in the two overlay (one and two-layer) welds amounted to 5.67 and 3.28 %, respectively. It was possible to obtain a very shallow penetration depth (below 0.3 mm), which, in turn, enabled the obtainment of a very low stirring degree. The analysis of the chemical composition of the overlay weld revealed that the iron content amounted to 3.47 and 2.75wt. %, i.e. considerably below the required criterion. The changes in the base material content in the overlay weld and the corresponding changes in the iron content on the overlay weld surface in relation to surfacing process conditions and parameters are presented below in Figure 8.

The hardness tests revealed that the hardness in the overlay weld metal amounted to approximately 274–336 *HV*10, where the highest value was obtained in the overlay welds made using the forced cooling of the tube (310–336 *HV*10). Such a high value could be attributed to the fast cooling of the overlay weld metal as well as the related deformation of the tube resulting in its (strain) hardening. Depending on an overlay weld subjected to a test, the HAZ hardness amounted to approximately 329–394 *HV*10, where the highest value was obtained in the overlay welds made using the forced cooling of the tube and was restricted within the range of 379–394 *HV*10, i.e. on the boundary of the allowed hardness amounting to 380 *HV*10 according to the requirements of EN ISO 15614-7 specifying the conditions of welding procedure qualification. The above-named increased hardness in the HAZ can be ascribed to the accelerated cooling of the area.

The microscopic metallographic tests revealed that the base material of the tube made of steel 13CrMo4 was the ferritic-pearlitic structure, typical of the aforesaid steel grade. In turn, in the heat affected zone adjacent to the fusion line, the intense thermal cycle accompanying the process of surfacing delayed the martensitic transformation. The structure of the above-named area was composed of martensite and bainite, responsible for the significant increase in hardness. The overlay weld microstructure in the fusion line contained a layer of entirely different colour than that of the remaining overlay weld area. The composition of the above-named area was identified in further tests involving the use of electron microscopy. In turn, the overlay weld consisted of the dendritic austenitic structure, typical of alloy Inconel 625, building up orthogonally towards the surface of the material subjected to surfacing.

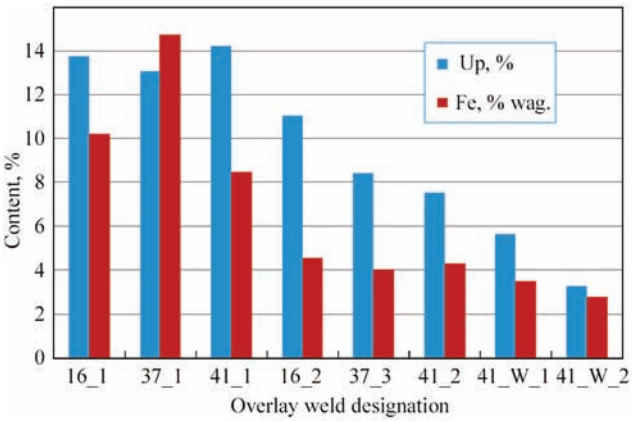

Figure 8. Base material content in the overlay welds (Up) and the iron content (Fe) on the overlay weld surface

The tests performed using electron microscopy revealed that the differently coloured layer (i.e. differing from the colour of the overlay weld metal) observed in the fusion line using the metallographic tests contained 17 % Cr, 23 % Fe, 52 % Ni, 1.5 % Nb and 5.5 % Mo. The analysis of the chemical composition of the overlay weld surface revealed the following contents of chemical elements: 63.64 % Ni, 21.09 % Cr, 8.25 % Mo, 3.44 % Nb and 2.75 % Fe. As can be seen, the key criterion requiring that the iron content on the overlay weld surface be below 5% was satisfied again. The analysis of the chemical composition of the overlay weld at the half of its thickness revealed that the contents of the primary chemical elements amounted to 60.4 % Ni, 21.4 % Cr, 6.6 % Mo, 3.0 % Nb and 8.2 % Fe and changed towards the base material to reach 39.9 % Ni, 13.2 % Cr, 4.1 % Mo, 1.6 % Nb and approximately 40.9 % Fe in the fusion line.

Conclusions

1. The TOPTIG technology enables the making of overlay welds characterised by very high quality and the minimum dilution of the overlay metal with the base material (at least 3.28 %) as well as the obtainment of the iron content on the overlay weld surface amounting to 2.75 % (if the forced cooling of the base material is used). Surfacing without cooling leads to a significantly higher base material content in the overlay weld (approximately 14 %), where the metal content on the overlay weld surface amounts to 8.47 %.

2. Single-sided surfacing without forced cooling does not enable the making of an overlay weld using

alloy Inconel 625, characterised by an iron content of below 5 % on the overlay weld surface.

3. Single-sided surfacing with forced cooling favours the formation of the martensitic structure in the HAZ area and the obtainment of high hardness (>380HV) values because of the cooling (inside the tube) involving the use of flowing water. However, the above-named technological aspect is necessary to satisfy the criterion of the maximum iron content on the overlay weld surface amounting to 5 %.

1. Rozmus-Górnikowska M. (2014) Badania mikrostruktury i mikrosegregacji składu chemicznego warstw ze stopu Inconel 625 napawanych techniką CMT na podłoże ze stali $16Mo_3$. *Przegląd Spawalnictwa*., **12**, 4–8.
2. Rutzinger B. (2012) Kierunki rozwoju w przemyśle energetycznym. Zastosowanie napawania metodą CMT w elektrowniach węglowych. *Biuletyn Instytutu Spawalnictwa*, **5**, 63–66.
3. Rutzinger B. (2014) Wpływ procesu napawania na stopień wymieszania napoiny wykonanej spoiwem ERNiCrMo-3 (stop typu 625) na podłożu ze stali niestopowej. *Ibid*., **5**, 72–74.
4. Adamiec P., Adamiec J. (2006) Aspekty napawania stopami Inconel 625 i 686 elementów w kotłach do spalania odpadów. *Przegląd Spawalnictwa*, **5/6**, 11–14.
5. Nowacki J., Wypych A. (2010) Mikrostruktura i odporność na wysokotemperaturowe utlenianie napoin nadstopu Inconel 625 na stali niskostopowej. *Biuletyn Instytutu Spawalnictwa*, **5**, 84–87.
6. Jarosiński J., Błaszczyk M., Tasak E. (2007) Napawanie stali stosowanych w energetyce stopami na osnowie niklu. *Przegląd Spawalnictwa*, **1**, 30–33.
7. Jarosiński J., Błaszczyk M. (2006) Napawanie stali stoso-wanych w energetyce stopami na osnowie niklu. Problem praktycznego pomiaru zawartości żelaza. *Spajanie*, **2**, 18–23.
8. Abioye T.E., McCartney D.G., Clare A.T. (2015) Laser cladding of Inconel 625 wire for corrosion protection. *Journal of Materials Processing Technology*, **217**, 232–240.
9. Abioye T.E., Folkes J., Clare A.T. (2013) A parametric study of Inconel 625 wire laser deposition. *J. Mater. Proc.Technology*, **213**, 2145–2151.
10. Pfeifer T., Winiowski A. (2014) Badania procesu napawania i spawania plazmowego oraz badanie procesów dyfuzyjnego lutowania i lutospawania połączeń różnoimiennych metali lekkich. *Praca badawcza Instytutu Spawalnictwa* no. Cf-93 (ST-333).
11. Pfeifer T. (2015) Opracowanie technologii napawania plazmowego proszkiem o składzie stopu Inconel 625. *Praca badawcza Instytutu Spawalnictwa* no. Cf-94.
12. Gladky, P.V., Pereplyotchikov, E.F., Ryabtsev, I.A. (2007) *Plasma surfacing*. Kiev: Ekotekhnologiya.
13. Ryabtsev, I.A., Senchenkov, I.K., Turyk, E.V. (2015) *Surfacing. Materials, technologies, mathematical modeling*. Gliwice, Poland: SPI.

Received 14.04.2017

doi.org/10.15407/tpwj2017.05–06.09

TECHNOLOGY OF ROBOTIC TIG WELDING OF STRUCTURE ELEMENTS OF STAINLESS STEELS

L.M. LOBANOV, E.V. SHAPOVALOV, P.V. GONCHAROV, V.V. DOLINENKO, A.N. TIMOSHENKO and **T.G. SKUBA**
E.O. Paton Electric Welding Institute, NASU
11 Kazimir Malevich Str., 03680, Kiev, Ukraine. E-mail: office@paton.kiev.ua

An approach was proposed to create the technology for TIG welding of structure elements of complex geometric shapes of stainless steel using a adaptive robotic system, which allows adapting to changes in the surface shape of workpieces during welding process and minimizing the probability of arising the defected welded joints and temper colors on the workpiece surface. The technology of robotic non-consumable electrode welding of fillet joint of thin-sheet structure elements of stainless steel of AiSi 304, 210, 430 grades with a thickness of joined sheets from 0.8 to 1.5 mm was developed. The results of welding experiments showed that the developed algorithms of interaction between technical means of adaptation can be used in automatic control systems for TIG welding process. 5 Ref., 2 Tables, 10 Figures.

Keywords: *TIG welding, stainless steel, complex geometric shape, adaptive robotic system, fillet joints, thin-sheet structure*

In this article an approach was proposed to create a technology for TIG welding of structure elements of complex geometric shape of stainless steel using a robotic adaptive system which allows adapting to changes in the shape of the surface of workpieces during welding and minimizing the probability of arising the defected welded joints and temper colors on the workpiece surface.

It is known that in order to provide a quality welded joint with the required geometric characteristics of the weld, it is necessary [1–3]:

- to provide constant height of the arc;
- to control the inclination of welding torch relative to the workpiece (angle of inclination) and position of welding torch when passing fillets and roundings;
- to provide constant welding parameters during welding process or their changes in case of specifying such requirements.

A promising direction for maintaining the abovementioned technological requirements is the use of adaptive robotic system. Such a system should provide scanning of welded butt, its state of assembly and should have a connection with the welding current source allowing the correction of welding mode at certain locations of the welded butt. This can be both adjustment of welding current, as well as the use of special welding modes (for example, pulse current), the ability of feeding the filler wire. Definitely, the adaptive robotic system can both realize a complicated algorithm for changing technological parameters of welding, as well as perform monitoring of trajectory of movements and position of welding torch.

The adaptive robotic system should include two subsystems: geometric adaptation and technological adaptation. The writing of the robot control program for realizing the problem of geometric adaptation consists of several stages:

- presetting the coordinate system of the tool «tool frame»;
- presetting the user's coordinate system (desktop) «user frame»;
- planning the trajectory of moving a welding torch along the joint of parts being welded;
- presetting welding mode parameters for different thicknesses of stainless steel plates being welded.

By default, the coordinate system of the tool is attached to the center of the flange on the last link of the robot (Figure 1). This position is called «tool center point» (TCP). To perform welding process, it is necessary to change the position of TCP in accordance with the configuration of a real model of the torch. TCP of welding torch for MIG welding is the tip of welding wire; for TIG welding it is the tip of tungsten electrode.

To preset the coordinate system of the tool, the method by 6 points is used. This method is based on the use of additional device in the form of a needle, fixed, for example, on the desktop. In the process of identification the operator moves the torch at different

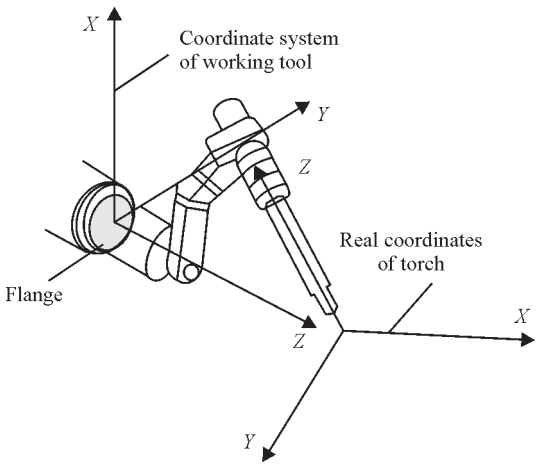

Figure 1. Coordinate system of working tool (welding torch)

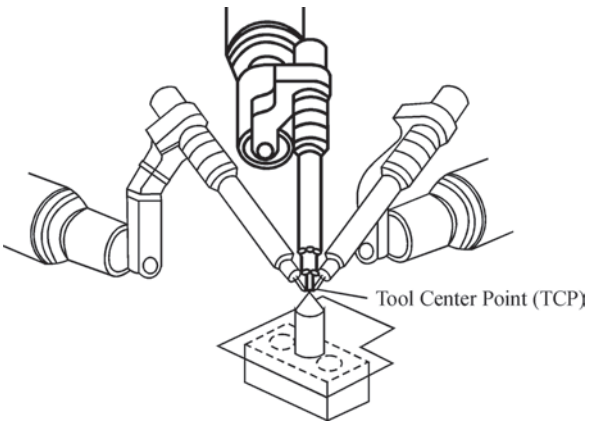

Figure 2. Orientation of torch in the process of identification of tool coordinate system

angles (Figure 2) to the tip of the needle and sequentially stores three configurations of the robot. Further, he moves the robot to the tip of the needle at such orientation of the torch, that its axis coincides with the axis of the needle and stores the 4th point. He moves it along the coordinate «*X*» and «*Z*» or «*Y*» and «*Z*» and stores the 5th and 6th points. As a result of subsequent calculations, we obtain the position of the electrode end and its orientation in 3D space.

We will perform all the measurements in the user's coordinate system. This means that the coordinates of the node points of welding trajectory will be counted down relative to the starting point of the desktop indicated during identification of the «user frame».

The planning of trajectory is performed either in the 3D-modeling package, or with the help of the «Teach Pendant» operator. The operator successively leads the welding torch to the welding start point, the intermediate points of the joint parts being welded, the welding end and stores the coordinates of these points in the robot program control code. In addition to the coordinates of the points of welding trajectory, additional information about the orientation of torch and configuration of the robot at each node point of the trajectory is stored.

The planned trajectory can be used without changes for a batch of products of one modification. However, at the end of welding process, the removal of workpiece from the rigging and fixing of a new workpiece, its position may change. To compensate the spatial position of the workpiece before starting the welding cycle it is necessary to perform the procedure of automatic search for a workpiece. Such procedure can be performed using touch sensor. Thus, for example, in the Fanuc Corporation this function is called «ARC START HEIGHT ADJUST». The algorithm of this function operation is shown in Figure 3.

After making the robot control program (planning of trajectory) and presetting the parameters of welding mode, the welding cycle can be started. However, the non-consumable electrode welding along a rigid trajectory without any means of adaptation during welding process does not guarantee the required weld quality. The disturbing factors are the errors in manufacture of rigging, which lead to changes in the butt position after performing the operation of changing the workpiece. Also the butt position can change during welding under the effect of thermal deformation.

To provide the required quality of welding, the additional sensors are applied, which adapt the trajectory of the robot to the butt trajectory (weld). One of

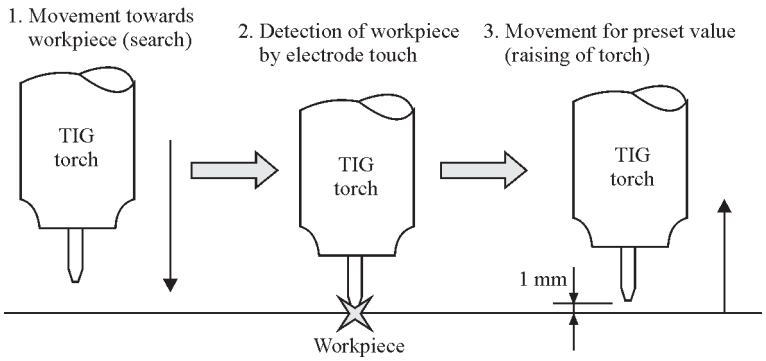

Figure 3. Algorithm of operation of function for torch correction in height

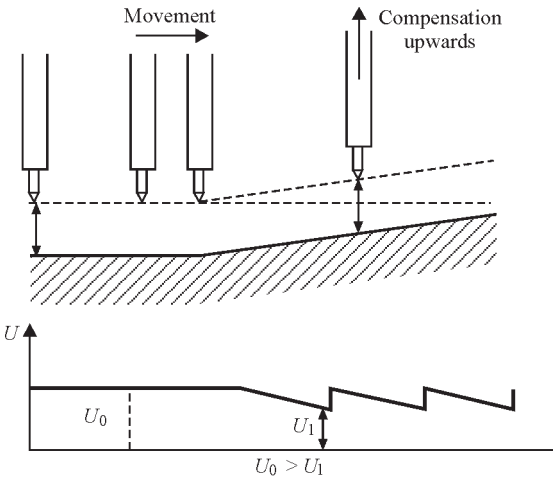

Figure 4. Method of automatic arc voltage control

such sensors, applied in the process of welding experiments, is the arc sensor and method «Automatic Voltage Control» (AVC) (Figure 4) to provide the constancy of power parameters of the welding mode.

AVC can be subjected to the effect of the following disturbing factors:

- change in type of electrode or its diameter;
- change in position of electrode relatively to weld pool as the result of action of welding thermal deformations;
- change in composition of shielding gas;
- change in parameters of oscillations (frequency, stop time in assemblies);
- surface condition of the products being welded.

AVC allows tracking the weld by monitoring the voltage. A typical application of AVC is the vertical tracking with the aim of stabilizing the arc voltage U_a by control the height of torch movement Z from the weld pool surface ($U_a = f(Z)$). The information, obtained with the help of AVC, allows correcting trajectory of the robot in accordance with the position of a real weld. If a weld is lowered relatively to the nozzle, then the arc voltage increases and the welding torch should be lowered. Otherwise, if a weld rises

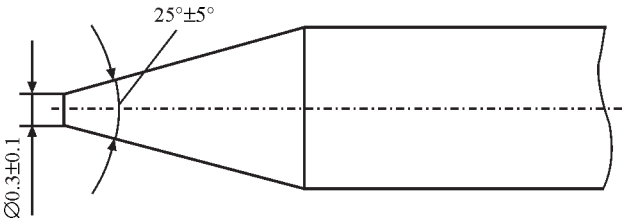

Figure 5. Shape of tungsten electrode sharpening

relatively to the nozzle, the arc voltage decreases and it is necessary to raise the welding torch.

As a result, the preset value of arc length is maintained and, thus, the width of a weld is constant.

AVC can be used for welding with oscillations across the weld. In this case, adaptation to the position of a butt in the horizontal plane is realized. If it is necessary to apply oscillations, then their shape should be sinusoidal (SINE). AVC can be applied for moving welding torch both along the linear as well as circular trajectory.

The welding of products from stainless steel sheets of small thickness (up to 1.2 mm) is accompanied by several factors which significantly affect the weld quality and its appearance. Such factors are welding thermal deformations and formation of oxide film on the surface of structure being welded. The first factor leads to arising of defects in the form of burn-outs or lacks of penetration of a weld. The second factor leads to arising of temper colors on the metal surface. The oxide film deteriorates the appearance of the product and is also considered to be a rejection.

In this work AVC is used for the robotic process of TIG welding of structure elements of complex geometric shape. The structure of a product implies producing a fillet joint, the thickness of the joined elements of stainless steel AiSi 304, 210, 430 is 0.8–1.5 mm. To produce this type of joint with obtaining the required characteristics of weld, the TIG welding was performed using pulsed current by setting «+» on the electrode (reverse polarity) without filler wire.

Table 1. Welded fillet joint U4 according to GOST 14771–76

Structural elements		s	b		n	e		g	
of prepared edges of parts being welded	of joint weld		Nominal	Limited deviation		Nominal	Limited deviation	Nominal	Limited deviation
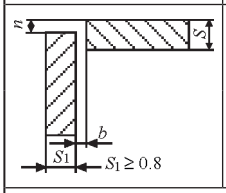	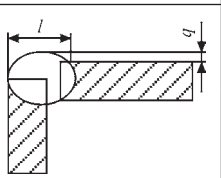	0.8–1.4	0	+0.5	0–0.5	3	±1	0	+1
		1.5–2.0				5			

Note. Conditional symbol of welded joint — U4, welding method — pulsed heating.

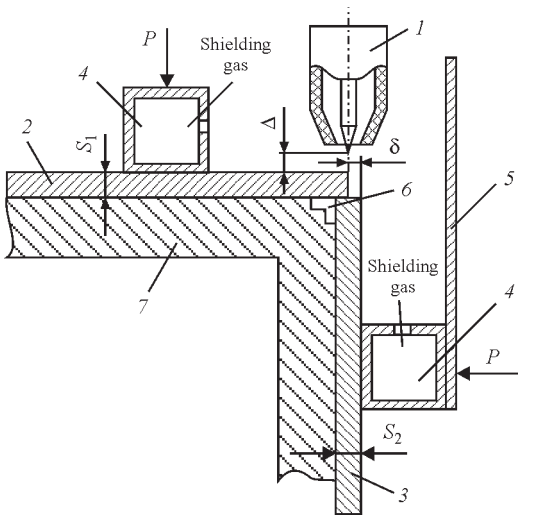

Figure 6. Scheme of assembly of structure elements before welding of fillet joint: *1* — welding torch; *2*, *3* — semi-products being welded; *4* — gas channel, for protection of outer side of the workpiece; *5* — protective screen; *6* — gas channel, for protect of back side of the workpiece weld; *7* — force part of rigging

As a non-consumable electrode, the tungsten electrodes of grade EVT-15, EVL-20 (GOST 23949) of 2.4 and 3.2 mm diameter were applied. To improve the stability of arc burning, the electrode was sharpened to a cone. The sharpening shape is presented in Figure 5. It is recommended to perform sharpening of tungsten electrodes using the specialized machine-tools.

As a shielding gas, argon of the highest grade was applied in accordance with GOST 10157 or its mixture with hydrogen: Ar + 2.5 % H, Ar + 5 % H.

Preheating and post-weld heat treatment are generally not required.

Applying this technology, the welding of fillet joint of the brake hammer of commercial equipment is performed. The geometric characteristics of the fillet joint U4 according to GOST 14771–76 are given in Table 1.

For automatic argon arc non-consumable electrode welding, the edges for welding are prepared mechanically, also using the specialized machine-tools for edge preparation. The angle of edges preparation is 90 ± 1°. In welding the joints of different thicknesses, the edge preparation for joined elements does not change, which is related to the thicknesses of semi-products being welded (0.8–1.5 mm).

Figure 7. Welded specimen of fillet joint without temper colors after argon arc welding in automatic mode

Before welding, the preparation of semi-products was performed: the burrs at the edges were eliminated by grinding. The mechanical treatment was carried out in a way to eliminate the arising of cavities on the edge of a semi-product being more than 30 % of its thickness. Also, before welding the metal surface was degreased with alcohol, acetone, aviation gasoline, white spirit or other solvents at a distance of at least 40 mm from the edges, to be welded.

The assembly of structure elements in the assembly and welding rigging was carried out in accordance with Figure 6. The superposition of the upper sheet *2* on the lower one *3* is carried out with overlapping the half of the thickness δ of second one. The fulfillment of this condition is necessary to produce a uniform weld as to its overlapping. It is also necessary to provide pressing of the workpieces to the assembly and welding rigging at the force which enables removing the gaps between sheets of semi-products and the assembly rigging (the value of pressing force is within the range P = 300–500 N, depending on thicknesses of metal being welded). To provide a tight abutment of semi-products to the rigging and to ensure the necessary heat removal, the pressing was performed by a uniform distribution of the force along the plane of clamping straps.

In case when it is impossible to provide the accuracy of fixing the semi-products, according to the scheme for making fillet joint the assembly of a workpiece should be performed by tacks using manual argon arc welding from the back side of fillet joint without a full penetration. Such arrangement of tacks will provide welding in automatic mode without disturbances of the process during welding arc passing through them.

The trajectory of movement of welding torch should be such that the tip of tungsten electrode was at the end of the edge of upper sheet, as is shown in Figure 6. The value of the arc gap between electrode and workpiece is set and maintained in the process of welding as equal to 1.5 mm applying AVC technology for all the types of materials and thicknesses being welded.

To produce welded joint without temper colors (Figure 7), the protection of welding zone and a part of the workpiece heated to the temperature of 200 °C, are provided. For this purpose zonal protection is per-

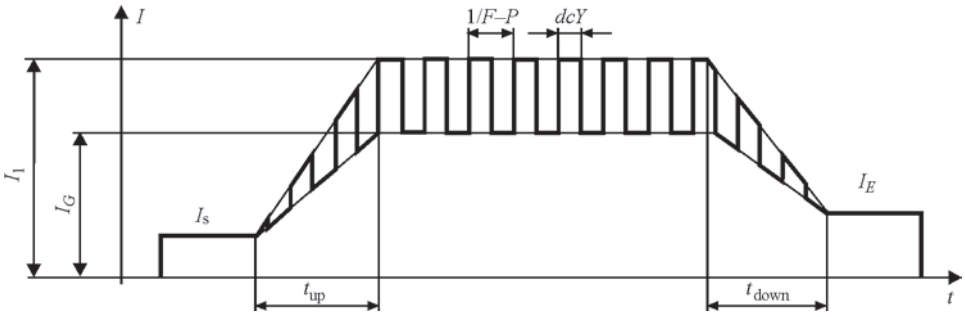

Figure 8. Cyclogram of pulsed welding current in TIG welding: TIG: I_s — starting current; I_e — end welding current; t_{up} — current increment; t_{down} — current drop; *F–P* pulse frequency (1/*F–P* — time interval between two pulses); *dcY* — working cycle; I_G — base current; I_1 — main current

formed, the shielding gas is supplied to the welding zone and to the area heated to 200 °C. Also, to protect the back side of the weld, the gas is supplied into the groove of rigging *6*, shown in Figure 7. The gas consumption is set in a flow meter in the amount, providing 6–8 l/min for protection of the back side of the weld, and 10–12 l/min for the outer side of the weld.

The use of pulsed arc makes it possible to expand the capabilities of welding by non-consumable electrode [1, 3–5]. Thus, the speed and quantity of heat introduced into the workpiece, are determined by the mode of arc pulsation, which, in its turn, is preset according to a certain program, depending on the properties of material being welded, its thickness, spatial position of the weld and so on. During welding by non-consumable electrode, the pulsed arc is intended for regulation of the process of base metal penetration and weld formation, while during welding by consumable electrode it is intended for regulation of the process of melting and electrode metal transfer [1, 3].

In this work, the welding was performed with pulsed arc at the frequency F = 1 kHz, the pulse and pause duration was 50 % of the total period. The main current was 10 % of the basic preset current. The duration of increment and drop of welding current t_{up}, t_{down} = 1.5 s. The cyclogram of pulsed welding current is shown in Figure 8.

The beginning and the end of automatic argon arc welding of fillet joint is performed on the run-in and run-out tabs to produce a defect-free welded joint on the main workpiece. The dimensions of run-in and run-out tabs should correspond to the duration of output for welding mode. The length of run-in and run-out tab is 30–40 mm.

The welding speed is preset in the control module of the robotic complex and should be 36 m/h (1 mm/s) for metal thicknesses being welded. Figure 9 shows the scheme of conducting the automatic welding of fillet joint. During welding process the welding torch should not deviate from the preset trajectory by more than ±0.2 mm.

Table 2. Modes of automatic argon arc welding of fillet joint of thin-sheet stainless steel

Thickness of semi-products to be joined S_1 + S_2, mm	Welding current I_w, A	Voltage U_a, V
0.8 + 0.8	100	9.0
0.8 + 1.0	105	9.2
0.8 + 1.2	115	9.5

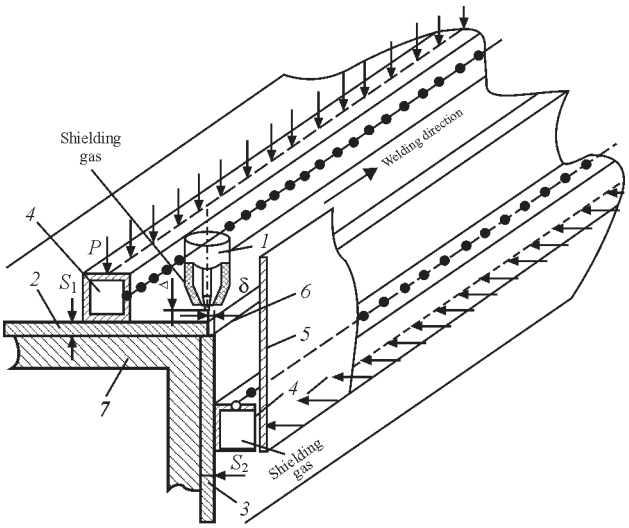

Figure 9. Scheme of moving welding torch along the butt: *1* — welding torch; *2*, *3* — semi-products to be welded; *4* — gas channel for protection of the outer side of the workpiece; *5* — protective screen; *6* — gas channel for protection of the back side of the workpiece weld; *7* — force part of rigging

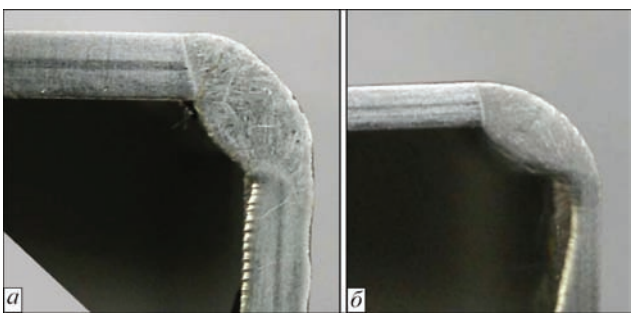

Figure 10. Macrostructure of fillet welded joint of stainless steel AiSi 304 of 1.2 mm thickness (*a*) and AiSi 201 of 0.8 mm thickness (*b*)

To reproduce the quality of welded joints, the robotic argon arc welding by non-consumable electrode should be performed in a premise with a controlled shop temperature. The given welding conditions (Table 2) were obtained at a room temperature of 18–22 °C. If there is a temperature difference by more than ±15 °C in the premice where the welding takes place, it is necessary to carry out correction of welding mode parameters.

In order to study the influence of technological welding modes on the structure of weld metal, a macro analysis of welded joint was carried out. The metallographic analysis of fillet welded joint of stainless steel AiSi 304, 210, 430 made on the basis of the developed technology of pulsed arc welding by non-consumable electrode with a full penetration, revealed certain features. As is shown in Figure 10, the weld has a solid cast structure with a smooth transition from horizontal plate to the vertical one without overlaps and also there are no visible defects such as pores, cracks or violation of weld integrity. Such results on the geometry of the weld allow concluding that the developed technology of robotic TIG welding of stainless steels of 0.8–1.5 mm thickness can be used in manufacture of workpieces made of stainless steel providing the quality weld with the required strength characteristics, appearance and color, similar to the color of base metal.

The results of welding experiments showed that the developed algorithms of interaction between technical means of adaptation can be used in the systems of automatic control for TIG welding process.

1. Savinov, A.V., Lapin, I.E., Lysak, V.I. (2011) *Non-consumable electrode arc welding*. Moscow: Mashinostroenie.
2. (2013) *FANUC robotics SYSTEM R-30iB arc tool setup and operations manual*. Doc. ID: MAROBAR8203131E, Rev. A., Version 8.20 series. FANUC Robotics America Corp.
3. Slivinsky, A.A., Zhdanov, L.A., Korotenko, V.V. (2015) Thermal-physical peculiarities of gas-shielded pulse-arc welding using non-consumable electrode (Review). *The Paton Welding J.*, **11**, 24–30.
4. Timoshenko, A.N., Gvozdetsky, V.S., Lozovsky, V.P. (1978) Energy concentration on arc anode of non-consumable electrode. *Avtomatich. Svarka*, **5**, 68–70.
5. Dudko, D.A., Shnajder, B.I., Pogrebitsky, D.M. (1977) Admissible gaps in pulse-arc welding of edge joints of small thickness metal. *Svarochn. Proizvodstvo*, **5**, 27–31.

Received 24.04.2017

doi.org/10.15407/tpwj2017.05–06.10

ROBOTIC SYSTEM OF NON-DESTRUCTIVE EDDY-CURRENT TESTING OF COMPLEX GEOMETRY PRODUCTS

V.V. DOLINENKO[1], **E.V. SHAPOVALOV**[1], **T.G. SKUBA**[1], **V.A. KOLYADA**[1], **Yu.V. KUTS**[2], **R.M. GALAGAN**[2] and **V.V. KARPINSKY**[2]
[1]E.O. Paton Electric Welding Institute, NASU
11 Kazimir Malevich Str., 03680, Kiev, Ukraine. E-mail: office@paton.kiev.ua
[2]NTUU «Igor Sikorsky Kiev Polytechnic Institute»
37 Peremogy Av., 03056, Kiev, Ukraine

An analysis was carried out for relevant state of development of automated and automatic systems of eddy-current non-destructive testing of complex geometry products. The necessity is shown in development of adaptive robotic systems, in which an operator is not directly engaged in testing process. The substantiation is given for the need of implementation of new efficient methodology of eddy-current signals processing. It uses a theory of discrete Hilbert transform in combination with the methods of theory of signals statistical manipulation. A structural scheme was proposed for a robotic automatic control complex consisting of industrial robot-manipulator, coordinate table with several degrees of freedom and device for tested object fixing, automatic station with a set of eddy-current converters of different types, block of machine vision probes, PC and electron block for control and processing of eddy-current signals. 12 Ref., 7 Figures.

Keywords: *automatic non-destructive eddy-current testing, adaptive robotic complex, machine vision probe, amplitude and phase characteristic of eddy-current signal*

Problem relevance. Operations of product quality control, which are based on application of non-destructive testing methods (NDT) [1, 2], take a relevant place in a structure of advanced productions at their different stages. Improvement of competitiveness and reliability of products to the most extent depend on rate of implementation of new structural materials and components, progressive technological processes, the latest achievements in fundamental and applied sciences. Under such conditions the developers of new products in their work should base on innovative methods and means of quality control, oriented on perspective materials with improved characteristics and parameters. Such means should accumulate the latest achievements from different branches of knowledges, i.e. physics, mathematics, engineering, electronics, computer engineering etc. This to the full refers to eddy-current testing (ECT), which is extremely informative and at the same time sufficiently complex from point of view of getting useful information and outlining diagnostic characteristics, particularly when this is a product of complex geometry.

Regardless implementation of modern design solutions, achievements of computer and information-measurement technologies, the considerable part of testing means is directed on «manual» scanning of tested object (TO) surface. Presence of human factor results in increase of subjectivity of testing, decrease the probability for correct diagnostic decision making. Therefore, practice shows that the manual method does not guarantee high testing quality even with available sophisticated testing procedures. Presence of a human-operator in technological testing chain significantly increase probability of acquiring wrong decisions that does not allow realizing high potential capabilities of NDT means in full scope.

Thus, increase of productivity and reliability of results of ECT of complex geometry products requires development of automatic testing systems, which obviously will use new approaches to testing procedure as well as mathematical support of flaw detector. Basic conditions for this are the next ECT peculiarities, namely need in absence of mechanical contact between TO and eddy-current probe (ECP); application of small size ECP designs; stability of ECP characteristics in operating temperature range as well as in time. One of the most perspective directions for realizing automatic ECT is development of robotic non-destructive testing systems.

Analysis of available solutions and problem statement. One of the main disturbances, which can significantly affects the results of automatic ECT is change of vision gap between the converter and TO. In the case of robotic testing such a gap is determined by:

- roughness of TO surface;
- accuracy of movement of eddy-current probe (ECP) on set trajectory;

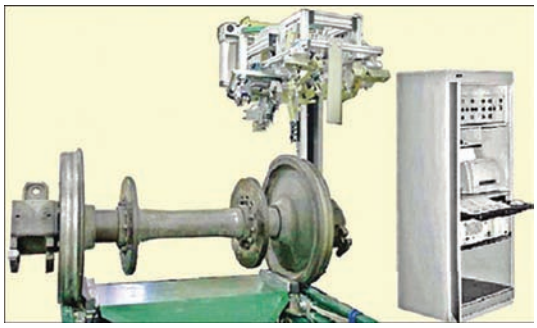

Figure 1. Automated module of ECT system for wheel pairs of railway cars PELENG-AUTOMAT

Figure 2. Mechanized system of ECT of pipes

● accuracy of approximation of computer geometry model of TO;

● accuracy of machine vision means (laser-triangulation video sensor) that is used at stage of adaptation to specific TO specimen [3].

Previous calculations show that uncontrolled change of a gap value in process of robotic eddy-current testing of large TO can reach ±0.5 mm. This disturbance can be significantly reduced in application of ECP with special spring-mounted fixture that provides tightness of ECP with TO surface, but increases testing time. Application of ECP with regular fixture, compensation of disturbance due to change of the gap value shall be performed by special mathematic module of robotic ECT system.

Mechanized and semi-automatic systems, that during some time fulfilled the industrial needs, preceeded the development of automatic NDT systems. Not very complex linear manipulators providing sufficient positioning accuracy [4] were used in such systems. For example, NDT of wheel pairs of cars used the automatic complex «PELENG-AUTOMAT» («ALTEC» Company, Russia). It consists of ECT module for the whole wheel surface and brake disk (Figure 1). Figure 2 shows mechanized ECT system for average diameter pipes (from 1.75 to 38´´) based on ChainXY-scanner from «Olympus» Company. Application of such a system is limited by testing of simple shape parts (plates, pipes etc.).

Testing systems with anthropomorphic robot-manipulators that have six and more degrees of freedom [5–7] are more flexible and productive. Such systems are used in the places which require high productivity or performance of testing of complex geometry products.

Robotic NDT systems can be conventionally divided on two classes, namely adaptive and non-adaptive. The non-adaptive systems are used for NDT of parts and products with not complex geometry. The main criterion of quality functioning of such systems is their productivity. These systems are mainly designed for testing of small parts with insignificant surface roughness. As an example of systems of such type Figure 3, *a* shows ECT robotic system «EloScan-system» for non-destructive testing. It is mainly designed for checking the symmetric rotation components in aircraft construction. Accuracy of TO posi-

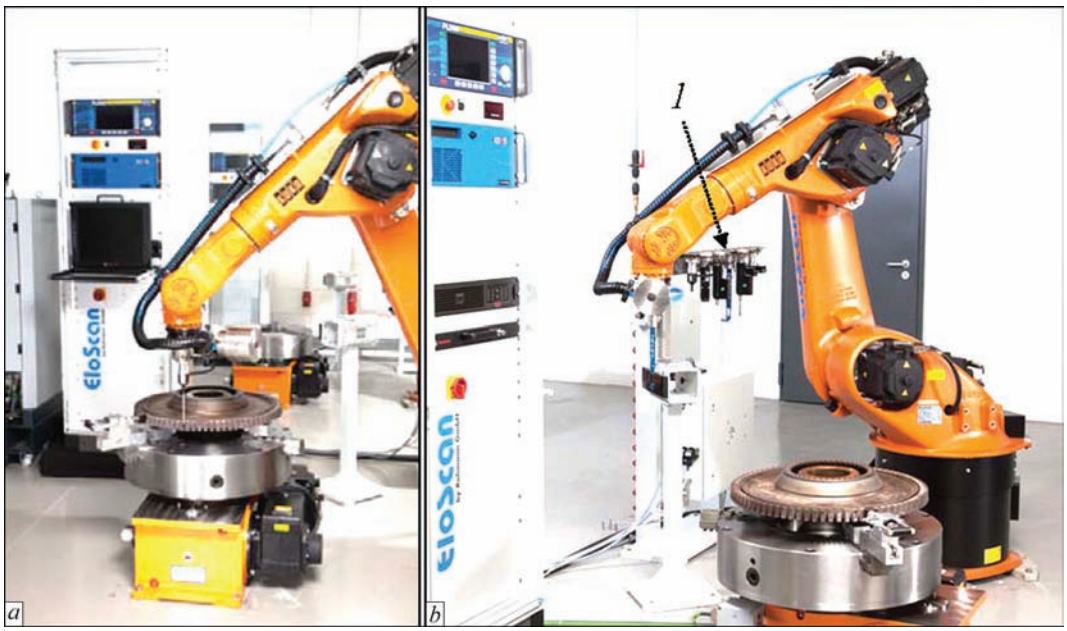

Figure 3. System of robotic ECT of complex-geometry parts «EloScan-system»: *a* — test process; *b* — process of probe adjustment (*1* — station for probe servicing)

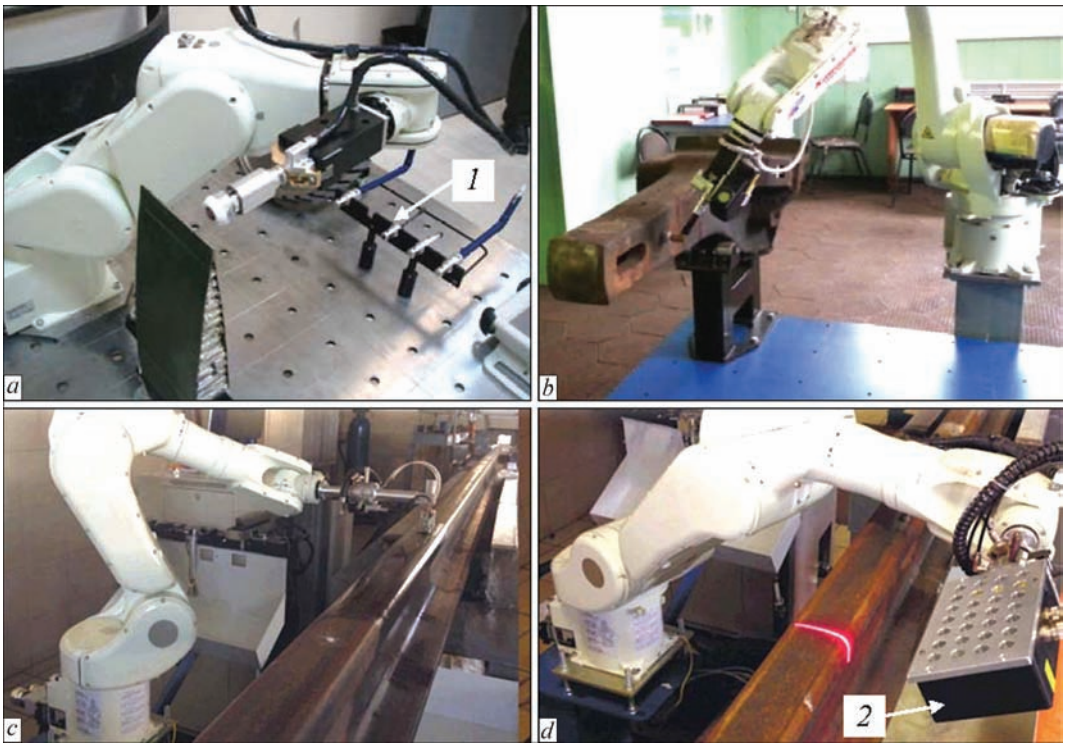

Figure 4. NTD system of «Roboskop VTM-3000» type for ECT: *a* — elements of plane wing; *b* — railway towing device; *c* — railway track; *d* — rail geometry (*1* — station for probe servicing; *2* — laser-TV video sensor)

tioning is provided by high manufacturing accuracy of the part being tested as well as application of special product manipulator of «lathe chuck» type. The system has a service station for probes (Figure 3, *b*) that allows quick replacement and effective readjustment of the probes during ECT for testing of the products with different geometry depending on task and type of test zone surface.

Adaptive robotic systems are used in the cases when it is necessary to carry out NDT of large parts and products with complex geometry. The main criterion of functional quality of such systems is a high level of possibility of defect detection at a determined level of testing productivity. This system can include laser-TV video sensor, productive work of which is provided by scattered reflection of laser light from surfaces being tested. The representatives of systems of this class are the robotic non-destructive ECT complexes of «Roboskop VTM-3000» type («WorldNDT» Company, Russia) [8] that are presented in Figure 4.

These systems consist of two anthropomorphic robots, laser-TV video sensor and station of eddy-current probes servicing. The laser-TV video sensor can be used in a complex with ECT for initial measurement of TO size or adapting to real size of specific TO as well as independently as a tool for determination and testing of product geometry parameters (Figure 4, *d*).

Application of that or another type of video sensor depends on required measurement accuracy as well as TO geometry. Testing of large products with flat surfaces can be carried out using video sensor with larger triangulation angle. A video sensor with smaller triangulation angle has significantly small dimensions, therefore it is reasonable to use if TO geometry includes narrow zones and noticeable deepening.

Efficient functioning of robotic ECT system is related with correct selection of eddy-current converters (ECC) with a specific set of probes, necessary for operational product testing [9]. ECC designs for each type of TO are determined by their designation, conditions of usage, frequency range of actuation current and other factors. Size of ECC coils is limited from the bottom by several millimeters in diameter and ECC mass by tens of grams (without taking into account fixing assemblies and displacement of ECC and interface elements).

Special attention shall be given to ECT devices. Current market is full of devices of different designation, including eddy-current flaw detectors that have high technical characteristics. Under conditions of manual scanning reliability of ECT results to a significant extent depends on preparation, experience and emotional state of flaw detector operator. However, their application in robotic NDT systems is limited by several factors. First of all, known eddy-current flaw detectors from the very beginning are oriented on operator, who makes decisions on visual signal in form of hodograph (Figure 5). Generally, such a hodograph is transferred to peripheral devices that creates certain inconveniencies for application of such signals in the automated systems. Obviously, that application of hodographs is very limited in robotic ECT systems.

Secondly, such devices for developer of NDT robotic systems are like «blackboxes». Process of selection of testing mode, calibration, algorithm of

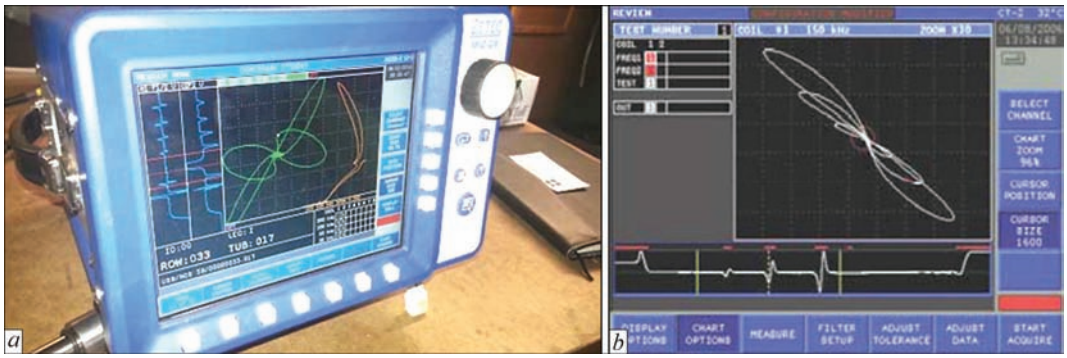

Figure 5. Graphic presentation of results of non-destructive ECT with manual scanning systems: *a* — portable system; *b* — stationary computer system

processing of experimental data is in whole «hidden» from the user that complicates integration of such devices in automation testing systems.

Thirdly, processing of ECC signals is based on analysis of signals' amplitude characteristics. Application of phase methods has auxiliary nature and can be directed, for example, on increase of testing selectivity [9]. At the same time, analysis of phase characteristics of ECC signals, including their statistical processing and determination of circle chart statistics [10] allows outlining additional diagnostics features that creates basics for expansion of functional possibilities of ECT, increase resolution ability of eddy-current flaw detection, implementation of new characteristics in ECT practice.

Thus, task of this work was formulated in the following way based on the results of carried analysis, i.e. it is necessary to substantiate general structure of robotic ECT system of products with complex geometry and propose procedure for ECC signals processing for such a system with the possibility of formation of diagnostic features from amplitude as well as phase characteristics of the signals with wide application of statistical methods of their manipulation.

Proposed technical solution. Based on carried analysis of known technical solutions it can be stated that typical robotic NDT complex shall include robot-manipulator, coordinate table with several degrees of freedom, automated station with a set of converters of different types, TO fixation device, machine vision devices, PC, block of electron control and signal processing.

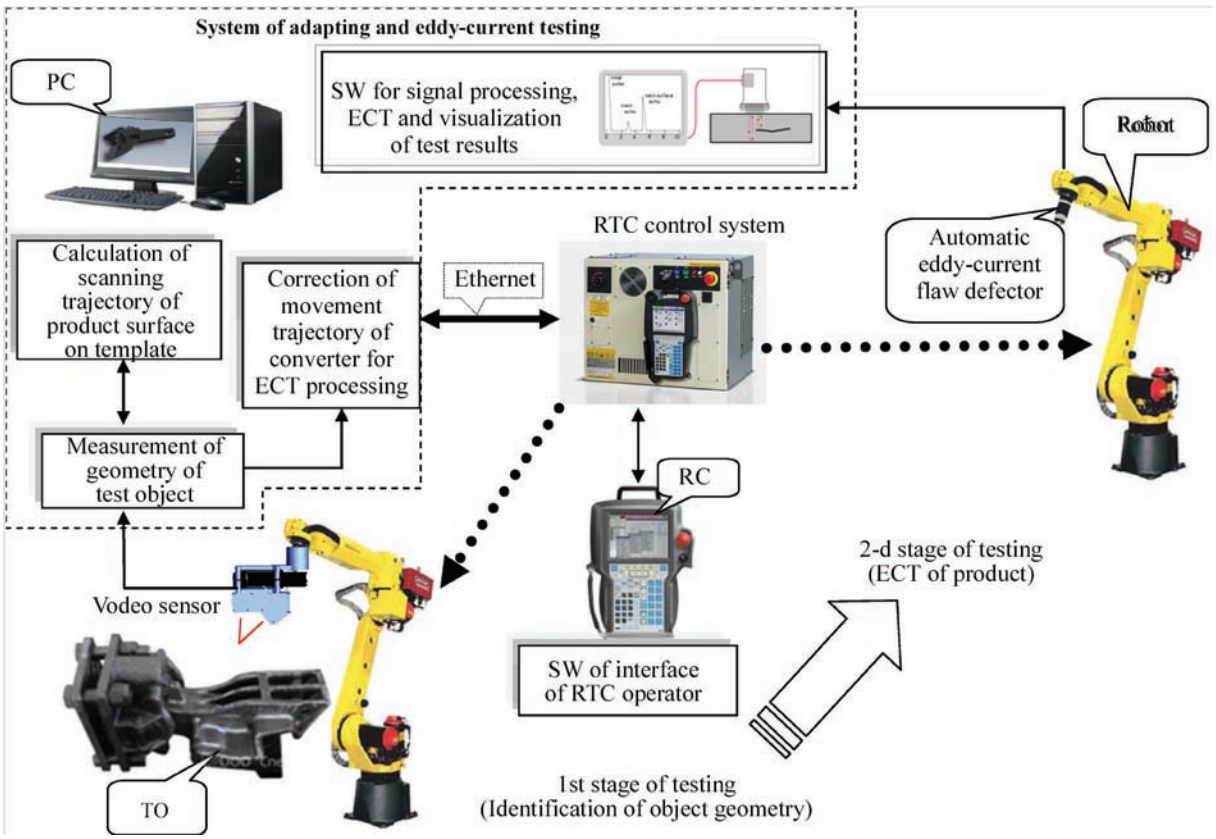

Figure 6. Structural scheme of robotic adaptive system of non-destructive ECT: RC — remote control; SW — software; RTC — robotic technical complex

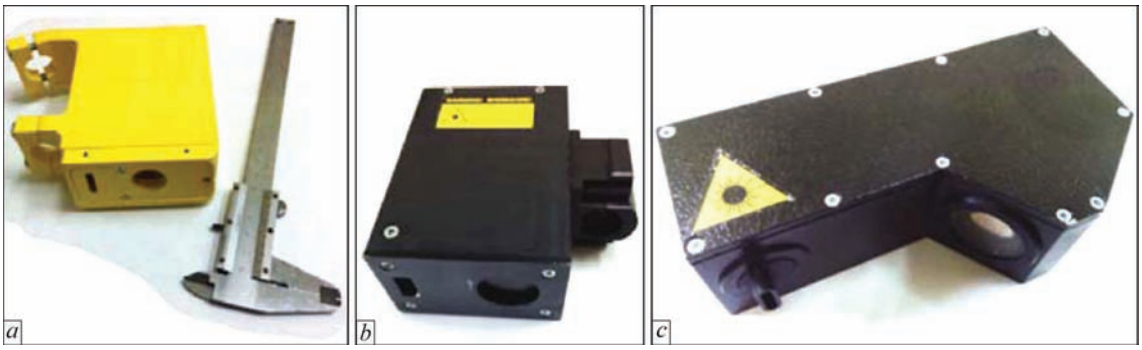

Figure 7. Laser-TV video sensors for robotic NDT systems with triangulation angles: *a* — 15; *b* — 20; c — 40°

The following structure of robotic adaptive ECT system, shown in Figure 6 (scheme does not show ECT service station and module for TO positioning), was proposed on the ground of mentioned above.

The robotic system of non-destructive ECT provides two-stage testing mode. Identification of TO geometry model is carried out at the first stage using laser-TV video sensor, i.e. machine vision probe. Such video sensors are an important element for adapting the robotic systems of non-destructive ECT to different TO. Currently, there are no versatile machine vision probes, therefore, such adapting devices are developed for specific tasks. E.O. Paton Electric Welding Institute has developed a range of models of laser-TV video sensors that can be used for identification of TO geometry in automatic systems. Figure 7 shows a range of such video sensors that differ by dimensions as well as value of triangulation angle.

System adaptability is realized at the expense of:

- algorithm of scanning of TO surface and registration of measurement results, which were gotten using laser-triangulation video sensor;
- algorithm of specification of key parameters of TO geometry model;
- algorithm of calculation of ECC scanning trajectory for product surface on set model;
- algorithm of calculation of amendments for robot control system at all scanning trajectory.

The second phase of testing is particularly directed on performance of ECT of a product. Such a testing is carried out in automatic mode. Operations on calibration, change of ECC type and re-adjustment of ECC operating mode are carried out without operator. Mathware of the PC generates corrections in a system of control of robotic technological complex (RTC) during regulation of robot trajectory. These corrections proceed in real time mode on Ethernet interface channel and result in correction of scanning trajectory that provides maximum sensitivity of ECC and prevents appearance of its collision with TO surface. This stage also includes start of work of mathematical module used for ECC signal processing and visualization. A decision on level of defectiveness of the controlled area of the product is formed based on the results of analysis of determined diagnostic characteristics.

Robotic NDT system stipulates for operator the possibility to perform some actions which are related with operations on installation and removal of TO from product manipulator. A remote control (RC) and special software which realize interactive communication in operator- RTC system are designed for this.

Typical peculiarity of mathematical and program software of the ECT robotic system is realization of paradigm of adaptability and versatility of technological process of testing. It can be reached due to possibility of ECC change for adapting to TO geometry and testing tasks as well as the following special function characteristics:

- determination of the coordinates of TO prepared for testing in 3D coordinate system;
- scanning of TO surface by set program;
- calculation of amplitude characteristic of ECC signal;
- calculation of phase and frequency characteristic of ECC signal;
- statistical processing of characteristics of ECC signals and other data;
- calculation and analysis of spectra of ECC signals;
- software control of parameters of signals for ECC actuation and modes of operation of system measurement channel;
- formation of diagnostic solutions as for determination of TO defectiveness and interactive communication with technologist-inspector based on the results of analysis of ECC signal etc.

Thus, the proposed structure of robotic system of non-destructive ECT allows realizing a paradigm of adaptive non-destructive testing of complex geometry products.

Realization of concept of complete ECT automation requires more general approach to ECT signals processing and formation of fields of informative features related with TO in coordinate system.

Mostly, ECC actuation is carried out using harmonic currents of the following type:

$$i_0(t) = I_0 \cos\left(2\pi f_0 t \pm \varphi_0\right), \quad t \in (-\infty, \infty), \tag{1}$$

where t is the present time; $I_0 > 0$ is the amplitude of actuation signal; $\varphi_0 \in [0, 2\pi)$ is the initial phase; $f_0 > 0$ is the frequency.

An output signal exists in a form of sine voltage that is observed at the background of additive noises $n(t)$. Localizing of the TO inhomogeneities in space during ECC scanning of TO surface in the robotic ECT systems results in time and space local changes (disturbances) of signals' parameters. Therefore, in general case the arguments of ECC signals are not only time t, but also vector of $\bar{p}_r$ parameters of «ECC–TO» system and space Cartesian coordinates $r = \{x, y, z\}$ of points of TO surface:

$$u\left(t, \bar{p}_r, r\right) = U\left(t, \bar{p}_r, r\right) \times \\ \times \cos\left(2\pi f_0 t - \varphi\left(t, \bar{p}_r, r\right)\right) + n(t), \ t \in T_a, \quad (2)$$

where T_a is the full time for analysis of the whole TO.

The first informative component of the signal (2) belongs to class of sine signals with locally concentrated disturbances of informative parameters. Space coordinates are limited by collection of values $\{x_{max} \dots x_{max}, y_{min} \dots y_{max}, z_{min} \dots z_{max}\}$ that are determined by technical characteristics of robot-manipulator. Range of values of vector components of $\bar{p}_r$ parameters is also limited and determined by physical parameters and characteristics of TO material and geometry characteristics of «ECC–TO» system.

Noise component $n(t)$ of the signal (2) is generated due to action of number of factors, i.e. noises of electron components of the system, electromagnetic guidance and mechanical vibrations etc. Usually, $n(t)$ substantiation as realization of Gaussian random process with zero mathematical expectation and σ^2 dispersion is not contradictory.

Signal (2) is non-stationary at all analysis interval. However, the conditions of testing process realizing allow the following simplification. Process of measurement of ECC signal parameters in digital systems takes place discretely in time in a finite collection of space points $r_g = \{x_g, y_g, z_g, g \in [1, G]\}$. Every separate measurement is carried out in T_g, $T < T_g << T_a$ time interval. Such a condition appears due to relatively small scanning rate or even the possibility of measurement after ECC stop in the next point g. Therefore, in specific time interval T_g, the signal $u(t, \bar{p}_g, r_g), \ t \in T_g$ can be assumed as locally stationary, parameters of which, amplitude and initial phase remain constant during T_g. Such the assumption allows significant simplification of ECC signal analysis.

ECC signal processing in modern ECT systems is carried out in digital form that provides discrete time sampling with $T_a << 1/f$ step. Signal discrete analogue is presented as

$$u\left[j, \bar{p}_g, r_g\right] = U\left[j, \bar{p}_g, r_g\right] \times \\ \times \cos\left[2\pi f_0 j - \varphi\left[j, \bar{p}_g, r_g\right]\right] + n[j], \\ g \in [1, G], \ j \in \left[1, \ T_a / T_a\right]. \quad (3)$$

There is a discrete Hilbert transform for model (3). This is a base model for processing of signals in ECT robotic systems.

From point of view of general algorithm processing of ECC signals in robotic testing systems can be conditionally divided on three stages, namely primary (formation and processing of analogue signal), secondary (processing of digital signal and its discrete characteristics) and ternary (visualization of testing results and their statistical processing).

The first step is carried out under traditional scheme [9], which provides formation of ECC actuation signals (1) and control of their parameters, software amplification of ECC signals (2), equalization (if necessary) of unbalance signals, analogue-digital transform of the signals.

The second stage of processing of eddy-current signal is designed for sampling of useful information in relation to defectiveness of controlled surface and formation of diagnostic features.

The general concept of ECC signal processing is based on combination of Hilbert discrete transform [10, 11] and statistical methods for processing of signal characteristics [12]. Application of algorithm of «moving average» with double window is the most efficient for getting evaluations of signal parameters that are continuous in real time.

The first window $W_1[j_k]$ with aperture k provides formation of present sample from sequence (3). Discrete Hilbert-image is calculated for the sample

$$u_H\left[j_k, \bar{p}_g, r_g\right] = \mathbf{H}\left\{u\left[j_k, \bar{p}_g, r_g\right]\right\}, \quad j_k = \overline{j, j+k}, \quad (4)$$

where $\mathbf{H}\{\cdot\}$ is the operator of Hilbert discrete transform.

Sequences (3) are associated to their complex significant analytical version $u\left[j_k, \bar{p}_g, r_g\right] + iu_H\left[j_k, \bar{p}_g, r_g\right]$, where $i = \sqrt{-1}$ for which the following characteristics can be determined:

- discrete amplitude characteristic

$$A\left[j_k, \bar{p}_g, r_g\right] = \sqrt{u^2\left[j_k, \bar{p}_g, r_g\right] + u_H^2\left[j_k, \bar{p}_g, r_g\right]}; \quad (5)$$

- discrete phase characteristic

$$\Phi\left[j_k, \bar{p}_g, r_g\right] = \operatorname{arctg}\frac{u_i\left[j_k, \bar{p}_g, r_g\right]}{u\left[j_k, \bar{p}_g, r_g\right]} + \\ + -\left\{2 - \operatorname{sign}\ u_i\left[j_k, \bar{p}_g, r_g\right]\left(1 + \operatorname{sign}\ u\left[j_k, \bar{p}_g, r_g\right]\right)\right\} + \quad (6) \\ + 2\pi\left[u\left[j_k, \bar{p}_g, r_g\right], u_i\left[j_k, \bar{p}_g, r_g\right]\right],$$

where sign is the sign function; **L** is the operator of development of phase characteristic out of the interval [0, 2π);

● discrete frequency characteristic

$$f[j]=\frac{\Phi\left[j_k,\overline{p}_g,r_g\right]-\Phi\left[j_k-1,\overline{p}_g,r_g\right]}{2\pi T_{\hat{o}}}; \quad (7)$$

● difference of discrete phase characteristics of two sequences, for example $u_1\left[j_k,\overline{p}_g,r_g\right]$ (determined for measuring signal) i and $u_2[i_k]$ (determined for reference signal)

$$\Delta\varphi\left[j_k,\overline{p}_g,r_g\right]=\Phi_1\left[j_k,\overline{p}_g,r_g\right]-\Phi_2\left[j_k\right]. \quad (8)$$

The second window $W_2[j_m]$ with aperture $m << k$ provides sampling of present values of discrete characteristics of signals, in particular, sequence (7) helps to determine new for ECT circular statistical characteristics [11]: circular sampling average, dispersion, length of resulting vector, median, mode etc.

The stage of ternary processing provides documenting and backup of testing results, defects classification, statistical processing of test results of single-series products or their fragments, construction and visualizing of the fields of diagnostic features in connected with TO coordinate system etc.

Discussion of received results. Combination of commercial robot-manipulators with ECT devices in scope of single diagnostic NDT complexes has the following advantages for flaw detection:

● complete automation of ECT process and improvement of its productivity;

● possibility for stabilizing of a gap between TO surface and ECC;

● enhancement of objectivity and probability of testing due to removal of human factor at all stages of testing from ECC signal forming to diagnostic decision making;

● possibility of presentation of testing results on 3D models and obtaining respective flaw patterns (documenting of testing results);

● possibility the binding the testing results to points on product surface in one space coordinate system;

● high accuracy and repeating of ECC positioning;

● possibility of retesting (or testing of different single-type products) in points with constant space coordinates that is necessary, for example, for realizing multiparameter ECT);

● possibility of adapting and fast readjustment of a complex for different types of ECC, TO geometry and testing tasks.

Expansion of possibilities of digital processing of ECC signal based on combination of discrete Hilbert transform and statistical methods of evaluation of signal characteristics allows increasing sensitivity and probability of testing using new for ECT circular statistics which are determined through phase characteristics of ECC signals.

Thus, robotics of ECT processes allows increasing productivity of non-destructive testing as well as improving its quality characteristics.

Conclusions

1. Combination of possibilities of modern robot-manipulators, methods of digital processing of signals and statistical methods of processing of measurement results allows developing current robotic ECT system with improvement of technical characteristics and novel possibilities that guarantee automatic non-destructive testing of complex geometry products.

2. Proposed was the effective procedure of ECC signal processing. It is based on application of Hilbert discrete transform in combination with statistical methods of processing of signals' characteristics.

3. A structure of robotic system for automatic non-destructive testing was proposed. It allows reaching new indices of productivity and reliability of NTD results of complex-geometry products.

1. (2003) *Nondestructive testing*: Refer. Book. Ed. by V.V. Klyuev. Moscow: Mashinostroenie.
2. *DSTU EN 12084:2005*: Nondestructive testing. Eddy-current testing. General requirements and recommendations.
3. Lobanov, L.M., Shapovalov, E.V., Kolyada, V.A. (2014) Application of modern information technologies for solution of problems of technological processes automation. *Tekhn. Diagnostika i Nerazrush. Kontrol*, **4**, 52–56.
4. Schwabe, M., Maurer, A., Koch, R. (2010) Ultrasonic testing machines with robot mechanics – a new approach to CFRP component testing. In: *Proc. of 2nd Int. Symp. on NDT in Aerospace* (22–24 Nov. 2010), Hamburg, Germany.
5. Louviot, P., Tachattahte, A., Garnier, D. (2012) Robotised UT transmission NDT of composite complex shaped parts. In: *Proc. of 4th Int. Symp. on NDT in Aerospace* (13–14 Nov. 2012, Augsburg, Germany).
6. Popov, E.P., Pismenny, G.V. (1990) *Fundamentals of robotics*. Moscow: Vysshaya Shkola.
7. Yurevich, E.I (2005) *Fundamentals of robotics*. 2nd ed. St.-Petersburg: BVKh-Petersburg.
8. Slyadneva, N.A. (2008) ROBOSKOP VT-3000 robotized complex of eddy-current control. Diagnostic devices. *Means and technologies of nondestructive testing*, **1**, 31.
9. Uchanin, V.M. (2013) *Surface mounted eddy-current transducers of double differentiation*. Lviv: SPOLOM.
10. Teterko, A.Ya., Nazarchuk, Z.T. (2004) *Selective eddy-current detection*. Lviv: N.V. Karpenko Physico-Mechanical In-te.
11. Kuts, Yu.V., Shcherbak, L.M. (2009) *Statistical phasometry*. Ternopil: Vyd-vo I. Pulyuya TTU.
12. Bendat, J., Pirsol, A. (1989) *Applied analysis of random data*. Moscow: Mir.

Received 19.04.2017

doi.org/10.15407/tpwj2017.05–06.11

DEVELOPMENT OF TECHNOLOGY OF SEALING HEAT EXCHANGER PIPES BY AUTOMATIC WET UNDERWATER WELDING

S.Yu. MAKSIMOV
E.O. Paton Electric Welding Institute, NASU
11 Kazimir Malevich Str., 03680, Kiev, Ukraine. E-mail: office@paton.kiev.ua

One of the alternative sources of energy is heat pumps. The heat exchangers, included into their composition, represent pipes with a diameter of 140–190 mm, going into the ground to the depth of 200 m and filled with a heat-carrying agent: a mixture of water with 25 % of special coolant FXC2 based on antifreeze with corrosion inhibitors. For the heat exchanger sealing a technology for welding-in bottom was developed using automatic flux-cored wire underwater welding. The influence of coolant and depth on the formation and structure of weld metal were determined, the main parameters of welding process were selected: wire feed speed, rotation speed of automatic machine, inclination angles of torch, optimal gap between the pipe wall and the end of welded-in bottom. A pilot industrial inspection was carried out. 2 Ref., 8 Figures.

Keywords: *wet arc welding, low-carbon steel, heat pumps, welding-in of bottom, flux-cored wire, process automation*

The constant increase in the cost of oil products and gas forces many countries to turn their attention to the methods of obtaining the so-called renewable energy. One of the typical solutions in this industry is heat pumps. In particular, the system «Geoscart^{TM}» developed by the Company «Greenfield Energy Limited» is operated on their base [1]. It is designed to control heat flows of public and commercial buildings and enterprises with continuous energy consumption of high density: modern supermarkets, high-class hotels, stationary hospital complexes, food and pharmacological industry enterprises. At the same time, geothermal heat exchangers of special design for quick and efficient transfer of surplus or deficit heat are applied, using high density and heat capacity of geological formations located much lower than the surface soils. The standard depths for heat exchange process are the intervals reaching 200 m below the surface level of the earth. Each complex consists of more than a dozen of heat exchangers, which represent pipes with a diameter of 140–190 mm filled with a mixture of water containing 25 % of special coolant FXC2 based on antifreeze with corrosion inhibitors. The lower end of pipes is sealed with a rubber plug of a special design. The practice of operating heat exchangers showed that after several years as a result of aging of plug material, a leakage of heat-carrier appears, leading to decrease in the efficiency of heat pumps.

Figure 1. Welding with coolant FXC2

The aim of the work was the development of technology of sealing the pipes of heat exchangers by automatic wet underwater welding using flux-cored wire in solution of antifreeze at the depth of 200 m.

The investigations were carried out in two stages: in the laboratory installation based on the tractor TS-17 and in a hydro-pressure chamber with a depth simulation. At the first stage, the surfacing was carried out using experimental flux-cored wires in antifreeze solution. The welding speed was 6.8 m/h, the wire feed speed was 250 m/h. The vapors formed at dissociation of the coolant solution, escaping to the water surface, were flamed (Figure 1).

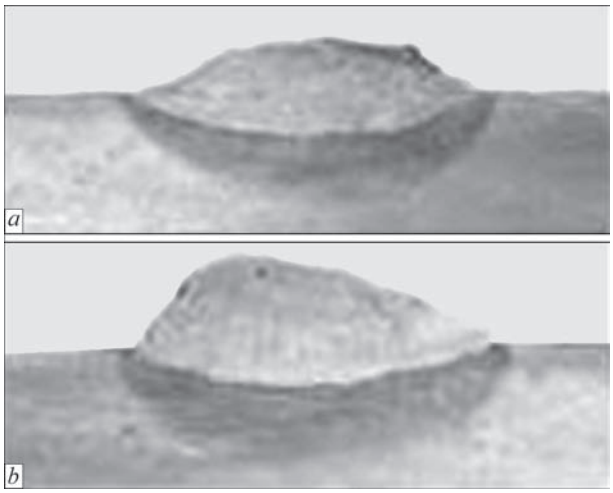

Figure 2. Macrosections of deposits produced in fresh water (*a*) and in 25 % solution of coolant FXC2 (*b*)

The macrosections of deposits produced by the flux-cored wire and selected for further investigations are shown in Figure 2. The presence of coolant did not actually have a noticeable effect on deposited bead formation.

To determine the effect of welding conditions on the structure of weld metal, the surfacing at the depth of 200 m was additionally performed. The metallographic examinations of specimens were carried out in the microscopes «Neophot-32» and Poluvar at different magnifications. The hardness was measured in the micro-durometer M-400 of the company LECO. The digital image was obtained with the help of the camera Olympus-5050. The results showed that the structure of weld metal during welding in fresh water represents ferrite with an ordered second phase (Figure 3, *a*), at the maximum hardness *HV*10 of 1950 MPa. During welding in 25 % solution of the coolant FXC2 a polygonal ferrite is formed in the weld metal, sometimes with a Wiedmanshtett orientation and finely-dispersed perlite precipitation along the boundaries of crystallites, the grain size is somewhat increased. In the body of crystallites several modifications of ferrite are formed: polyhedral and two modifications of a lamellar one with an ordered second phase and with a disordered one (Figure 3, *b*). The hardness is somewhat decreased (*HV*10 — 1820 MPa). During welding at the depth of 200 m, the structure of weld metal represents a fine-grained granular perlite and the areas of free ferrite (Figure 3, *c*). The separate large pores appeared. The hardness decreased to *HV*10 — 1600 MPa. Thus, the addition of the coolant FXC2 does not lead to a significant degradation of the microstructure of weld metal.

At the second stage, the welding technique was mastered as-applied to welding-in the bottom applying automatic machine in the hydro-pressure chamber. The specimens represented T-joint (Figure 4). A horizontal flange of 10 mm thick simulated the bottom.

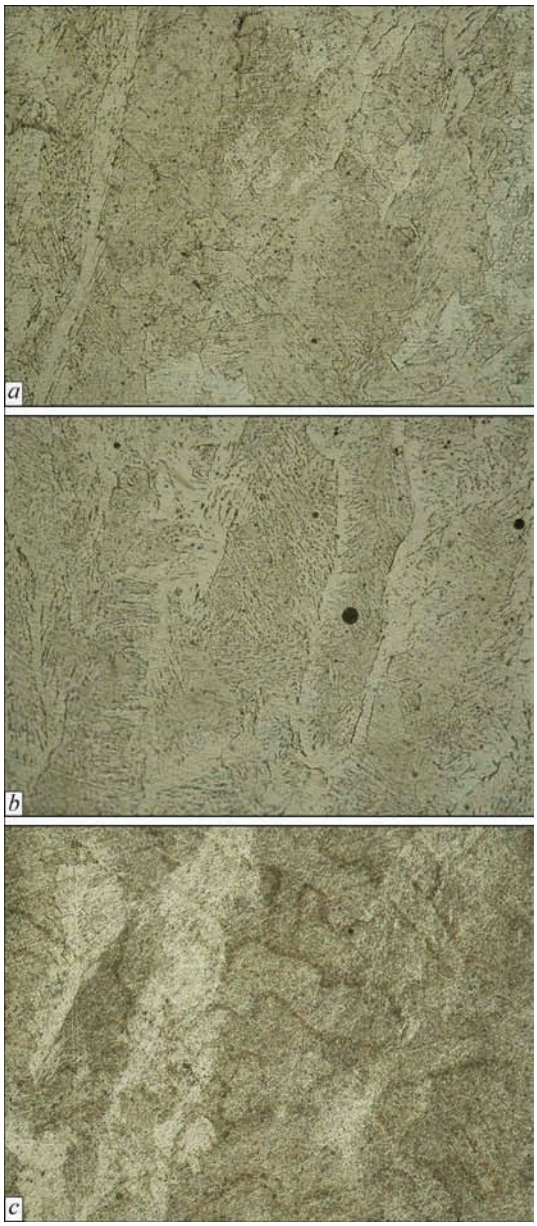

Figure 3. Microstructure of deposits produced in fresh water (*a*) and in 25 % solution of coolant FXC2 at the depth of 0.2 (*b*) and 200 m (*c*) (×250)

Figure 4. Specimen for welding

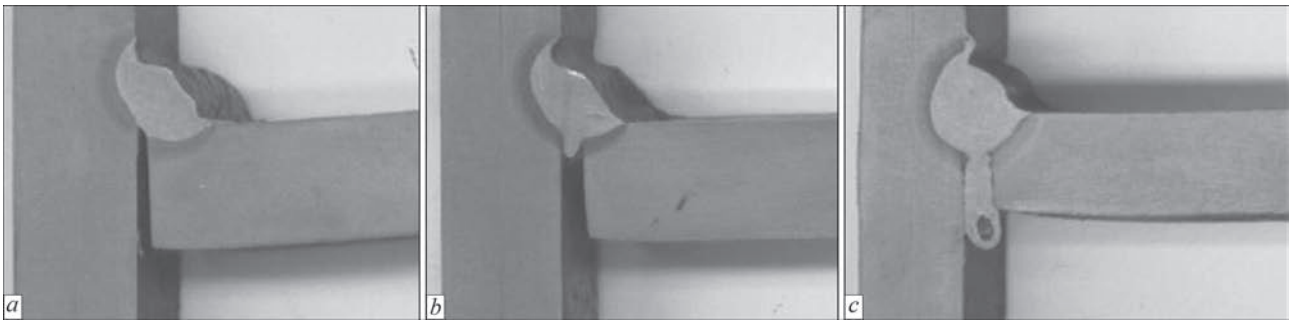

Figure 5. Examples of welded joints of specimens with different parameters of assembly and welding

Based on the design peculiarities of the automatic machine [2] and delivery terms of the bottom to welding site, it is desirable that a gap between its edges and the pipe wall was as large as possible. On the other hand, the increase in a gap can result in a loss of liquid metal. Therefore, the specimens for welding were assembled with a gap from 0 to 5 mm. Also, the inclination angle of the holder was varied in the vertical and horizontal planes and the place of ignition of the arc was varied on the wall or bottom at a different distance from the edge. The welding speed varied between 2.8–6.8 m/h, the wire feed speed was 160–260 m/h. The welding was performed by experimental flux-cored wire with diameter of 1.6 mm at the reverse polarity. The open-circuit voltage was 40–42 V.

Figure 5 shows macrosections of typical welded joints. The most acceptable results were obtained at the value of gap of 4 mm between the horizontal and vertical flanges of T-joint. The ignition was carried out in the horizontal flange at distance of 1–2 mm from the edge. The inclination angle of the electrode

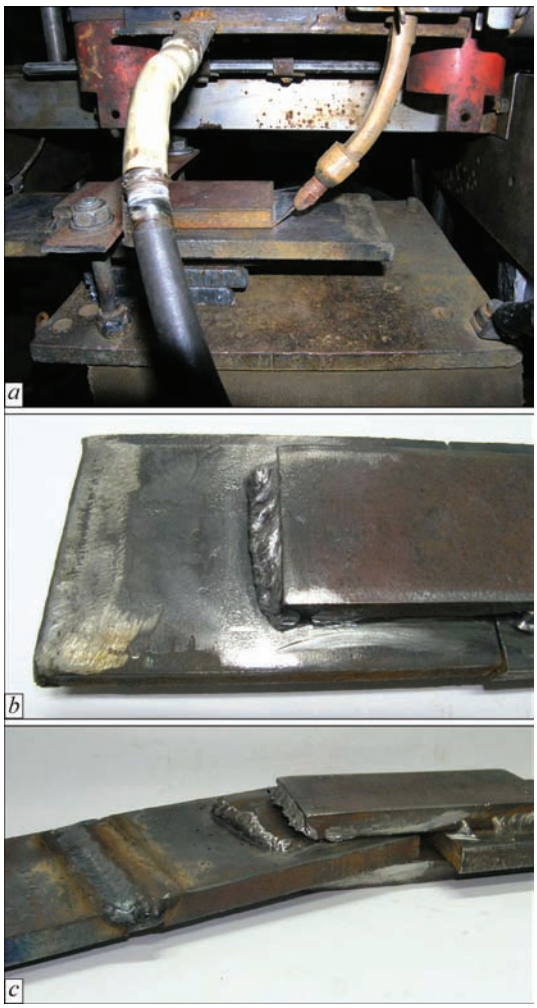

Figure 6. Specimen for rupture tests: before welding (*a*), after welding at the depth of 200 m (*b*) and after test (*c*)

Figure 7. Results of welding-in the bottom to the pipe inner surface: *a* — circumferential weld with overlapping; *b* — real gap between bottom and pipe; *c* — shape of welded joint

in the vertical plane was 40–50° and in the horizontal it was about 20°. The welding speed was about 5 m/h, the wire feed speed was 220–240 m/h.

To determine the shear strength of weld metal, the specimens were welded simulating a fillet joint (Figure 6) and tested for tension. The welding speed was 5.1 m/h, the wire feed speed was 240 m/h, $U_{o\text{-}c}$ = = 41 V. The failure force was 9150 kg or 438 MPa in terms of failure section. Taking into account that the bottom undergoes the pressure of a water column of 200 MPa, it can be concluded that the formed welded joint has a significant margin of safety.

At the final stage the developed technology was tested in automatic mode in the special testing stand, designed at the EDTB of the PWI. The welding was performed in two stages. With the help of a tack the bottom was fixed relative to the pipe wall to prevent rotation of the bottom together with the automatic machine inside the pipe. Then the machine moved to the opposite side of the bottom and the welding of circumferential weld was performed. The welding time was selected taking into account the overlapping in 2–3 cm of weld beginning. The appearance of welded-in bottom and macrosections are shown in Figure 7.

In industrial conditions the welding was carried out in Crayford, Great Britain, in the pipe of 119 mm diameter. The object consisted of 15 wells with the depth from 180 to 210 m, the angle of well location relative to the vertical was from 0 to 15°. Before the start of welding operations, the wells were checked

Figure 8. Appearance of welded-in bottom

by a special set of models with the diameters of 118, 117 and 116 mm for passing ability of welding machine and for determination of the bottom diameter. The welding speed was 6.3 m/h; the welding time was 3 min 18 s; the welding current was 200–220 A; the voltage was 50 V. After welding, the weld quality was evaluated visually with the help of a special video camera (Figure 8) and with an excessive pressure of 1 MPa for 30 min.

The obtained results showed that the developed technology of welding-in the bottom inside the pipe provides its sealing, preventing the loss of expensive coolant and reducing the efficiency factor of the heat pump.

1. Stickney, K. (2009) Introduction to geoscart TM and the benefits to refriaeration systems. *Greenfield Energy Ltd*., 18.
2. Lebedev, V.A., Maksimov, S.Yu., Pichak, V.G. et al. (2014) Automatic machine for wet underwater welding in confined spaces. *The Paton Welding J*., **9**, 39–44.

Received 21.04.2017

doi.org/10.15407/tpwj2017.05–06.12

DEVELOPMENT OF A ROBOTIC COMPLEX FOR HYBRID PLASMA-ARC WELDING OF THIN-WALLED STRUCTURES

V.N. KORZHIK[1,2], **V.N. SYDORETS**[1,2], **SHANGUO HAN**[1], **A.A. BABICH**[1,2], **A.A. GRINYUK**[2,3] and **V.Yu. KHASKIN**[1,2]

[1]Guangdong Welding Institute (China-Ukraine E.O. Paton Institute of Welding)
363 Changxing Str., Tianhe, Guangzhou 510650, China
[2]E.O. Paton Electric Welding Institute, NASU
11 Kazimir Malevich Str., 03680, Kiev, Ukraine. E-mail: office@paton.kiev.ua
[3]NTUU «Igor Sikorsky KPI»
37 Pobedi Prosp., 03056, Kiev, Ukraine

The objective of this work is development of a complex of equipment and technology of hybrid consumable electrode plasma-arc welding with coaxial wire feed for structures from steels and aluminium alloys 5–12 mm thick, using industrial robots. Mathematical modeling of processes in the arc in hybrid plasma-arc welding was the basis for selection of welding mode parameters allowing for mutual influence of the column of nonconsumable electrode constricted arc and consumable electrode arc, which enabled defining technical requirements to welding current power sources. Proceeding from mathematical and physical modeling of the process of hybrid welding, a complex of equipment and basic technologies were developed for robotic welding of thin-walled structures from steels and aluminium alloys. Developed system of complex control anabled synchronizing the functioning of two welding sources and auxiliary equipment with movements of an anthropomorphic industrial robot for realization of a stable process of hybrid consumable electrode plasma-arc welding. Application of this welding process allowed reducing electrode metal consumption by 40 %, compared to consumable electrode pulsed-arc welding at comparable speeds. Here, the level of longitudinal deflection of welded samples at hybrid process application was 3 times smaller, compared to the process of consumable electrode pulsed-arc welding. 20 Ref., 1 Table, 10 Figures.

Keywords: *robotic complex, plasma, consumable electrode arc, hybrid process, aluminium alloys, steels, welding modes, joint quality*

At present, the tendencies of welding production robotization and automation are becoming ever more urgent for large-scale production. Robot application in conveyor lines in car manufacturing can be an example of it [1]. Another important example is application of industrial robots in ship-building [2]. Here, welding robots are applied for manufacturing elements of ship hulls, deck superstructures, switching systems and diverse ship equipment [3]. The main advantage gained here is improvement of efficiency and quality of welded joints due to replacement of manual welding by automatic welding. Moreover, the requirement for highly qualified specialists–welders is reduced, and performance of high-productivity welding in difficult-of-access places becomes possible. Application of aluminium and its alloys instead of steel in ship- and car-building for manufacturing body elements allows their mass to be reduced by 50–60 %. As result, it becomes possible to increase the carrying capacity of ships and railway transport.

Well-known traditional arc processes are most often used to perform robotic welding [3]. These, primarily, are consumable (MIG/MAG) and nonconsumable (TIG) electrode welding. However, welded joints produced by these processes do not always fully meet the requirements to surface quality and level of residual deformations after welding of the produced structures. At robotization of welding processes, it is rational to apply accessible high-efficient technology, allowing minimization of the level of residual welding deformations.

One of the welding processes, which allow solving the defined task, is hybrid consumable electrode plasma-arc (Plasma-MIG) welding [4]. This process was patented for the first time in 1972 by Wilhelm Essers and other staff members of Philips Company (The Netherlands) [5]. In such a welding process, a heat source for hybrid plasma-arc welding is formed, which consists of nonconsumable electrode constricted arc, encompassing the consumable electrode arc. Additional constriction of the latter provides reduction of spatter and possibility of increasing base metal penetration depth at smaller values of electrode wire feed rate (welding current of consumable electrode

arc is smaller). Application of such a process for welded structure fabrication can provide formation of fine-grained structures of welds, as well as high quality and efficiency of welding [6].

Conventional nonconsumable pin electrode was used earlier in the designs of torches for hybrid consumable electrode plasma-arc welding. In modern designs it was replaced by hollow-annular electrode [7]. Modern modified process of hybrid plasma-arc welding has not yet become widely accepted, being, however, actively studied by researchers [8]. Technologies of welding different materials by this process are at the development stage.

The objective of this work was development of equipment and technology for hybrid consumable electrode plasma-arc welding with coaxial wire feed for robotic welding of structures from steels and aluminium alloys with 5–12 mm wall thickness.

The following tasks were solved to achieve the defined objective:

1. Modeling of the process of hybrid consumable electrode plasma-arc welding, allowing for mutual influence of nonconsumable electrode constricted arc and consumable electrode arc, which is the base for preselection of hybrid welding mode parameters.

2. Defining requirements to welding power sources.

3. Synchronizing the operation of welding sources and auxiliary equipment with anthropomorphous industrial robot.

4. Development of welding torch for hybrid plasma-arc welding, designed for continuous robotic welding.

5. Development of a robotic complex and optimization of the technology of hybrid plasma-arc welding of structures from steels and aluminium alloys with 5–12 mm wall thickness.

For preselection of parameters of the mode of hybrid consumable electrode plasma-arc welding the processes of consumable electrode heating were considered at the following assumptions (Figure 1): phases of heating of electrode extension and its melting are sufficiently well separated and interaction proceeds so that final heating conditions are initial conditions for melting; electrode extension is heated by plasma of discharge with nonconsumable electrode and welding current; molten zone length is much smaller than electrode extension length; and electrode metal transfer is of drop type. These assumptions coincide with those made in [9]. Therefore, the mathematical model was constructed similarly. The difference between MIG and Plasma-MIG welding processes consists in that electrode extension is additionally heated by plasma of discharge with nonconsumable annular electrode (anode).

Electrode wire is located inside the plasma discharge along its axis. Its temperature rises due to convection and radiation heating. Considering that plasma temperature T_p = 5500–15000 K, it is easy to show that the fraction of energy supplied to electrode wire through convection heating, is extremely small. Therefore, we did not allow for convection heating, when solving the heat problem. Radiation heating obeys Stefan-Boltzmann law, and differential equation, describing the change of temperature T in time t, has the following form:

$$\frac{dT}{dt} = \frac{2\beta\sigma_{SB}}{\gamma c r_w}\left(T_p^4 - T^4\right), \qquad (1)$$

where σ_{SB} is the Stefan–Boltzmann constant; β, γ, c, r_w are the degree of blackness, specific heat conductivity, electrode wire radius, respectively.

Solution of differential equation (1) has an implicit form:

$$t = \frac{\beta\sigma_{SB}T_p^3}{\gamma c r_w}\left[\operatorname{atanh}\left(\frac{T}{T_p}\right) - \operatorname{atanh}\left(\frac{T_0}{T_p}\right) + \operatorname{atan}\left(\frac{T}{T_p}\right) - \operatorname{atan}\left(\frac{T_0}{T_p}\right)\right], \qquad (2)$$

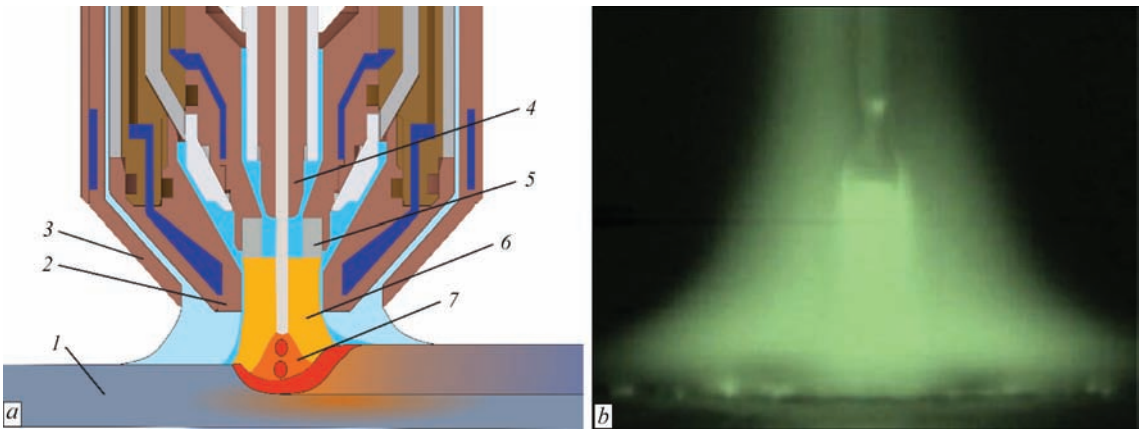

Figure 1. Technological schematic of the process (*a*) and photo of simultaneous action of constricted arc and consumable electrode arc (*b*) in hybrid plasma-arc welding: *1* — sample being welded; *2* — plasmaforming nozzle; *3* — shielding nozzle; *4* — consumable electrode nozzle; *5* — plasmatron annular electrode (anode); *6* — constricted direct arc; *7* — consumable electrode arc

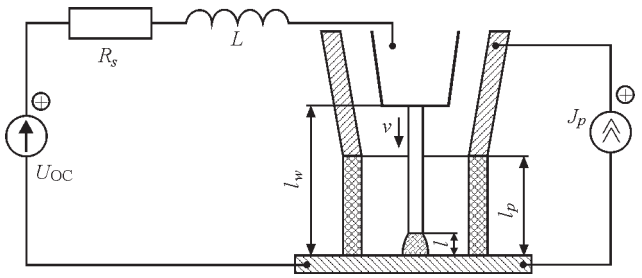

Figure 2. Schematic of connection of power sources in hybrid plasma-arc welding process

where T_0 is the initial temperature of electrode wire.

It is difficult to use solution (2) for further studies. It is simplified, considering that electrode wire melting temperature T_m is much smaller than plasma temperature T_p. In this case we obtain a simple solution

$$T = T_0 + \frac{2\beta\sigma_{SB}T_p^4}{\gamma c r_w}t. \qquad (3)$$

Difference between the solutions at melting temperature T_m is equal to 0.2 for steel and 0.02 % for aluminium (1.2 mm electrode wire diameter). This provided a base for us for further application of formula (3).

Energy accumulated in the metal of electrode extension due to welding current passage, and plasma radiation, summing up with energy evolving in near-electrode (near-cathode) region, is consumed for metal heating and melting. Electrode melting rate can be derived from this condition:

$$v_m = \frac{\pi r_w^2 U_c i + \rho i^2 (l_w - l) + 2\pi^2\beta\sigma_{SB}T_p^4 r_w^3 (l_p - l)}{\pi^2\gamma r_w^4 \left[c(T_m - T_0) + \lambda \right]},$$

where i is the welding current (MIG process current); l is the arc length; U_c is the cathode voltage drop; l_w, l_p are the distance from the tip to the item and from plasmatron nozzle to the item (Figure 2); ρ, λ are the specific resistance and latent heat of electrode metal melting.

It is obvious that electrode melting dynamics is described by differential equation, the essence of which consists in that the change of arc length is equal to the difference of electrode melting rate and electrode feed rate v

$$\frac{dl}{dt} = \frac{\pi r_w^2 U_c i + \rho i^2 (l_w - l) + 2\pi^2\beta\sigma_{SB}T_p^4 r_w^3 (l_p - l)}{\pi^2\gamma r_w^4 q} - v, \qquad (4)$$

where $q = c(T_m - T_0) + \lambda$.

In keeping with Kirchhoff's law, open-circuit voltage U_{OC} of the power source is equal to the sum of voltage drops across the circuit elements (see Figure 2) — ohmic resistance R_S and inductance L of the power source and connecting cables, ohmic resistance of electrode extension and arc voltage drop El (E is the electric field resistance in the arc)

$$U_{OC} = R_S i + L\frac{di}{dt} + \rho\frac{l_w - l}{\pi r_w^2} i + El + U_{an} + U_c, \qquad (5)$$

where U_{an} is the anode voltage drop.

Equations (4) and (5) make up a system of nonlinear differential equations, which describe the dynamics of «power source–consumable electrode arc» system during the process

$$\begin{cases} \dfrac{dl}{dt} = \dfrac{\pi r_w^2 U_c i + \rho i^2 (l_w - l) + 2\pi^2\beta\sigma_{SB}T_p^4 r_w^3 (l_p - l)}{\pi^2\gamma r_w^4 q} - v \\ \dfrac{di}{dt} = \dfrac{1}{L}\left(U_{OC} - R_S i - \rho\dfrac{l_w - l}{\pi r_w^2} i - El - U_{an} - U_c \right) \end{cases}. \qquad (6)$$

In order to find special points, which determine the static state, it is necessary to equate the right-hand parts of system (6) to zero. Equations for determination of static values of arc length l_0 and welding current i_0, have the following form:

$$\rho\left(r_w E^2 + 2\rho\beta\sigma_{SB}T_p^4\right) l_0^3 - \rho\Big[r_w E\left(2\bar{U}_{OC} + U_c + El_w\right) + 4\beta\sigma_{SB}T_p^4\left(\pi r_w^2 R_S + \rho l_w\right) + \rho\left(2\beta\sigma_{SB}T_p^4 l_p - \gamma q v r_w\right)\Big] \times$$
$$\times l_0^2 + \Big[\Big[r_w U_c E + 2\rho\left(2\beta\sigma_{SB}T_p^4 l_p - \gamma q v r_w\right)\Big] \times$$
$$\times\left(\pi r_w^2 R_S + \rho l_w\right) + \rho r_w \bar{U}_{OC}\left(\bar{U}_{OC} + U_c + 2El_w\right) + 2\beta\sigma_{SB}T_p^4\left(\pi r_w^2 R_S + \rho l_w\right)^2\Big] l_0 -$$
$$-\Big[r_w U_c \bar{U}_{OC}\left(\pi r_w^2 R_S + \rho l_w\right) + \rho r_w \bar{U}_{OC}^2 l_w + \left(2\beta\sigma_{SB}T_p^4 l_p - \gamma q v r_w\right)\left(\pi r_w^2 R_S + \rho l_w\right)^2\Big] = 0;$$
$$\rho R_S i_0^3 - \rho\left(\bar{U}_{OC} + U_c - El_w\right) i_0^2 + \pi r_w\Big[2\beta\sigma_{SB}T_p^4\Big[\pi r_w^2 R_S + \rho\left(l_w - l\right)\Big] + r_w\left(U_c E + \gamma\rho q v\right)\Big] i_0 - -\pi^2 r_w^3 \times$$
$$\times\Big[2\beta\sigma_{SB}T_p^4\left(\bar{U}_{OC} - El_p\right) + \gamma q v E r_w \Big] = 0,$$

where

$$\bar{U}_{OC} = U_{OC} - U_{an} - U_c.$$

To study the properties of these solutions let us use conditions of existence, the essence of which is as follows: Plasma-MIG process can be physically realized, when static welding current is greater than zero

$$i_0 > 0, \qquad (7)$$

and static value of arc length is in the range from zero (electrode contact with the item) up to the distance from the nozzle to the item (electrode burning-off)

$$0 < l_0 < l_w. \qquad (8)$$

Application of these conditions allows determination of maximum plasma temperature at which Plasma-MIG process proceeds

$$T_{p\max} = \left(\frac{\gamma q v E r_w}{2\beta\sigma_{SB}\left(El_p - U_{OC} + U_{an} + U\right)} \right)^{1/4}.$$

Our assessments showed that maximum temperature for steel is T_{max} = 7960 K; for aluminium

it is $T_{p\,max}$ = 7340 K (process parameters, for which calculations were performed, are given in [10]). This result is in good agreement with experimental results of temperature measurement [11].

In hybrid Plasma-MIG process mutual effect of gas discharges on each other is in place. Impact of plasma discharge on electrode wire melting was considered above. Electrode wire melting, in its turn, influences the electric parameters of plasma discharge [12, 13], in particular, its volt-ampere characteristic (VAC). These features were taken into account at selection of power sources and development of equipment for Plasma-MIG process [14]. However, dependence of electrical characteristics on technological parameters of Plasma-MIG process cannot be derived at application of currently available resistive models [15].

Arc model developed at PWI was improved to describe plasma discharge of hybrid Plasma-MIG process [16, 17].

Plasma arc is considered phenomenologically as heat macroobject, which is the element of electric circuit with static VAC $U_p(i)$. The law of energy conservation for such a heat macroobject has the following form

$$\frac{dQ}{dt} = P - P_\theta.$$

This law connects three energy parameters of plasma arc column: internal energy Q, applied P and removed P_θ power. Internal energy of arc column Q is the sum of all the plasma energies: energy of thermal motion, ionization energy, vibrational and rotational energy of molecules, etc., and it depends on arc radius and length, i.e. on its volume. By the term applied power P we mean power consumed from the power source, and by the term removed power P_θ we mean the power, which the arc column releases into the environment through heat conductivity and radiation.

Application of the term of state current [16] and introduction of variable i_θ enables expressing arc energy parameters through electric parameters

$$P = \frac{U_p\left(i_\theta\right)}{i_\theta} i_p^2, \quad P_\theta = U_p\left(i_\theta\right) i_\theta,$$

$$Q = 2\theta \int_0^{i_\theta} U_p\left(i_\theta^*\right) di_\theta^*,$$

where i_p is the plasma arc current; θ is the plasma arc time constant) and deriving the differential expression of the model

$$\theta \frac{di_\theta^2}{dt} + i_\theta^2 = i_p^2. \qquad (9)$$

Equation (9) is complemented by a formula of relation between plasma arc current and its voltage

$$u = \frac{U_p\left(i_\theta\right)}{i_\theta} i_p,$$

which is part of equation corresponding to Kirchhoff laws.

In the case of plasma arc with gas blowing, an additional mechanism of energy scattering is in place, alongside natural convection. This mechanism is based on forced convection, the power of which P_v can be allowed for directly

$$P_v = \frac{W_A}{V_A} Q = \frac{v_{ShG}}{l_p} Q,$$

where V_A is the volume taken up by plasma arc column; W_A is the volume of plasma consumed per a unit of time for longitudinal blowing $W_A = \pi(r_{Aout}^2 - r_{Ain}^2)v_{ShG}$, v_{ShG} is the speed of blowing with shielding gas; r_{Ain} and r_{Aout} are the inner and outer radii of plasma discharge column.

Power balance equation in this case becomes

$$\frac{dQ}{dt} = P - P_\theta - P_v.$$

Equation of the model of an arc with longitudinal blowing is as follows

$$\theta \frac{di_\theta^2}{dt} = i_p^2 - i_\theta^2 \left[1 + \frac{v_{ShG}}{l_{pl}} \frac{Q}{P_\theta}\right] \qquad (10)$$

It is promising to use equation (10) to describe the dynamics of plasma arc, where longitudinal blowing with shielding gas is an essential part of the process.

When electrode wire moves inside the cylindrical plasma discharge, there appears one more mechanism of energy removal, associated with its heating. It should be taken into account in the law of energy conservation.

$$\frac{dQ}{dt} = P - P_\theta - P_v - P_w.$$

Electrode wire heating due to plasma discharge radiation was considered above. Using these results, we obtain the following formula for power

$$P_w = 2\pi r_w \beta \sigma_{SB} T_p^4 \left(l_p - l_0\right).$$

Equation of generalized dynamic model of plasma arc for Plasma-MIG process has the following form

$$\theta \frac{di_\theta^2}{dt} = i_p^2 - i_\theta^2 \left(1 + \frac{P_v + P_w}{P_\theta}\right).$$

To obtain plasma discharge VAC in Plasma-MIG process we will use the procedure described in paper [18]. As a result, a parametric dependence of plasma discharge voltage on its current was derived (Figure 3)

$$U_{\text{Plasma-MIG}}\left(i_\theta\right) = U\left(i_\theta\right)\left(1 + \frac{P_v + P_w}{P_\theta}\right)^{1/2};$$

$$I_{\text{Plasma-MIG}}\left(i_\theta\right) = i_\theta\left(1 + \frac{P_v + P_w}{P_\theta}\right)^{1/2}.$$

In these formulas i_θ variable has the role of a parameter.

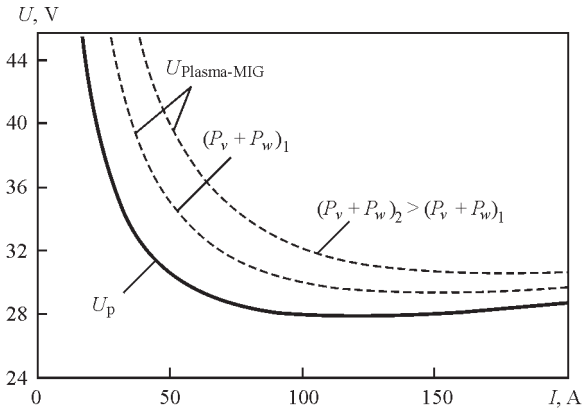

Figure 3. VAC of plasma discharge in Plasma-MIG process (*dashed lines*) compared to VAC of plasma discharge without MIG process (*solid line*)

The graph presented in Figure 3, demonstrates the tendency to voltage rise in plasma discharge in Plasma-MIG process. This is in good agreement with the phenomena, which were observed during technological experiments at comparison of Plasma and Plasma-MIG processes [10, 19, 20].

Proceeding from the conducted calculations, specification for design or selection of welding power sources has been developed. So, it is determined that power source of plasma component should provide the possibility of running of nonconsumable electrode constricted arc at reverse polarity direct current with current load from 50 up to 250 A and up to 45 V arc voltage. Power source of consumable electrode arc should provide welding current from 10 up to 350 A at 100 % duty cycle. Here, the power sources should have the capability of communication with the control system via bus interface, using the most common communication protocols. Technical requirements were the basis to select welding inverter sources, the most suitable to the developed specification. These sources are fitted with bus interface for exchange of control and feedback signals with the overall control system of the complex. For reliable operation of plasma module in RPDC welding mode, reconnection of pilot arc connectors was performed to ensure its excitation at reverse polarity. Control system of welding power sources and plasma module is based on programmable PLC controller, it provides an algorithm of sequential switching on and off of electric components of the complex of equipment for hybrid consumable electrode plasma-arc welding, acquisition of data on the welding mode, monitoring of parameters of the complex component operation for possible emergencies (Figure 4). Communication between the power sources proceeds via buses by CAN bus protocol. Algorithm of the sequence of switching-on the components of equipment complex uses current and voltage feedback signals, generated by power sources.

A typical algorithm for the process of hybrid consumable electrode plasma-arc welding is as follows: when power is applied to welding current sources, «Ready for work» signals are generated, and they come to control system controller. In the absence of the signal, further process of switching-on is blocked. When «Welding start» command is issued, the signal passes via the bus to power source of consumable electrode arc, which is followed by arc excitation. When consumable electrode arc is running, «Main current» signal from consumable electrode power source to control system controller is formed. When this signal is received, a command is generated for plasma module for arc excitation. After pilot arc excitation, a signal is generated with a time delay for excitation of the arc by plasma component power source. At excitation of nonconsumable electrode constricted arc by plasma component power source, «Main current» signal is generated, which is sent to control system controller. After passing of «Main current» signal from plasma component power source, starting of the system of displacement of the torch or the part proceeds with the selected time delay. Absence or removal of each of «Main current» signals during the process is a signal for interruption of the algorithm of switching-on the power sources, and the hybrid consumable electrode plasma-arc welding process proper.

The system performs control of external displacement devices (welding column, welding rotator, or other device), or provides interaction of the complex of welding power sources with welding robot controller and synchronizing of welding cycle stages with its actions. The main technical characteristics of robotic complex of hybrid plasma-arc welding equipment (Figure 5) are given below.

Main technical characteristics of equipment complex for hybrid plasma-arc welding

Voltage of three-phase AC mains with 50 Hz frequency, V	400 (±15 %)
Working voltage of consumable electrode arc, V	0–50
Working current of consumable electrode arc in hybrid plasma-arc welding, A	50–250
Working voltage of plasma welding source, V	15–34
Limits of regulation of different-polarity asymmetrical current, A	10–350
Limits of regulation of straight and reverse polarity direct current, A	10–350
Limits of regulation of the duration of current flowing at straight polarity, %	15–85
Shielding gas	Ar, Ar + He
Plasma gas in hybrid welding torch	Ar
Working gas pressure at power source input, MPa	0.2–0.4
Gas flow rate, l/min:	
shielding	10–40
central	1–10
plasma	0.1–10.0
Filler and electrode wire diameters, mm	1.2; 1.6

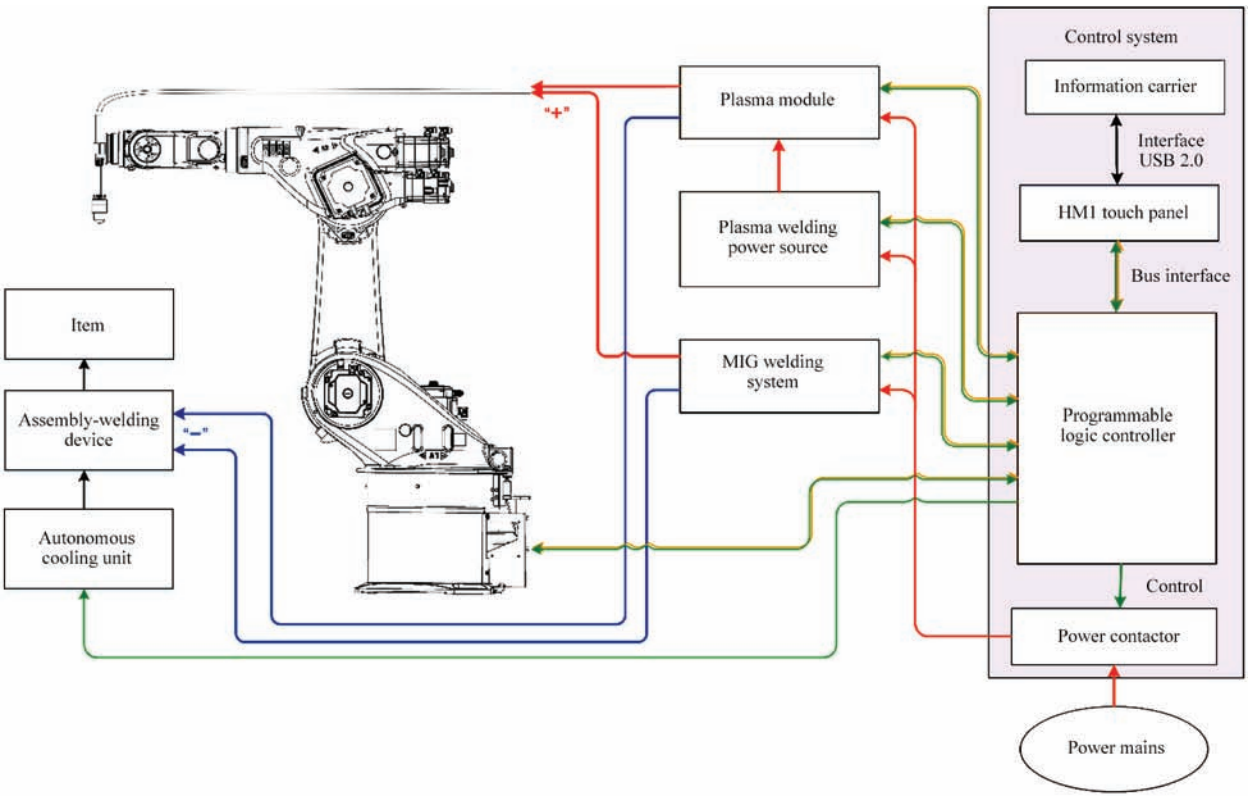

Figure 4. Block-diagram of robotic complex of hybrid plasma-arc welding

Application of bus interface, operating by CAN bus protocol, is envisaged for communication with robot controller. The problem of interaction of control system of the complex of hybrid consumable electrode plasma-arc welding equipment and robot controller is based on «Master–Slave» principle. Robot controller acts as «Master». After switching on the control system of welding equipment complex, a survey of readiness for work and serviceability of power sources is performed. In the absence of malfunction signals, «Ready» signal is formed and sent to robot controller. The robot controller at «Welding start» command moves the welding torch to the point of welding start, and transfers the command to the controller of control system of welding equipment complex to start the algorithm of arc excitation at hybrid plasma-arc welding. Control system starts the algorithm of hybrid arc excitation, and after passage of «Main current» signals, issued by power sources at arc excitation, it generates a signal for robot controller to start welding head movement by a program, installed on robot controller. After the torch has reached the welding

Figure 5. Equipment of the complex for robotic hybrid Plasma-MIG welding: *a* — control panel of the complex for hybrid Plasma-MIG welding; *b* — power sources for plasma and arc components with wire feed mechanisms; *c* — welding torch in the arm of KR 60 HA robot of KUKA Company (Germany)

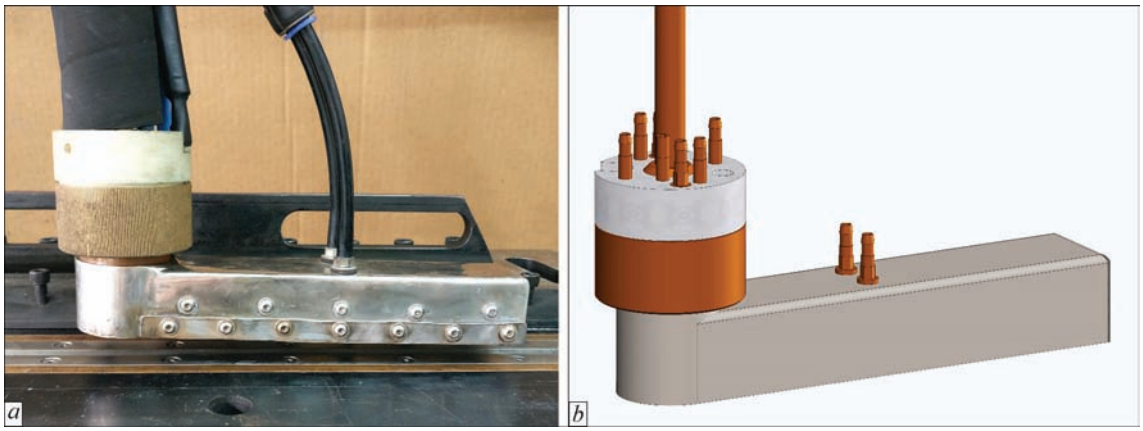

Figure 6. Appearance (*a*), and schematic (*b*) of the torch for robotic hybrid plasma-arc welding with additional shielding nozzle

end point, the controller stops movement, and issues a command to the controller of welding equipment complex control system for extinguishing the hybrid arc. Control system controller performs disconnection of power sources and plasma module by an algorithm installed in it. After removal of «Main current» signal from consumable electrode power source and completion of welding cycle, a signal is transferred to robot controller to bring the welding torch back to the initial point.

This algorithm of interaction of the system of control of the complex of welding equipment for hybrid consumable electrode plasma-arc welding and welding robot controller enables simplifying the process of welding equipment integration with robots of different manufacturers. Here, the robot controller takes over the functions of monitoring the welding tool movement; it also issues commands to control system of welding equipment complex for welding arc excitation and extinction in hybrid plasma-arc welding.

A welding torch with an assembly of additional gas shielding was developed to produce sound welds (Figure 6). Diameters of replaceable plasmaforming nozzles were selected in the range of 6–10 mm. Anode design was composite, consisting of a copper body with refractory (tungsten) insert. A hole is made in the tungsten for electrode wire feed. Working distance between plasmaforming nozzle and sample being welded should be equal to 6.0 mm. This distance was selected from the conditions of existence (7) and (8) that ensured variation of the length of electrode extension (distance from current-conducting tip for electrode wire to the item) in the range of 16–18 mm. Here, minimum spatter deposition on plasmaforming and shielding nozzles of plasmatrons in hybrid plasma-arc welding is achieved.

To optimize the technology of robotic hybrid plasma-arc welding of structures from steels and aluminium alloys 5–12 mm thick, samples of butt joints of 400×200×δ mm size from SUS304 steel (δ = 12 mm), Steel 20 (δ = 10 mm) and aluminium alloys 5083 (δ = 8.0 mm) and 1561 (δ = 8.0 mm) were prepared. Welding was performed without edge preparation. Removable backing was used to form the root part of the weld: for steels — copper, water-cooled, with 4×1.5 mm groove size; for aluminium alloys — from non-magnetic austenitic steel with groove dimensions of 8×3.0 and 6×2.0 mm. Sound weld formation was the criterion for final selection of the welding mode (Figures 7–10). To determine presence or absence of internal pores, produced samples were subjected to X-ray inspection. This resulted in determination of the modes of robotic hybrid consumable electrode

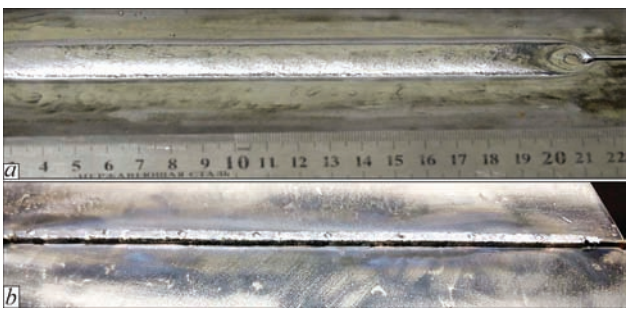

Figure 7. Butt joint of SUS304 steel (δ = 12 mm), produced by hybrid Plasma-MIG welding in the developed robotic complex: *a* — upper bead; *b* — lower bead

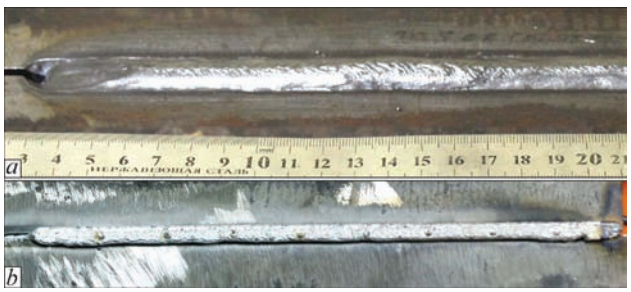

Figure 8. Butt joint of steel 20 (δ = 20 mm), produced by hybrid Plasma-MIG welding in robotic complex; *a* — upper bead; *b* — lower bead

Parameters of the modes of hybrid plasma-arc welding (Plasma-MIG) of steels and aluminium alloys with argon shielding, using electrode wires of 1.6 mm diameter

Grade of steel or alloy	Sample thickness δ, mm	Welding speed, m/min	Constricted arc current, I_p, A	Constricted arc voltage, U_p, V	Plasma gas flow rate, Q_p, l/min	Consumable electrode arc current, I_{MIG}, A	Consumable electrode arc voltage, U_{MIG}, V	Electrode wire feed rate, v_w, m/min
SUS304	12.0	0.25	240	39	7	300	28	7.5
Steel 20	10.0	0.25	200	37	6	240	28	8.0
5083	8.0	0.4	168	23	5	213	23	7.0
1561	5.0	0.6	115	26	5	165	18	7.6

Figure 9. Butt joint of 1561 alloy (δ = 5 mm) produced by hybrid Plasma-MIG welding in the developed robotic complex: *a* — upper bead; *b* — lower bead

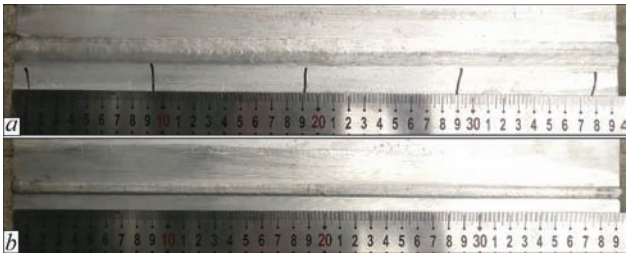

Figure 10. Butt joint of 5083 alloy (δ = 8 mm), produced by hybrid Plasma-MIG welding in the robotic complex: *a* — upper bead; *b* — lower bead

plasma-arc welding, allowing production of sound welded joints (Table).

At consumable electrode pulsed-arc welding, welding current is directly proportional to electrode wire feed rate. This causes in some cases the need to perform edge preparation to accommodate molten electrode metal. In hybrid consumable electrode plasma-arc welding with coaxial feed of electrode wire, the electrode wire feed rate can be reduced to values, required to form the geometry of penetration and convexity of the weld, in keeping with normative document requirements, by selection of the ratio of energy of nonconsumable electrode constricted arc and energy of consumable electrode arc. At application of the developed technology, there is no need to perform edge preparation for welding structures from steels and aluminium alloys with 5–12 mm wall thickness. Moreover, as shown by comparison of the derived results with those of consumable electrode arc welding, weld width and reinforcement in hybrid plasma-arc welding are reduced to 40 %.

Another result of comparison of robotic hybrid plasma-arc process with processes of plasma and MIG/MAG welding is determination of the possibility of increasing the welding speed by 25–40 %. The level of longitudinal and transverse deformations is decreased due to increasing the welding speed and reducing the quantity of deposited electrode metal. So, for 1561 alloy at the same values of welding speed, the level of longitudinal deflection of the sample at hybrid plasma-arc welding is reduced 3 times, compared to the sample, made by consumable electrode pulsed-arc welding.

Conclusions

1. Proceeding from the results, obtained at modeling of the process of hybrid consumable electrode plasma-arc welding with coaxial feed of electrode wire, equipment and basic technologies were developed for robotic welding of structures from steels and aluminium alloys with 5–12 mm wall thickness.

2. Developed control system of the complex allows synchronizing operation of two welding sources and auxiliary equipment with the actions of anthropomorphous industrial robot for realization of the process of hybrid consumable electrode plasma-arc welding.

3. Application of the developed robotic complex of hybrid plasma-arc welding and process of welding steels and aluminium alloys 5–12 mm thick allows increasing welding speed by 25–40 %, compared to consumable electrode pulsed-arc welding and reducing by 40 % the quantity of electrode wire, required for welded joint formation, in keeping with the normative documents, as well as lowering the level of residual welding deformations of welded items.

The work was performed with the support of the program of State Administration of Foreign Experts No. WQ20124400119 «1000 Talents» (PRC), Guangdong Innovative Research Team (PRC) No. 201101C0104901263, Project of Guangdong Academy of Sciences (PRC) «Capacity-building of innovation-driven development for special fund

projects» 2017GDASCX-0411; Projects of Guangdong Province (PRC) No. 2015A050502039 and 32016B050501002.

1. Skhirtladze, A.G., Bochkarev, S.V., Lykov, A.N. et al. (2013) *Automation of technological processes*. Moscow: LLC TNT.
2. Vodovozov, V.M., Myadzel, V.N., Rassudov, L.N. (1986) *Robots in ship hull productions (Control, teaching, algorithmization)*. Moscow: Sudostroenie.
3. Ovchinnikov, V.V. (2012) *Equipment, mechanization and automation of welding processes*. Practical work. Moscow: Academiya.
4. Essers, W.G., Jelmorini, G. (1975) *Method of plasma-MIG-welding*. Pat. US3891824. U.S. Philips Corp., USA.
5. Essers, W.G., Liefkens, A.C. (1972) Plasma-MIG welding developed by Philips. *Machinery and Production Eng.*, **12**, 632–633.
6. Essers, W.G., Willemes, G.A. (1984) Plasma-MIG-Schweissen von Aluminium Aufragschweissen und Zweielektrodenschweissen, von autahl. DVS-Berichte, **90**, 9–14.
7. Dedyukh, R.I. (2014) Specifics of consumable electrode plasma welding process (Review). *Svarochn. Proizvodstvo*, **5**, 34–39.
8. *Tao* Yang, Hongming Gao, Shenghu Zhang et al. (2013) The study on plasma-MIG hybrid arc behaviour and droplet transfer for mild steel welding. *Rev. Adv. Mater. Sci*., **33**, 459–464.
9. Sydorets, V.N., Zhernosekov, A.M. (2004) Numerical simulation of the system of power source-consumable-electrode arc. *The Paton Welding J*., **12**, 9–15.
10. Korzhyk, V., Grynuk, A., Khaskin, V. et al. (2016) The hybrid plasma-arc welding of thin-walled panels made of aluminum alloy. *First Independent Sci. J*., **12/13**, 28–36.
11. Ton, H. (1975) Physical properties of the plasma-MIG welding arc. *J. Phys. D: Appl. Phys*., **8**, 922–933.
12. Hertel, M., Fuessel, U., Schnick, M. (2014) Numerical simulation of the plasma-MIG process – interactions of the arcs, droplet detachment and weld pool formation. *Welding in the World*, **58**, 85–92.
13. Yang, T., Xu, K., Liu, Y. et al. (2013) Analysis on arc characteristics of plasma-MIG hybrid arc welding. *Transact. China Welding Inst*., 34(**5**), 62–66.
14. Kornienko, A.N., Makarenko, N.A., Granovskij, A.V. et al. (2001) A universal source for plasma-MIG surfacing and welding. *Svarochn. Proizvodstvo*, **9**, 25–26.
15. Oliveira, M.A. de, Dutra, J.C. (2007) Electrical model for the plasma-MIG hybrid welding process. *Welding & Cutting*, 6(**6**), 324–328.
16. Pentegov, I.V., Sidorets, V.N. (1990) Energy parameters in a mathematical model of a dynamic welding arc. *Welding International*, 4(**4**), 272–275.
17. Pentegov, I.V., Sydorets, V.N. (2015) Comparative analysis of models of dynamic welding arc. *The Paton Welding J*., **12**, 45–48.
18. Pentegov, I.V., Sydorets, V.N. (1991) Quasistatic and dynamic volt-ampere characteristics and time constant of blown and moving arcs. *Ibid*., **3**, 361–364.
19. Gao, H.-M., Bai, Y., Wu, L. (2008) Comparison between plasma-MIG and MIG procedures on 5A06 Aluminum Alloy. *Mat. Sci. Forum*, **575–578**, 1382–1388.
20. Matthes, K.-J., Kohler, T. (2002) Electrical effects and influencing quantities in the case of the hybrid plasma-MIG welding process. *Welding & Cutting*, **2**, 87–90.

Received 11.05.2017

doi.org/10.15407/tpwj2017.05–06.13

MONITORING OF TECHNOLOGICAL PROCESS OF ARC ROBOTIC WELDING

I.O. SKACHKOV
NTUU «Igor Sikorsky Kyiv Polytechnic Institute»
37 Peremogy Av., 03056, Kiev, Ukraine. E-mail: i.skachkov@kpi.ua

Continuous monitoring of welded structure production is important to provide under conditions of robotic welding. As for MIG/MAG welding the preference should be given to control of electric parameters of arc, which generalize the conditions of technological process during 1 s. A complex evaluation of the electric parameters can be carried out in «arc current–arc voltage» area. The conclusions on presence of the disturbances should be made using coefficients of Haar wavelet decomposition. 5 Ref., 1 Table, 2 Figures.

Keywords: *gas-shielded consumable electrode welding; robotization, quality monitoring, 2D Haar wavelet transforms*

Assurance of welded joint quality under production conditions is mostly resulted in stabilizing production conditions in all aspects. This requires strict control of technology, equipment condition and support of respective personnel qualification. Robotization promotes fulfillment of indicated conditions, and, at the same time requires their strict execution. However, even strict keeping all the quality assurance requirements necessitates application of technological process control and testing of finished products. The most widespread procedures of production quality conformity assessment are as a rule statistically valid plans for random control using the procedures [1] adequate as for selected groups of defects. In regard to welding all known methods of joint quality control have limited application sphere, i.e. they can determine only some groups of defects.

These control procedures can be divided on two classes by their effect on material or product, namely methods of destructive and non-destructive testing. Obviously, that destructive testing methods are used only optionally and can provide evaluation of quality of the products being subjected to running with some probability. All non-destructive methods used in industry for welded joint testing are directed on detection of specific defects that result in violation of the conditions as for integrity, geometry, physical-mechanical properties or physical-chemical properties of the weld as well as near-weld zone. Due to technical and economical reasons the methods of non-destructive testing in the majority of cases are also used optionally and, therefore, can provide only probabilistic assessment of product quality.

This provokes a necessity in monitoring the process of welded structure manufacture that includes testing of quality of finished or intermediate product by destructive and non-destructive testing methods as well as control of conformity of the parameters of technological process to set ones.

Preparation of production in robotic welding is directed on development of the conditions that provide stability of welding conditions together with solution of other problems. However, this can not completely eliminate appearance of different formation defects and metallurgical defects, which appear due to series of energy, kinematic and technological disturbances, caused by random outside factors such as variation of mains voltage as well as failure of equipment. The latter can pollute welded surfaces with oil, break gas shield, etc. Some technological disturbances, as a rule, take place due to technical and economical restrictions on increase of accuracy of part preparation for welding. It is often impossible on technical or economical reasons to measure or at least evaluate the level of pollution in robotic welding. This, first of all, refers to such factors as break of gas shield, change of gap or exceed of edges, presence of pollution on the part surface. However, such disagreements of the conditions of welding process can have significant effect on weld formation. In robotic welding, joint quality control is carried out only at specific stages of technology process of structure manufacture. Therefore, disagreements in welding process can result in substantial material expenses.

Traditionally, monitoring of technological process mode parameters is carried out by means of registration of their deviations from set values. The number of parameters is determined by welding method and

possibility of measurement of controlled parameters in welding of specific product. Some generalized evaluation of the parameter, i.e. average or root-mean-square value is subjected to control.

Large number of controlled parameters provokes a problem of their complex evaluation. Combination of values of large number of the parameters, which are within the limits of set tolerances, can sometimes result in a defect due to their unfavorable combination. Reduction of the tolerances at that can result in declaration of some part of quality products as invalid ones.

The most acceptable and physically grounded method of continuous monitoring of quality of welded joint made by electric welding is the analysis of energy parameters of welding process [2]. Presence of natural feedbacks between a heat source and a joint, that is formed, allows evaluating the process of joint formation using electric parameters of the heat source. Natural variation of formation process leads to appearance of stochastic component in electric parameters of the heat source. The stochastic component gives different reflection of process of joint formation for different methods of welding. Thus, in MIG/MAG welding, presence of the disturbances results in change of movement of electrode spot on pool surface and violation of axisymmetry of the forces acting the electrode metal drop, i.e. electrode metal transfer. This effects the instantaneous values of current and arc voltage and enters some stochastic components in oscillograms. So, the main idea of monitoring lies in comparison of some ideal image of stochastic process with current one.

The investigations were carried out in welding of sheet steel using consumable electrode ER-49-1 (Sv-08G2S) of 0.8 mm diameter in MIX1 (82 % Ar + 18 % CO_2) mixture at 80A current. Variations of arc electric parameters under disturbances effect were investigated.

Record of the arc electric parameters in welding was carried out by measurement system that included PC, probes of current LA-305S/SP1 and voltage LV-25P based on Hall effect, analogue-digital converter E-140 and PC with installed in it L-graph program. Frequency of analogue-digital conversion made 10 kHz for each channel.

Process of gas-shielded consumable welding can be divided on a range of similar cycles of melting and electrode metal transfer. Electric parameters of each cycle have some, often significant, differences from other due to presence of large number of various disturbances. Thus, evaluation of the process may be statistical and conclusions on presence of substantial disturbances of the process or defect formation are probabilistic.

Previous preparation of data lied in withdrawal of error values caused by electromagnetic interferences, from received oscillograms. Such error values are random, have significant amplitude and occur quite rarely, namely one-two for 30–50 thou of measurements. This allows changing them on an average sample value without loss of statistical reliability. In order to elimi-

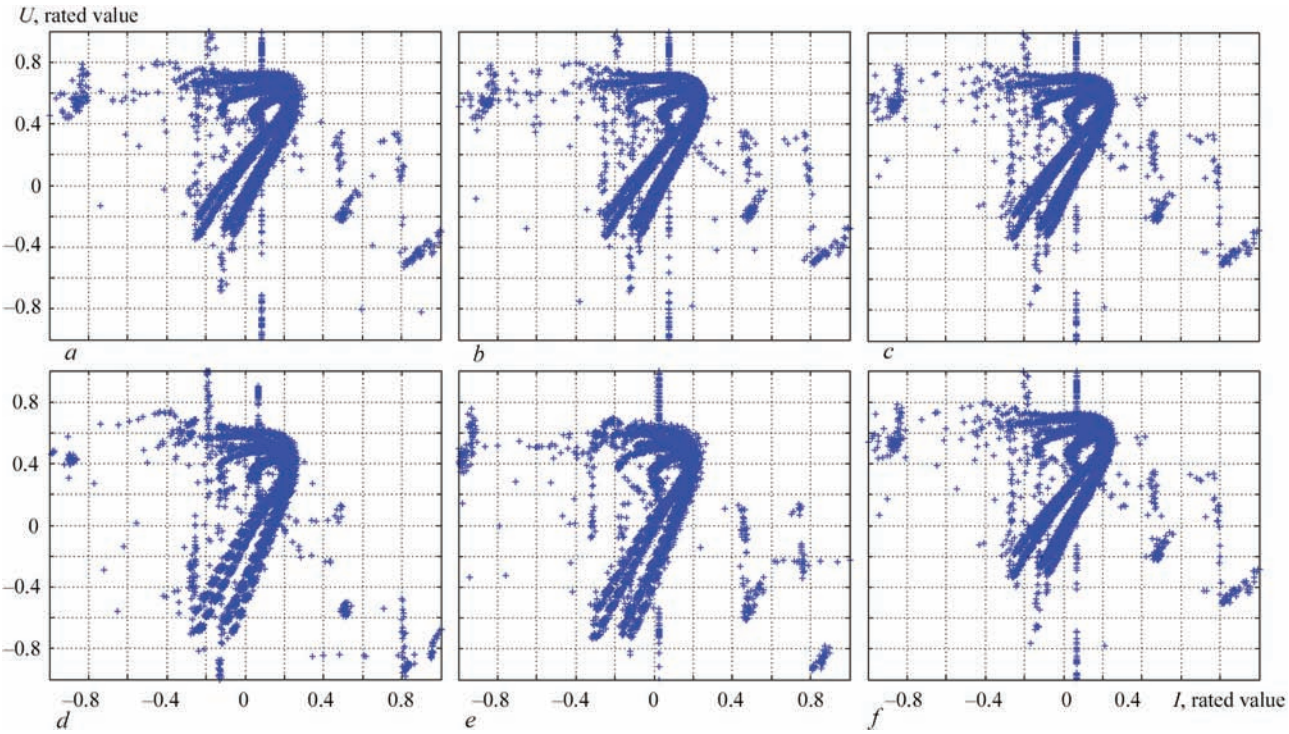

Figure 1. Rated diagrams of «current–voltage» of welding process (description *a–f*) see in the text)

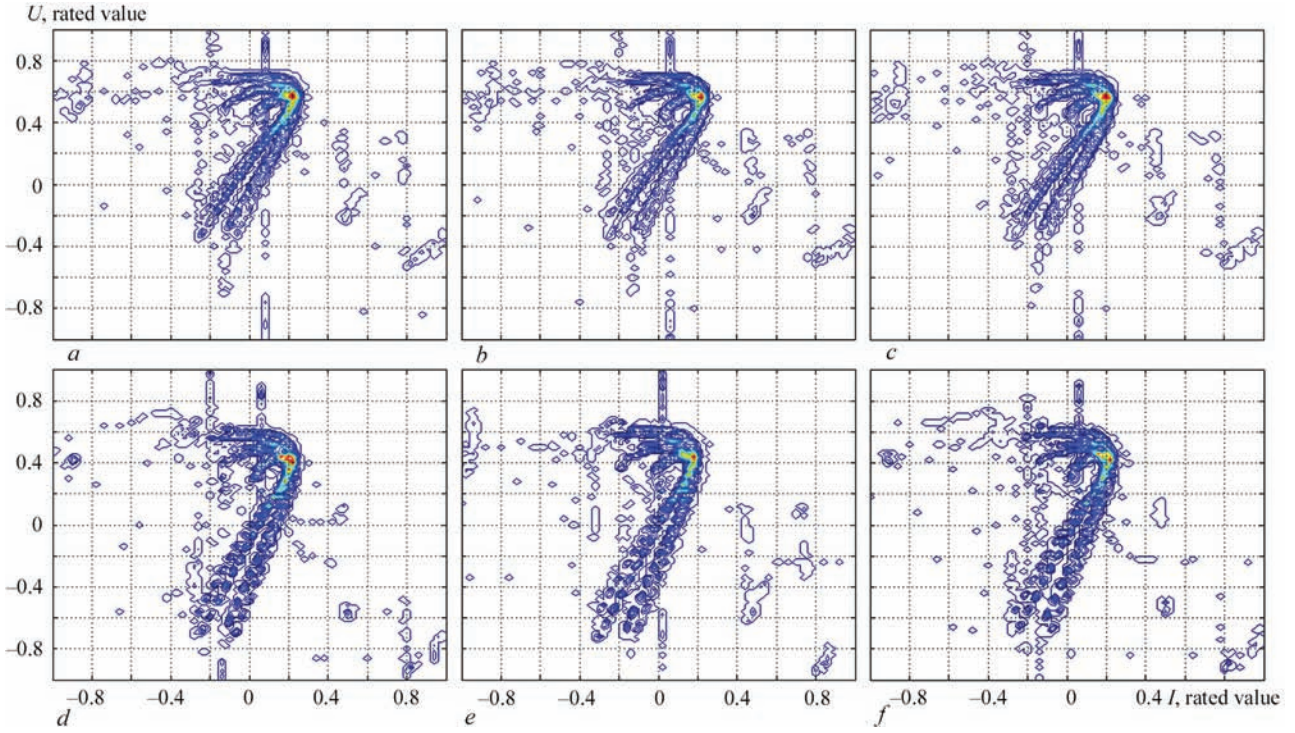

Figure 2. Density of location of points in «current–voltage» diagrams (*a–f* see Figure 1)

nate effect of scale factor in the analysis the welding process evaluation was carried out using rated to [–1, 1] range of current and voltage oscillograms.

Stability of arc burning in welding was evaluated on density of points location on a diagram of voltage-to-current dependence (Figure 1), received from current and voltage oscillograms. If process is stable, the diagram points should clearly match one with another forming even a complex trajectory line. However, stochastic nature of the process of electrode metal transfer, caused by random actions of different nature and intensity, results in diffusion of the diagram. It is reasonable for analysis to evaluate a process progress in a period of time that is insufficient for formation of joint defects, but not too long for «absorption» of effect of disturbances due to sample averaging. For the weld made without disturbances, the diagrams (Figure 1, *a–c*) of process progress in time intervals 10–11 s, 20–21 and 30–31 s have stationary stochastic component, i.e. the process can be regarded as ergodic. Introduction of a disturbance in welding (oil pollution of the specimens) results in change of diagram form with obvious increase of the stochastic component (Figure 1, *d–f*). Presence of the disturbances provokes not only increase of points spread, but also transform stochastic process in non-ergodic.

It is reasonable to calculate density of points location in Figure 1 on «current–voltage» area (Figure 2) for quantity evaluation of level of process stochastic property.

It can be seen that such a representation allows data reduction. Dividing the «current–voltage» area on 0.01×0.01 squares the amount of data for analysis of the process progress during 1 s decreases 10000 times. Received in such a way matrix of whole numbers can be analyzed as digital image. The main task of processing is to find effective presentation, which allows providing image in compact form. Current processing theory and practice widely use wavelet transforms [3–5].

The wavelets that are determined as a function of one real variable are used very often in practice. 2D discrete wavelet transform, that is based on one-dimensional wavelet transform and does not depend on number of columns and rows of the image, are used for the analysis. Therefore, the preference is given to horizontal and vertical directions. Haar wavelets made a good showing for processing of discrete

Specifying coefficients of Haar wavelet decomposition

Specifying coefficients of level 6		Diagram
–25.5787037037037	0.810185185185186	Fig. 1, a
–67.4479166666667	0.192901234567901	
–45.1976102941177	0.0574448529411765	Fig. 1, *d*
–59.2026654411765	0.0114889705882353	
–27.1956699346405	0.714869281045752	Fig. 1, *b*
–71.5788398692811	0.224673202614379	
–40.5063291139241	1.84928797468355	Fig. 1, *e*
–52.7986550632912	0	
–22.8591160220995	0.656077348066299	Fig. 1, *c*
–59.4872237569061	0.129488950276243	
–39.6990740740741	0.578703703703704	Fig. 1, *f*
–52.8549382716050	0.0385802469135803	

one-dimensional and 2D signals. Haar transform does not require complex calculations and is divisible.

The significant difference of the problems of traditional image analysis from the problems that requires monitoring of technological process progress is a need in evaluation of level of noises and not their suppression. In practice this means that it is necessary to evaluate the values of only specifying coefficients of wavelet transform.

Matrix of 100×100 size can have Haar decomposition up to level 7. However, the difference between a set of specifying coefficients becomes apparent only at level 6 (4 coefficients). Increase of level to the second allows determining more differences between the diagrams, but at the same time rises the number of coefficients for analysis (26×26) (Table).

Automation of the analysis is possible in application of methods of artificial intelligence based on artificial neuron nets.

Conclusions

1. Monitoring of conformity of technological process of MIG/MAG welding is reasonable to perform using arc electric parameters.

2. Monitoring should be carried out following the data, which average conditions of technological process progress in 1 s.

3. Complex evaluation of arc electric parameters on «arc current–arc voltage» area is reasonable for reduction of time of information processing without its loss.

4. Conclusions on presence of the disturbances is appropriate to make using the specifying coefficient of Haar wavelet decomposition.

1. Tatarychkin, I.O. (2002) *Statistical methods of quality assurance of products of welding production*. Lugansk: V. Dal EUNU.
2. Li, X.R., Shao, Z., Zhang, Y.M. et al. (2013) Monitoring and control of penetration in GTAW and pipe welding. *Welding J.*, **6**, 90–196.
3. Gonzalez, R.C., Woods, R.E. (2001) *Digital image processing*. Boston: Addison Wesley.
4. Pratt, W.K. (2001) *Digital image processing*. N.Y.:Wiley Intersci.
5. Chui, Ch. (2001) *Introduction to wavelets*. Moscow: Mir.

Received 25.04.2017

doi.org/10.15407/tpwj2017.05–06.14

INFLUENCE OF FLASH BUTT WELDING PROCESS PARAMETERS ON STRENGTH CHARACTERISTICS OF RAILWAY RAIL BUTTS

P.M. RUDENKO, V.S. GAVRISH, S.I. KUCHUK-YATSENKO, A.V. DIDKOVSKY and **E.V. ANTIPIN**
E.O. Paton Electric Welding Institute, NASU
11 Kazimir Malevich Str., 03680, Kiev, Ukraine. E-mail: office@paton.kiev.ua

The analysis of basic parameters of flash butt welding was carried out according to the data of current technological reports formed by the computer control system during welding of rails. The opportunity to develop the model for predicting the output quality index of welded butt of a rail, i.e. fracture load of specimen and deflection, was shown based on the parameters of welding process applying different methods of statistical analysis, in particular, correlation and regression analysis and neural networks. The calculations were carried out according to the experimental data obtained at the Kiev rail welding enterprise during welding of rails in the welding machine K1000. 6 Ref., 2 Tables, 5 Figures.

Keywords: *flash butt welding, statistical models of monitoring and control, monitoring of process parameters, statistical control*

During welding of railway rails in the stationary and suspended flash butt welding machines, the monitoring of the mode technological parameters is carried out with their registration by the computer system for each welded butt. Simultaneously, ultrasonic testing of these butts is carried out. Periodically, mechanical tests of welded rails are carried out and the conclusion on the conformity of this technological mode to the required welding quality is issued. The monitoring of the process is carried out by checking the presence of mode parameters in the allowances preset by technical specifications (TS) [1].

At the present time the stationary and mobile rail welding machines of the new generation of K1000, K920, K922 types are equipped with the computerized control systems. The schemes for control of the machines are designed on the basis of SIEMENS industrial controllers. The modern element base allowed a high accuracy reproducing the values of the mode parameters, regulated by TS for welding of railway rails. However, even in this case, it is impossible to exclude the probability of defects arising in welded joints, if under the influence of random external factors the heating zone, plastic deformation or stability of flashing changed. In the industrial conditions different technological and electrical disturbances arise, which lead to violation of the process stability and deterioration of the welding quality. It is necessary to find new parameters and algorithms of control which increase the probability of predicting the quality of welded joints.

The aim of this work is the development of algorithms for control of flash butt welding process in the stationary and field conditions, providing the control of quality of butts based on the process parameters and monitoring the technical condition of welding equipment. These algorithms are embodied into a two-level system of monitoring and control. Such system besides a direct digital control of welding process and monitoring of process parameters in accordance with allowances, performs the following functions:

- prediction of the quality of welded butt by the process parameters and increase in its validity due to application of more advanced algorithms and involving the qualified specialists in the prediction;
- monitoring of technical condition of welding equipment, systematization of types of wear of welding equipment components, their dividing into common ones for all machines of the given type and specific ones for definite machines, working out of recommendations and planning the maintenance of welding equipment;
- detection and recognition of emergency situations (inadmissible deviations in welding process parameters, technical condition of equipment, performance of auxiliary technological operations, data of mechanical tests, inadmissible voltage deviation, cooling, etc.) for immediate intervention to the technological process;
- systematization of deviations of welding process parameters, which can lead to deterioration of the quality indicators of welded joints, working out of

recommendations on the correction of welding mode parameters;

● indirect control during welding process deviations in the implementation of auxiliary technological operations (preparation of edges for welding), in the state of auxiliary objects (transformer substation, equipment for edges preparation).

The control algorithms are based on the analysis of welding process parameters, which are displayed in the technological report of the computer control system. An example of the report is given below: v_{fl} — 0.108 mm/s; S — 26.1 mm; T — 67 s; U_1 — 412 V; U_2 — 320 V; I — 359 A; v_f — 1 mm/s; P_a — 136 atm; L_{ups} —15.5 mm; T_{upsI} — 1.4 s; $Z_{sh.-c}$ — 104.5 μOhm; Q — 2271 W·h; v_{ups} — 68 mm/s; P_{fr} — 2400 kN; L_{defl} — 48 mm.

Here, v_{fl} is the flashing speed; S is the allowance for flashing; T is the welding duration; U_1 is the voltage at the 1st stage; U_2 is the voltage at the 2nd stage; I is the welding current; v_f is the forcing speed; P_a is the pressure; L_{ups} is the allowance for upsetting; T_{upsI} is the upsetting duration; $Z_{sh.-c}$ is the short circuit resistance of the machine circuit; Q is the total energy; v_{ups} is the upsetting speed; P_{fr} is the fracture load; L_{defl} is the deflection.

The aim of investigations was checking the opportunity to develop a model for predicting the output quality index of welded butt of a railway rail, i.e. the fracture load of specimen and deflection according to the parameters of welding process using different methods of statistical analysis, in particular, correlation and regression analysis and neural networks. The design strength of welded rails is determined by testing for static transverse bending. Here the value of fracture load P_{fr} and deflection of the rail L_{defl} are registered under the action of this load. The admissible values of these parameters are regulated by TS. The experiments were conducted at the Kiev rail welding enterprise in the welding machine K1000. The data

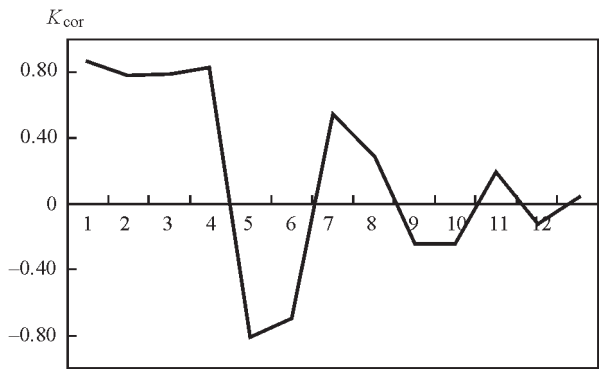

Figure 1. Correlation coefficients of process parameters with the value of fracture load of specimen in descending order: *1* — U_1; *2* — U_2; *3* — I; *4* — L_{ups}; *5* — S; *6* — v_{fl}; *7* — T_{upsI}; *8* — P_a; *9* — v_{ups}; *10* — $Z_{sh.-c}$; *11* — Q; *12* — T; *13* — v_f

of process parameters (162 sets) were measured and monitored by the monitoring and control system of welding machine. All the further investigations were carried out with the help of programs Excel 2010 (Microsoft) and Statistica v.10 (StatSoft, Dell) [2].

Each of the controlled parameters determines the course of the process at separate stages: 1 — fusion of the bevel (U_1); 2 — flashing (U_2, I, v_{fl}, Q); 3 — forcing (v_f, $T_{sh.-c}$); 4 — upsetting (v_{ups}, L_{ups}, P_a, T_{upsI}).

The parameter S characterizes the process before upsetting (1, 2, 3 stages), T characterizes the process over the welding time (1, 2, 3, 4); $Z_{sh.-c}$ — technical condition of welding machine.

To control the process the presetting of each stage is carried out according to the travel of a moving column, i.e. on achievement of the preset S (typical mode for the machines K920 and K1000). Thus, the parameter S, as well as U_1, U_2, L_{ups}, P_a, T_{upsI} are stabilized by the control system. Other parameters like I, v_{fl}, Q, v_f, $T_{sh.-c}$, v_{ups}, $Z_{sh.-c}$, T are determined by the conditions of running process (presence of disturbances, technical condition of welding equipment, qualification of welder and auxiliary workers).

If a particular parameter has a constant value, there is no sense to introduce it into the model [3, 4]. However, all the abovementioned parameters except of $T_{sh.-c}$ have scattering from ±8 to ±100 % and are appropriate for study.

The deviation of the process parameters (±) in the investigated experiments is the following: v_{fl} — 99 mm/s; S — 17 mm; T — 68 s; U_1 — 8 V; U_2 — 8 V; I — 41 A; v_f — 67 mm/s; P_a — 9 atm; L_{ups} — 14 mm; T_{upsI} — 56 s; $Z_{sh.-c}$ — 9 μOhm; Q — 49 W·h; v_{ups} — 79 mm/s; P_{fr} — 38 kN; L_{defl} — 39 mm.

From the data of correlation analysis (Table 1) the following parameters in the descending order (Figure 1) have the greatest relation with the output–fracture load P_{fr} (Figure 1): U_1 ,U_2, I, L_{ups}, S, v_{ups}, T_{upsI}, P_a, v_{ups}, $Z_{sh.-c}$, Q, T, v_f. The latter two of them are lower than the Student's value (0.159) and 6 are lower according to the Chaddock 0.3). To evaluate the relation strength in the theory of correlation, the scale of the English statistician Chaddock is applied: weak — from 0.1 to 0.3; moderate — from 0.3 to 0.5; significant — from 0.5 to 0.7; high — from 0.7 to 0.9; very high (strong) – from 0.9 to 1.0.

From the coefficients of mutual correlation between the parameters, it follows that:

● high relation (0.7–0.9) between U_1, U_2, I, L_{ups}, S;

● high relation of v_{fl} with this group except of S (0.67) and Q (0.64);

● Q has a high relation with T (0.8) and an average one with v_{fl} (0.64);

Table 1. Correlation coefficients between welding process parameters

v_{fl}	S	T	U_1	U_2	I	v_f	P_a	L_{ups}	T_{upsI}	$Z_{sh.-c}$	Q	v_{ups}	P_{fr}	L_{defl}	
1.00	0.67	–0.34	–0.78	–0.67	–0.70	–0.14	0	–0.82	–0.45	0.12	–0.64	0.15	–0.69	–0.46	v_{fl}
	1.00	0.30	–0.89	–0.82	–0.88	0.13	–0.46	–0.74	–0.38	0.37	–0.05	0.35	–0.81	–0.54	S
		1.00	–0.09	–0.16	–0.23	0.14	–0.35	0.05	0.03	0.35	0.80	0.17	–0.13	–0.04	T
			1.00	0.87	0.83	–0.03	0.32	0.91	0.62	–0.28	0.25	–0.29	0.86	0.59	U_1
				1.00	0.74	–0.09	0.32	0.81	0.62	–0.18	0.15	–0.20	0.78	0.47	U_2
					1.00	0.07	0.22	0.75	0.33	–0.40	0.27	–0.34	0.79	0.51	I
						1.00	–0.49	0.10	0.09	–0.03	0.31	0.07	0.03	0.13	v_f
							1.00	0.11	0.17	–0.32	–0.37	–0.13	0.29	0.13	P_a
								1.00	0.72	–0.14	0.39	–0.17	0.82	0.58	L_{ups}
									1.00	0.10	0.24	0.05	0.55	0.37	T_{upsI}
										1.00	0.13	0.22	–0.24	–0.16	Z
											1.00	0.01	0.19	0.12	Q
												1.00	–0.24	–0.14	v_{fl}
													1.00	0.67	P_{fr}
														1	L_{defl}

● rest parameters T_{upsI}, P_a, v_{ups}, $Z_{sh.-c}$, T, v_f have a relation with other parameters below the average one.

Checking the correlation relations of second-order parameters at the stage of flashing showed that these parameters changed little the pattern of relation with P_{fr}.

The analysis of data with deflection shows a clearly worse dependence, which can be connected with the measurement accuracy.

Taking into account the data of theoretical and experimental investigations, at the first stage the linear regression from the following parameters was plotted:

$$v_{fl}, S, U_2, I, P_a, L_{ups}, Z_{sh.-c}, v_{ups}.$$

Further, taking into account the correlation coefficients, the models with different combinations of parameters were calculated:

$$v_{fl}, S, U_2, I, P_a, L_{ups}, Z_{sh.-c}, Q, v_{ups}; v_{fl}, S, U_2, P_a, L_{ups};$$
$$v_{fl}, S, P_a, L_{ups}; v_{fl}, S, U_2, I, L_{ups}, S, L_{ups}.$$

All the mentioned models have a root-mean-square-deviation (RMSD), which equals to 73 kN for P_{fr} and 2.35 mm for L_{defl}.

Table 2. Neural networks based on MLP for the value of fracture force P_{fr} and deflection L_{defl} of specimens

Number	Output variable networks	Input variable networks	Structure	RMSD
1	P_{fr}	v_{fl}, S, L_{ups}, U_2	4-8-1	66.4
2	L_{defl}	v_{fl}, S, L_{ups}, U_2	4-10-1	2.27
3	P_{fr}	v_{fl}, S, L_{ups}	3-4-1	66.1
4	L_{defl}	v_{fl}, S, L_{ups}	3-3-1	2.33
5	P_{fr}	S, L_{ups}	2-4-1	66.8
6	L_{defl}	S, L_{ups}	2-4-1	2.3

Neural networks for modeling the process. Artificial neural network is a mathematical dependence which models a method for processing a definite problem. Obviously, it is considerably simplified and primitive as compared to the biological neurons [5, 6].

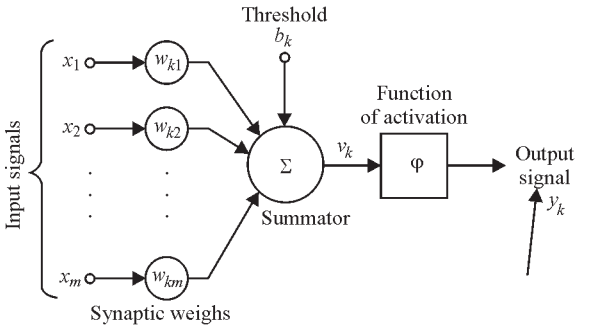

Figure 2. Schematic diagram of artificial neuron

Input signals

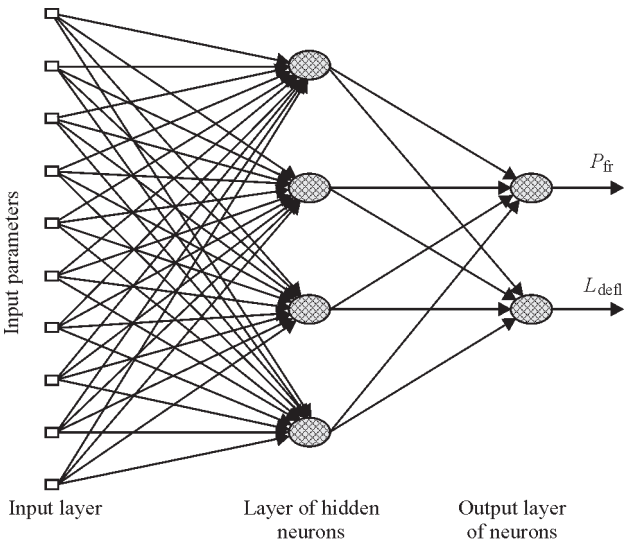

Figure 3. Multilayer perceptron MLP

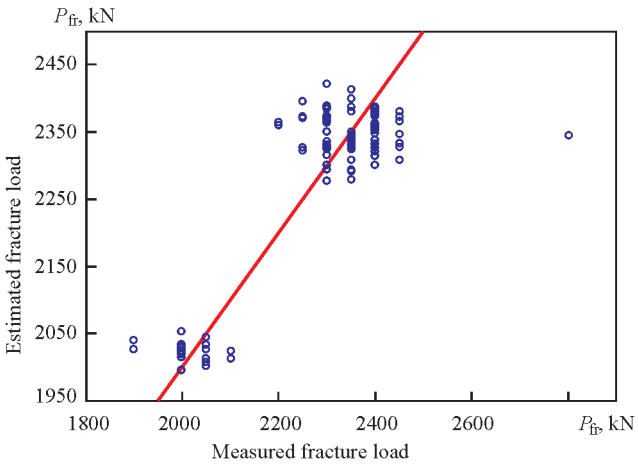

Figure 4. Prediction error P_{fr} by networks 3-4-1, 0.87, 79 kN

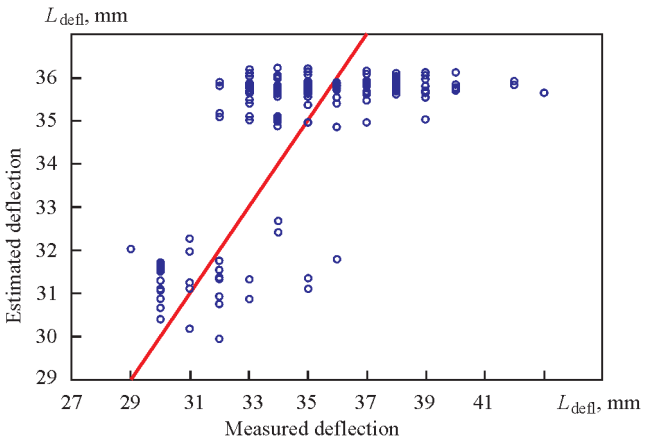

Figure 5. Prediction error L_{defl} on networks 4-10-1, 0.88, 2.27

Having signals or their numerical values at the input of the network, the output signal is uniquely determined by the formula (Figure 2):

$$v_k = \sum_{j=1}^{m} w_{kj} x_j + b_k, \quad y_k = \varphi(v_k).$$

Error of prediction according to the neural network

$$e_k(n) = Y_k(n) - y_k(n),$$

where $Y_k(n)$ is the actual value of output; $y_k(n)$ is the estimated value.

The cost function where the number of step n of the iterative process of adjustment of synaptic weights of the neuron k.

When developing the neural networks, the same input parameters were used as for nonlinear regression without second-order terms. The network structure was in MLP with a one hidden layer, in which non-linearities of approximated dependence are worked out. As a function of activation of internal neurons the hyperbolic tangent and output — identity function [6] were used. The initial weight coefficients were not preset. The training was conducted according to the algorithm BFGS. First, the search for the best network was performed in ANS (automated network search) mode, and then in CNN (custom neural networks) to select the same structure of the hidden layer. The results of calculation are given in Table 2. The prediction errors were shown in the diagrams (Figures 4, 5).

Conclusions

1. The regression models and neural networks with input parameters v_{fl}, S, L_{ups}, U_2, which are included in the technological report of the system for control of welding machine, can be used to predict the strength characteristics of welded butts of railway rails.

2. The developed models have approximately the same prediction error, and a root-mean-square-deviation (RMSD) equals to 73 kN for P_{fr} and 2.35 mm for L_{defl}.

1. Mojseenko, K.V., Mala, T.L. (2016) New welded rails for railways. Specifications. *TU U 24.1-40075815-002:2016*.
2. *Neural Networks*: Manual. www.statsoft.com
3. Mastitsky, S.E., Shitikov, V.K. (2014) *Statistical analysis and visualization of data using R*. Moscow: DMK Press.
4. Dreiper, N., Smith, G. (2007) *Applied regression analysis*. Moscow: Williams.
5. Kruglov, V.V., Dli, M.I., Golunov, R.Yu. (2001) *Fuzzy logic and artificial neural networks*. Moscow: Fizmatlit.
6. Osovsky, S. (2002) *Neural networks for information processing*. Moscow: Finances and Statistics.

Received 12.05.2017

doi.org/10.15407/tpwj2017.05–06.15

DEVELOPMENT OF AUTOMATED EQUIPMENT FOR MANUFACTURING 3D METAL PRODUCTS BASED ON ADDITIVE TECHNOLOGIES

V.N. KORZHIK[1], **A.N. VOJTENKO**[1,2], **S.I. PELESHENKO**[3,4], **V.I. TKACHUK**[1,2], **V.Yu. KHASKIN**[1] and **A.A. GRINYUK**[1,5]

[1]E.O. Paton Electric Welding Institute, NASU
11 Kazimir Malevich Str., 03680, Kiev, Ukraine. E-mail: office@paton.kiev.ua
[2]RPC «PLAZER»
1 Build., 17A General Naumov Str., Kiev, Ukraine
[3]Institute of Mechanical Engineering and Car-Making of South-China University of Technology
381 Build., 381 Wushan Str., Guangdong, Guangzhou, 510641, China
[4]Weihan Science and Technology Company
A4 Bld., Xi'an Av. 1001, Shenzhen, Guangzhou, 518071 China
[5]NTUU «Igor Sikorsky KPI»
37 Pobedi Prosp., Kiev, Ukraine

Additive technologies have huge potential for lowering the energy and material costs for development of the most diverse kinds of products. An increase of the proportion of welding technologies in additive manufacturing of bulk metal products is currently observed. This is associated both with high efficiency of arc welding (surfacing) and with its low cost. The paper describes an automated complex for 3D printing of metal products. It is shown that the developed automated complex allows manufacturing bulk metal products by the methods of additive consumable electrode arc surfacing (at up to 80 A currents), plasma surfacing with wires (at up to 120 A currents) and microplasma surfacing with powder materials (at up to 50 A currents). 10 Ref., 7 Figures.

Keywords: *additive building-up, microplasma surfacing, wires, powders, equipment complex, technological research, metallography*

In the modern world there has been a steady increase in the interest to additive manufacturing processes (3D printing technologies). It is anticipated that application of these processes will fundamentally change industrial production. This is related to such capabilities of additive manufacturing technologies, as realization of automatic part design, flexibility and speed of their manufacture, redistribution of manufacturing from large enterprises to small ones, part manufacturing directly in the user facility [1]. 3D printing technologies allow «building-up» products of any complexity at minimum costs. At the same time, there are practically no production wastes, and the number of service personnel is reduced. Additive technologies have huge potential in terms of lowering the energy and material costs in development of the most diverse kinds of products.

The fullest use of 3D printing capabilities requires availability of technologies of producing high-strength bulk products from metals and alloys, including those of high hardness [2]. Application of metallic materials enables direct manufacturing of a finished product, and not its prototype, as often is the case now [3]. Therefore, development of technologies of additive manufacturing of finished metal bulk products is an urgent task. Such technologies, primarily, include welding processes (for instance, surfacing).

In terms of producing 3D metal products of the highest quality, the processes of Selective Laser Melting (SLM) and Electron Beam Melting (EBM) are the most promising. However, EBM process application has been rather limited, because of complexity, high cost and bulkiness of the used equipment [4].

SLM processes have become very widely accepted now for manufacturing high-strength bulk metal products [5]. This process enables manufacturing products by fusing powders of various metals and alloys by the laser beam. The advantages are high degree of element detailing, high density (up to 99 %), as well as accuracy of about ±5 μm. On the other hand, SLM process, for all its effectiveness and flexibility, also has several limitations, which narrow its application:

- need to apply expensive and energy-consuming equipment with high maintenance costs, that causes a high cost of the process of 3D printing and leads to a high cost of manufactured products;

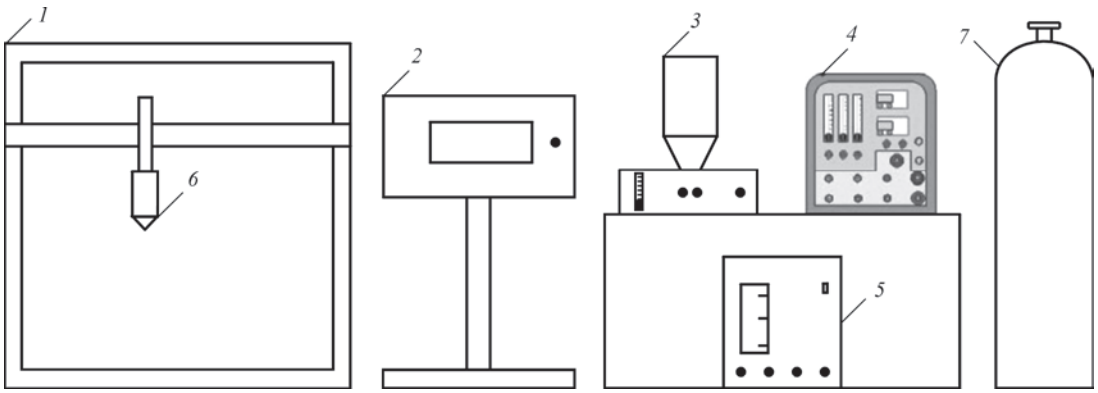

Figure 1. Functional diagram of the equipment complex for manufacturing bulk metal products on the base of plasma and arc surfacing technologies: *1* — three-coordinate positioner; *2* — control system; *3* — powder feeder (wire feed mechanism); *4* — power source module; *5* — autonomous cooling module (ACM) of surfacing head (plasmatron); *6* — replaceable surfacing head; *7* — shielding gas (argon)

● relatively low productivity of 3D printing (usually not more than 10 cm^3/h of incremented metal for the most common machines);

● material limitations — SLM uses expensive powders with strict requirements to granulometric and chemical composition, flowability and other characteristics;

● insufficiently high strength properties of manufactured products.

Application of arc and plasma welding technologies (for instance, surfacing) for manufacturing bulk metal products is of high interest for industry, owing to their technical and economic accessibility. At present research work on 3D arc welding is performed at the University of Nottingham (Great Britain), Wollongong University (Australia) and Southern Methodist University (USA) [6]. Research teams from Indian Institute of Technology (Mumbai, India) and Fraunhoffer Institute for Manufacturing Engineering and Automation (Germany) presented their conceptual ideas of combining welding with milling. Ways of eliminating characteristic defects of formation of bulk products by welding processes have been developed [7]. Need to monitor the temperature of incremented layers was demonstrated. Special attention was given to development of products from titanium [7] and nickel [8] alloys for aerospace applications.

Thus, increase of the fraction of welding technologies in additive manufacturing of metal bulk products is currently observed. This is related both to high productivity of arc welding (surfacing), and to its low cost. Therefore, development of an automated complex for 3D printing of metal products using such technologies, as well as detailed study of their features and prospects for further industrial application, is of interest.

The objective of the work is development of an automated complex for manufacturing bulk metal products by additive technologies of arc and plasma surfacing and investigation of the features of the processes for manufacturing metal 3D products (primitives).

To achieve the defined goal, it was decided to use block-modular architecture of the designed complex. Such an architecture allows easily eliminating the currently used and integrating new required components in one system, combining accessibility and simplicity of complex components with the required technological flexibility and capability of equipment adaptation for various tasks, arising during its industrial operation. Application of this type of complex architecture allowed using three replaceable surfacing heads: arc head with consumable electrode (MIG/MAG), plasma and microplasma heads. This allows readily switching from one surfacing process to another, using their advantages. If it is necessary to build-up large volumes of metal, it is rational to apply MIG/MAG surfacing, and if it is necessary to increase accuracy, reduce the thickness of the deposited wall and lower the roughness, microplasma surfacing should be applied. In addition, gantry-type three-axis positioner was used instead of expensive anthropomorphous robot, in order to increase the competitiveness and reduce the cost of designed complex. Technical advantages of such equipment are simplicity of manufacturing large-sized products, as well as higher accuracy of surfacing tool movement.

As a result, a schematic given in Figure 1, was selected for development of automated complex, according to which control of movement of replaceable surfacing heads *6*, attached to positioner carriage *1*, is performed from the tower of control system *2* in the manual or automatic mode by a preset program. This assembly also controls start/stop signal for power source module *4*. In its turn, module *4* controls the start/stop signal for wire feed mechanism or powder feeder *3* and monitors availability of water flow, supplied by ACM *5*. During operation of the proposed

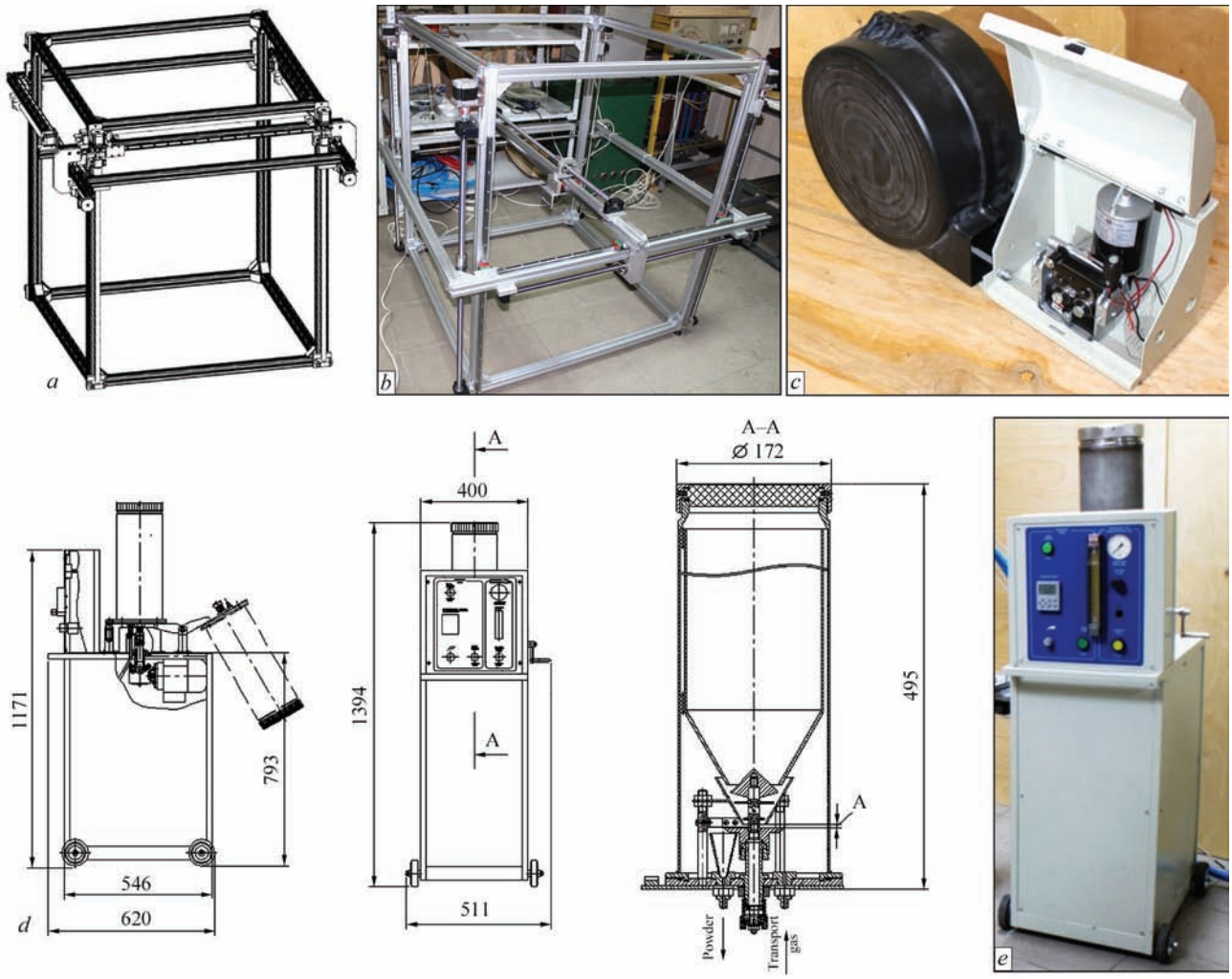

Figure 2. Blocks of automated complex for additive surfacing of bulk metal products: 3D computer model (*a*) and appearance (*b*) of three-coordinate positioner, wire feed mechanism (*c*), drawing (*d*) and appearance (*e*) of surfacing powder meter

complex, the platform on which bulk product is created, is placed on three-axis positioner *1* which performs additive surfacing by spatial movements of head *6* by a program, entered into control system *2*.

Accepted block-modular architecture of automated complex allowed manufacturing its individual blocks irrespective of each other that accelerated and simplified this process. An original inexpensive and adaptable-to-fabrication three-axis positioner of replaceable surfacing heads was developed (Figure 2, *a*, *b*). The positioner working zone accommodates the process platform for manufacturing bulk metal product. As both powders and wires are used as consumable filler materials in such heads, the developed complex was fitted with wire feed mechanism (Figure 2, *c*) and powder meter (Figure 2, *d*, *e*).

Developed automated complex for additive microplasma surfacing of bulk metal products has two power sources, which are inverter-type converters. One of them is designed for realization of additive technologies of plasma surfacing with wire (0.8/1.2 mm diameter) at up to 120 A welding currents and powder microplasma surfacing at up to 50 A welding currents, and the other one is for technology of MIG/MAG arc surfacing with wire (0.8/1.2 mm diameter) at up to 100 A welding currents. Accordingly, the complex is fitted with three replaceable surfacing heads: arc and plasma heads for wire surfacing and microplasma head for powder surfacing. Such heads were designed using Solidworks Flow Simulation design software package [9]. This package uses for modeling one of the subsections of computational fluid dynamics, namely continuum mechanics, including a set of physical and mathematical numerical methods, designed for calculation of flow process characteristics. Owing to this software package, different models of surfacing heads were designed. Modeling of heads for microplasma powder surfacing and virtual check of their performance can be an illustration of it (Figure 3). It was established that the variant of the model of microplasma surfacing head with inner powder feed is the most successful (Figure 3, *f*, *g*, *h*). As a result, designs were selected and heads were manufactured for

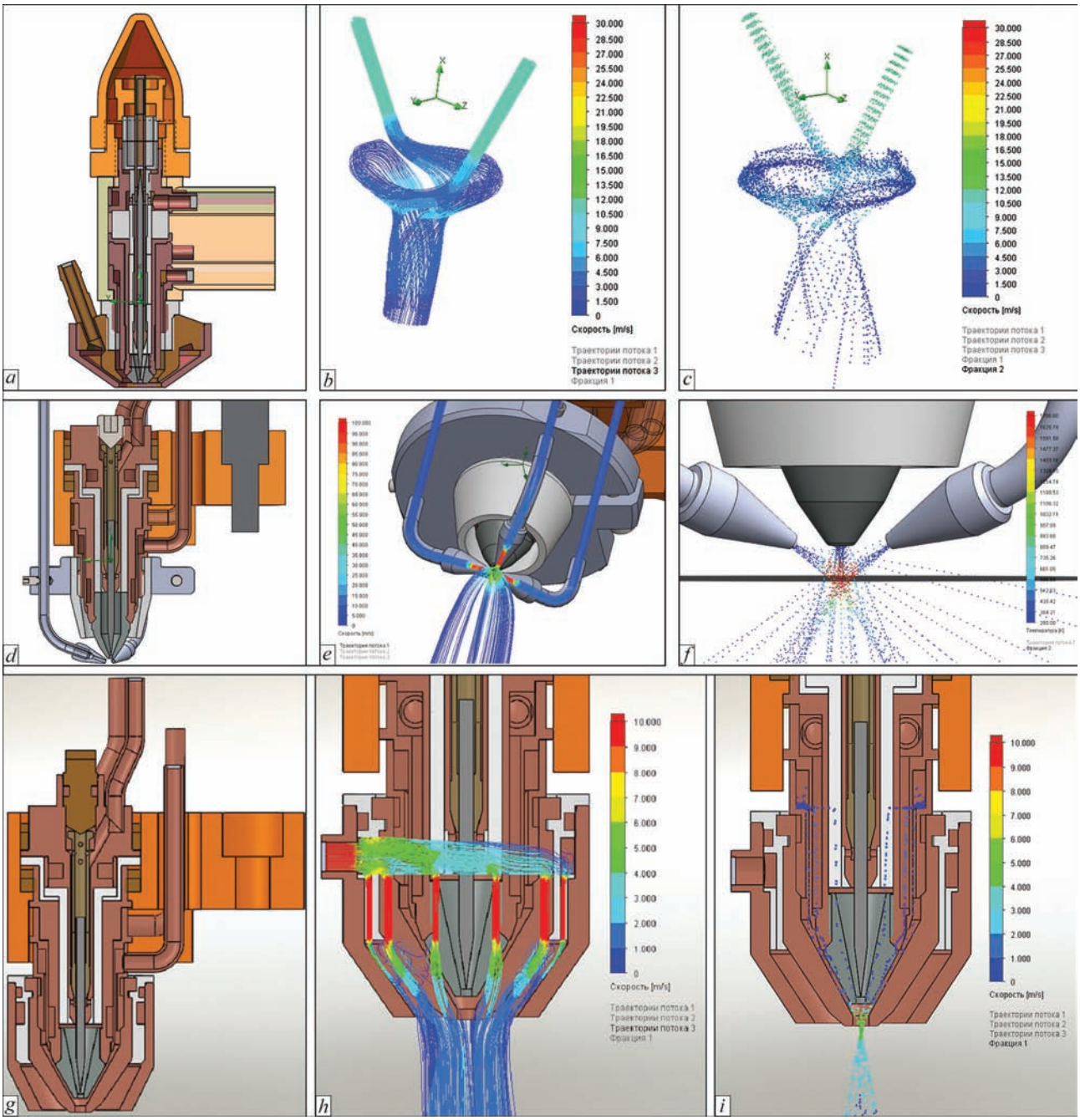

Figure 3. Design (*a*, *d*, *g*), speed and direction of flows of transport gas (*b*, *e*, *h*) and particles of surfacing powder (*c*, *f*, *i*) of various models of microplasma heads; *a–c* — upgraded plasmatron MPU-4; *d–f* — head with powder feeding with three external tubes; *g–i* — head with inner powder feed

the three surfacing processes: MIG/MAG, plasma and microplasma (Figure 4).

The complex includes three-axes positioner of ingenious design with working zone of surfacing head displacement of 900x900x900 mm (Figure 5, *a*). MIG/MAG head operates at direct current. Plasmatrons can operate in the modes of straight polarity direct and pulsed current, mode of different polarity pulses, etc [10]. Control of surfacing head positioning and feeding of wire or consumable powder is performed by CNC system, which is combined with powder source and control panels of wire feed mechanism and powder meter (Figure 5, *b*). Automated additive surfacing complex is controlled by common PLC-controller with the capability of exchanging data of 3D printing modes and controlling commands with the computer.

Developed complex for additive surfacing of bulk metal products was used to perform a number of experiments on manufacturing metal 3D primitives. Used for this purpose was welding wire Sv-08G2S GOST 2246–70 (1.0 and 1.2 mm diameter) and surfacing powder PG-10N-04 TUU 322-19-004–96 (60–100 μm fraction). Products of the type of «wall», «sleeve», «cone», «semisphere» were manufactured

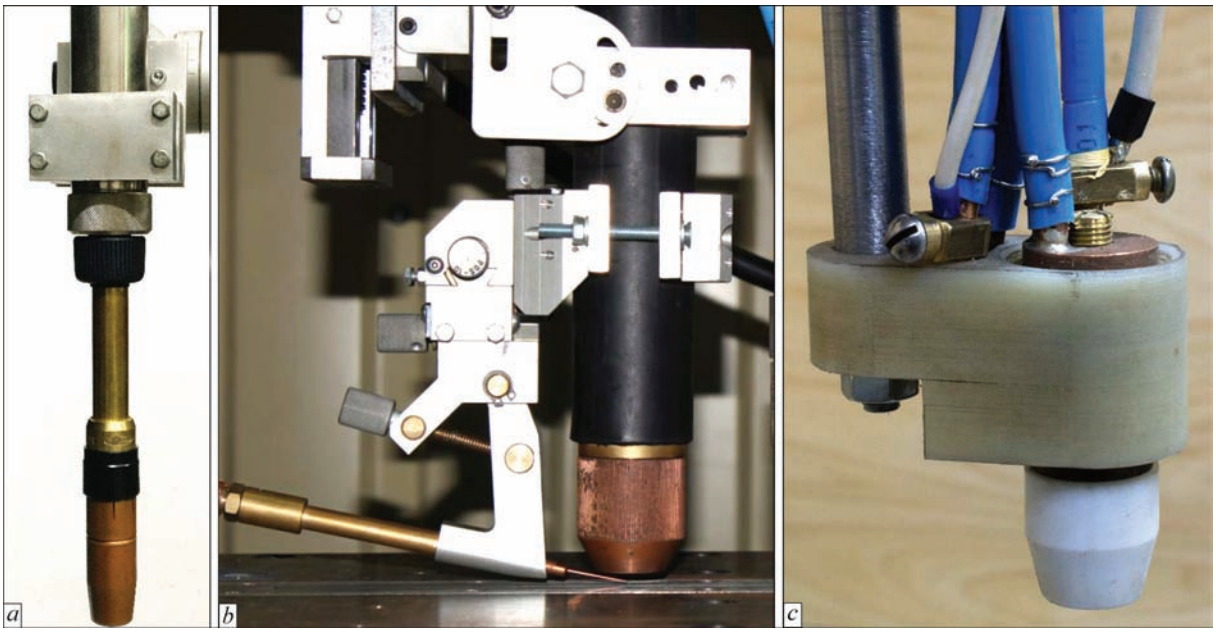

Figure 4. Appearance of surfacing heads: *a* — for surfacing by consumable electrode arc (MIG/MAG); *b* — for plasma surfacing with wires; *c* — for microplasma powder surfacing

(Figure 6). To determine the accuracy of manufacturing these products, their measurement was performed, using a caliper with the price of division of 0.05 mm. It was found that deviations of products produced by additive surfacing from nominal size are in the range of ±0.5 mm. In addition to accuracy determination, also metallographic and mechanical investigations of the manufactured bulk products were performed.

To study the structural features of metal deposited with Sv-08G2S wire (1.2 mm diameter) templates were cut out of «wall» type samples, they were ground and polished, and then etched in 4 % solution of nitric acid. Revealed structures were studied in «Neophot-31» microscope. Polished unetched samples were used to detect porosity and nonmetallic inclusions. These investigations showed that porosity of deposited walls does not exceed 1–2 % (Figure 7, *a*). Studying the sample structure revealed coarsening of dendritic grains in the upper part and availability of finer equiaxed grains in the middle and lower part (Figure 7, *b*). This is attributable to recrystallization of previous deposited layers at deposition of subsequent ones. There are no gaps between the contacting layers or along the fusion line (Figure 7, *c*). Size of HAZ from the built-up layer is equal to 2 mm. Structure of both fusion zone (Figure 7, *d*), and deposited metal is equiaxed, layer mixing is extremely low.

Deposited metal strength was assessed by averaging test results under the conditions of uniaxial static tension of three samples. Testing of samples cut out of deposited walls of type XIII GOST 6996–66 was conducted in an all-purpose servo-hydraulic tensile

Figure 5. Automated complex for additive surfacing of bulk metal products: *a* — manipulator with plasmatron and powder meter-feeder; *b* — appearance of power and control block with open face panel

Figure 6. Metal products, manufactured in the developed complex: *a* — 5×70 mm wall; plasma surfacing with Sv-08G2S wire (1.2 mm diameter) in 50 passes; *b* — cone, surfacing with Sv-08G2S wire (1.0 mm diameter); *c* — 80 mm diameter sleeve, MIG/MAG surfacing with Sv-08G2S wire (1.2 mm diameter); *d* — 40 mm diameter sleeve, microplasma surfacing with PG-10N-04 powder

testing machine MTS 810. Their results showed that mechanical strength of products made by additive plasma surfacing with Sv-08G2S wire is equal to about 90–95 % of that of cast metal.

The main disadvantages of the developed technological processes are:

- considerable unevenness and roughness of walls, formed by additive arc and plasma surfacing of products;
- overheating of product walls during surfacing, leading to their thermal deformation.

To eliminate the first of these disadvantages, it is rational to use traditional machining, for instance, turning (Figure 6, *c*). The second disadvantage can be eliminated by application of laser pyrometer, continuously monitoring the temperature of deposited walls and transmitting information to the control system. The latter can correct the surfacing mode in accordance with the level of product heating. Another variant of elimination of this drawback can be forced cooling of the deposited walls of the product.

Thus, the developed automated complex allows manufacturing bulk metal products by the methods of additive consumable electrode arc surfacing (at up to 80 A currents), wire plasma surfacing (at up to 120 A currents) and microplasma surfacing with powder materials (at up to 50 A currents).

Studying the features of the processes of manufacturing metal 3D primitives of «wall», «sleeve», «cone» and «semisphere» type showed that deviations from the nominal size in their manufacturing do not exceed ±0.5 mm, porosity is within 1–2 %, and mechanical strength is of the order of 90–95 % of that of the cast metal. Deposited material structure is fine-grained, equiaxed and layer mixing is extremely low.

1. Kruth, J.P., Leu, M.C., Nakagawa, T. (1998) Progress in additive manufacturing and rapid prototyping. CIRP Annals — Manufact. *Technology*, 47(2), 525–540.
2. Slyusar, V.I. (2003) Fabber-technologies. New mean of three-dimensional simulation. *Elektronika: Nauka, Tekhnologiya, Biznes*, **5**, 54–60.
3. Korzhik, V.N., Khaskin, V.Yu., Grinyuk, A.A. et al. (2016) 3D-printing of metallic volumetric parts of complex shape based on welding plasma-arc technologies (Review). *The Paton Welding J.*, **5/6**, 117–123.
4. Bruce, M.R., Riley, S.F., Cola, M.J. et al. (2012) Measurement and simulation of titanium alloy deposit temperature in electron beam additive manufacturing. In: *Proc. of 9th Int. Conf. on Trends in Welding Research 2012* (June 4–8 2012, Chicago, USA), 963–969.
5. Kruth, J.P. (2004) Selective laser melting of iron-based powder. *J. Mater. Process. Technol.*, **149**, 616–622.

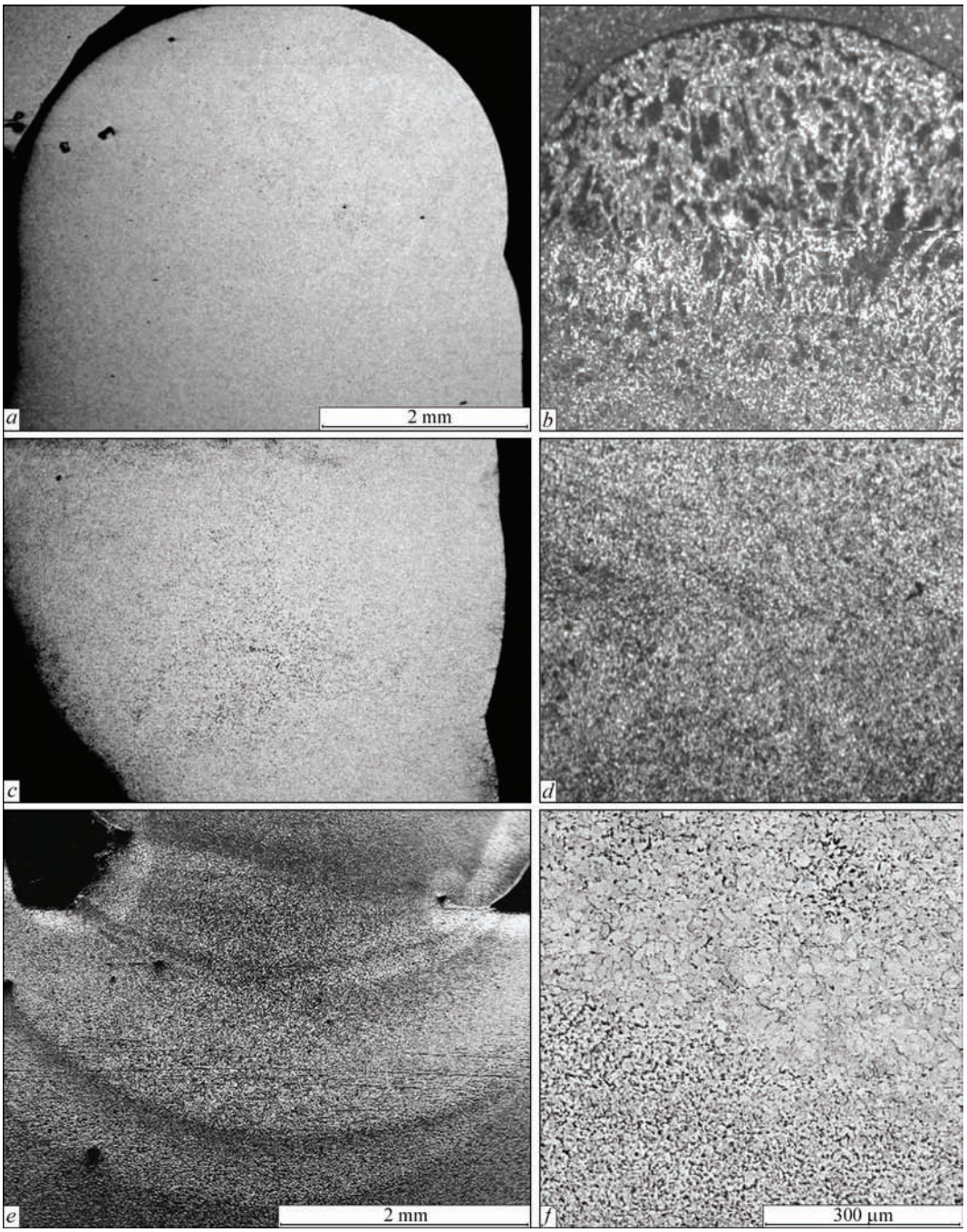

Figure 7. Structures of additive plasma surfacing of «wall» type primitive, using Sv-08G2S wire: *a* — unetched section of upper part; *b* — structure of upper part after etching, ×63; *c* — unetched section of middle part; *d* — structure of middle part after etching, ×63; *e* — fusion line and HAZ; *f* — fusion zone, ×200

6. Alhuzaim, A.F. (2014) *Investigation in the use of plasma arc welding and alternative feedstock delivery method in additive manufacture*: Syn. of Thesis for Master of Sci. Degree. USA: University of Montana.
7. Baufeld, B., Van der Biest O., Gault, R.S. (2010) Additive manufacturing of Ti–6Al–4V components by shaped metal deposition: Microstructure and mechanical properties. *Materials & Design*, **31**, 106–111.
8. Clark, D., Bache, M.R., Whittaker, M.T. (2008) Shaped metal deposition of a nickel alloy for aeroengine. *J. Materials Proc. Technology*, **203**, 439–448.
9. (2009) *Main elements of SolidWorks (SolidWorks 2010)*. Dassault Systems SolidWorks Corp.
10. Grinyuk, A.A., Korzhik, V.N., Babich, A.A. et al. (2016) Unified plasmatron for non-consumable electrode constricted arc welding. In: *Proc. of Int. Conf. on Innovative Technologies and Engineering in Welding — PoliWeld-2016* (26–27 May 2016, Kiev, Ukraine,). Kiev: NTUU KPI.

Received 12.05.2017

doi.org/10.15407/tpwj2017.05–06.16

AUTOMATION OF WELDING PROCESSES WITH USE OF MECHANICAL WELDING EQUIPMENT

I.V. LENDEL[1], V.A. LEBEDEV[2], S.Yu. MAKSIMOV[1] and G.V. ZHUK[2]
[1]E.O. Paton Electric Welding Institute, NASU
11 Kazimir Malevich Str., 03680, Kiev, Ukraine. E-mail: office@paton.kiev.ua
[2]EDTB of the E.O. Paton Electric Welding Institute, NASU
15 Kazimir Malevich Str., 03680, Kiev, Ukraine. E-mail: dktbpaton@gmail.com

The article gives examples of robotization, automation and mechanization of welding and related processes based on mechanical welding equipment (MWE). The composition of complexes and installations applied for welding or surfacing processes includes both serial models of MWE, as well as specially designed ones, taking into account individual features of the product design and technological peculiarities of its manufacture. The wide range of solved problems and the possibility of the domestic manufacturer of MWE to design and manufacture modern high-tech complexes and installations for welding and surfacing are shown. The possibility of designing special MWE for new welding and surfacing technologies in the composition of robotic complexes and automatic installations is noted. 9 Ref., 6 Figures.

Keywords: *arc welding, surfacing, mechanical welding equipment, automation, mechanization*

The performance of welding operations is associated with the need to use a complex of equipment which, often with the participation of welder, provides welds of specified quality and configuration. The influence of dimensions and shape of semi-products, the quality and accuracy of assembly, as well as the change in workpiece dimensions due to thermal deformations on welding conditions is greater than of any other technological process of metal treatment. Therefore, many requirements are specified and great attention is paid to the equipment used for welding operations [1–4].

Depending on the range of components the composition of the complex of technologically interconnected equipment, which provides welding operations, includes:

- power source and welding machine with units of control, adjustment of the process and electrode holder;
- mechanical and auxiliary equipment designed to manipulate workpiece being welded in the process of weld laying-on and to fix and move welding machines;
- technological assembly and welding devices which provide fast and accurate assembly of parts for welding, their holding in the required position during operation and prevention or reducing the distortion of workpiece to be welded.

In each individual case the complex or welding installation can have all the abovementioned elements or some of them. As far as significant time is spent on auxiliary, assembly and additional works, reducing the efficiency of application of advanced high-efficient welding methods, the shortening of production cycle and a high quality of welds can be achieved only with the complex mechanization and automation of welding, assembly and auxiliary operations. The level of complex mechanization determines the presence of technological devices, mechanical, auxiliary and other equipment (transport, control and the like) in the composition of installation [1–5].

As is known, the installation for automatic welding contains devices for laying, assembly and rotation of workpiece being welded, welder's platform and other equipment. In it, at least, two basic operations of welding process are mechanized: electrode feeding and arc movement along the edges being welded. Accordingly, the installations, where only one of these operations is mechanized, are considered to be installations for semiautomatic welding [1–4].

The presence of mechanical and auxiliary equipment in the composition of welding installation has a decisive importance for complex mechanization of welding process. According to the work [6], mechanical welding equipment (MWE) includes: horizontal, vertical and universal manipulators, roller and balancing rotators; chain tilters; pipe rotators. In addition, this type of equipment also includes welding gantries, trolleys, welder tables, and also columns for welding automatic and semiautomatic machines.

Some rigging or the simplest models of auxiliary MWE can be manufactured by the machine-building

Figure 1. Installations for surfacing and restoration of parts: RM-09 (*a*); RM-15 (*b*); IZRM-05 (*c*)

enterprises, in the technological cycle production of which the welding works are present, themselves at their own production facilities. However, often in such cases they turn to the specialists of specialized enterprises who are ready to offer a professional, complex solution for automation and mechanization of welding and related processes.

In Ukraine, an enterprise like that is the PJSC «Ilnitskiy plant of mechanical welding equipment» («IZMSO»), which started its activities since 1964. This enterprise was created for designing and implementation of equipment for automation and mechanization of welding operations. Beginning from the moment of its foundation, it mastered the production of ever more new types of MWE and simultaneously increased the volume of production, which allowed a full satisfaction of the country's needs. In close cooperation with the All-Union Planning and Design Institute for Welding Production (VISP), the production of welding rotators (universal, horizontal, vertical, roller), as well as columns for automatic and semi-automatic welding machines was mastered. Together with the E.O. Paton Electric Welding Institute the production of new models of torches of such types as A1231 and GDPG-305 for electric arc welding was mastered, as well as modernization of the torch A-547uM was carried out. The joint work of Ukrainian partners made it possible to produce the equipment and complexes for surfacing and restoration of parts of metallurgical companies and repair plants.

This is confirmed by such complexes as: RM-04, RM-05, RM-06, RM-09 (Figure 1, *a*)

- for automatic arc surfacing of wheels of hoisting cranes; RM-15 (Figure 1, *b*) is the universal installation for surfacing of rope blocks of up to 2.5 m diameter and other cylindrical and plane parts; RM-165 and IZRM-05 (Figure 1, *c*)
- for automatic arc surfacing of small-sized cylindrical parts with diameter of up to 0.5 m, length of up to 1 m and mass of up to 120 kg; RM-10 — for surfacing of rolling tool with diameter of up to 0.6 m, length of up to 2 m, mass of up to 5000 kg and a number of other installations. Depending on the design features and mass-dimensional characteristics of the deposited workpieces, the installations include universal manipulators, columns, roller rotators, welder tables of the PJSC «IZMSO» production in their serial or special version.

To increase the degree of technical and technological characteristics of the produced MWE, the specialists of the PJSC «IZMSO» carry out constant modernization of the manufactured products to provide the possibility for the consumer to install, activate and use systems with new technological solutions and all advantages of modern welding and surfacing equipment, for example, with pulsed technologies. Thus, in a close cooperation with the SE «EDTB of the E.O. Paton Electric Welding Institute of the NAS of Ukraine» the modernization of the installation IZRM-05 was made to enable its equipping with gearless systems for electrode wire feed on the basis of brushless electric motors with the control from computerized regulators. Such systems provide operation with modes modulation and controlled pulsed electrode wire feed. The new feeding systems due to efficient control of electrode metal transfer and reduction of heat inputs to the workpiece in the combination with the considered equipment allow:

- obtaining welding-surfacing with energy- and resources-saving effects;
- reducing deformation of product;
- providing quality process in all spatial positions, including producing horizontal welds in vertical plane and in overhead position.

The rationality of applying manipulators, rotators, mobile columns, and recent developments in the welding and surfacing equipment in the systems is predetermined also by the ability of this equipment to maintain the preset parameters of working movement even in long cycles, with a high degree of accuracy for the working tool positioning. As an example, it can be noted that moving welding columns can perform a high-efficient welding of long products such as of deck type with the possibility of high-precision scanning of relief of surfaces being welded, which is pro-

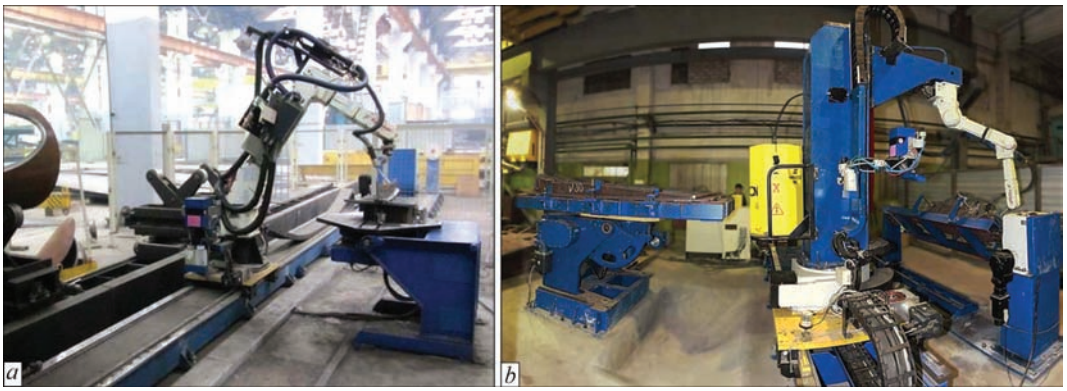

Figure 2. Robotic complexes with application of universal manipulator (*a*), universal and double-post horizontal manipulator (*b*)

vided by using modern computerized electric drives and sensors of distance to the surface being welded.

The next example of complex automation and robotization of welding, surfacing and cutting processes with the use of products of the PJSC «IZMSO» production is the developments of the holding Company «Belfingrupp». This Company specializes in designing and development of robotic technologies and deals with industrial robotics. The specialists of «Belfingrupp» developed and implemented the robotic complex (RTC), which solves such problems as cutting pipes of different diameters and lengths along the complex 3D trajectories. This RTC not only provides a high-precision cutting of holes, but also cutting and trimming of pipes. The equipment allows cutting pipes with a length of up to 12 m and a diameter of up to 1.2 m (Figure 2, *a*).

RTC (Figure 2, *b*) solves more universal tasks for arc welding. The presence of two different types of manipulators in the composition of RTCmanufactured by the PJSC «IZMSO» guarantees the possibility of welding a large and diverse range of products. At present, both RTCs are put into operation and involved in serial production.

There is a large number of realized projects of complex automation and mechanization of welding and surfacing processes, proposed by the experts of the PJSC «IZMSO» using a special MWE of the own design.

They include the complex for welding railway tank cars (Figure 3, *a*) for the PJSC «Kryukov railway car building works», consisting of the bicycle type column KVT-05 and roller rotator. For the Share Holding Company «NIKIMT-Atomstroy» the complex (Figure 3, *b*) of mechanized welding of pipelines with diameter of up to 0.3 m, length of up to 6 m and mass of up to 2000 kg, used at nuclear power engineering facilities, as well as the complex (Figure 3, *c*) for welding elements of up to 2 m in diameter and mass of up to 3000 kg in the active zone of nuclear reactors were designed and manufactured. In the case presented in Figure 3, *b* the complex consisted of a special double-post horizontal rotator, including column for welding machine, and in Figure 3, *c* it consisted of universal manipulator, roller stand and column. The last complex (Figure 3, *c*) was equipped with the special system for butt tracking, which allowed making correction of the rotation speed of driving rolls of the stand to obtain a constant welding speed. For the LLC «MPVF» Energetik», a unique welding complex was developed (Figure 3, *c*), including the special column T-31060 with more than 3 m travel of working body along the horizontal and vertical and the tandem roller stand with a load capacity of up to 5000 kg, which were interconnected by the software. The complex carries out two-sided automatic submerged arc welding of longitudinal and circumferential welds of steam boiler drums, shells of vessels of large diameter and thickness.

In addition, the unique models of MWE were designed and manufactured for the LLC «MPVF «Energetik» at the PJSC «IZMSO», among which the moving gantry (Figure 4, *b*) for welding workpieces with length of up to 7 m and the installation (Figure 4, *c*) for semi-automatic submerged arc welding of circumferential and longitudinal inner welds of vessels of up to 3 m length and the diameter from 0.4 m. The installation (Figure 4, *c*) consists of the column with a stationary beam. At the end of the beam the flux hopper, welding torch and elements of welding process monitoring system are installed. The gantry and the column (Figure 4, *b*, *c*) are able to move along the rail track at a welding speed. Also, to carry out mechanization of welding and related processes, the universal manipulator with a load capacity of 7000 kg (Figure 4, *a*) and the balancing rotator with a load capacity of 40000 kg (Figure 4, *d*) were designed and manufactured for the Ilyich Iron and Steel Works in Mariupol.

The features of the manipulator are the increased dimensional characteristics of a faceplate (1.4 m diameter) and the presence of water cooling of spindle and bearing units of the table. Moreover, the balanc-

Figure 3. Complexes of automation and mechanization of welding processes with use of special MWE

ing rotator has an ability to move along the rail track and, depending on diameter of the workpiece, change the distance between the rollers supports.

It should be noted that in addition to serial equipment, the enterprise solves problems of creating unique equipment with high operation characteristics.

Figure 4. Unique models of MWE: universal manipulator of 7000 kg loading capacity (*a*), moving gantry (*b*), installation for semi-automatic submerged arc welding of circumferential and longitudinal inner welds (*c*), balancing rotator with a load capacity of 40000 kg (*d*)

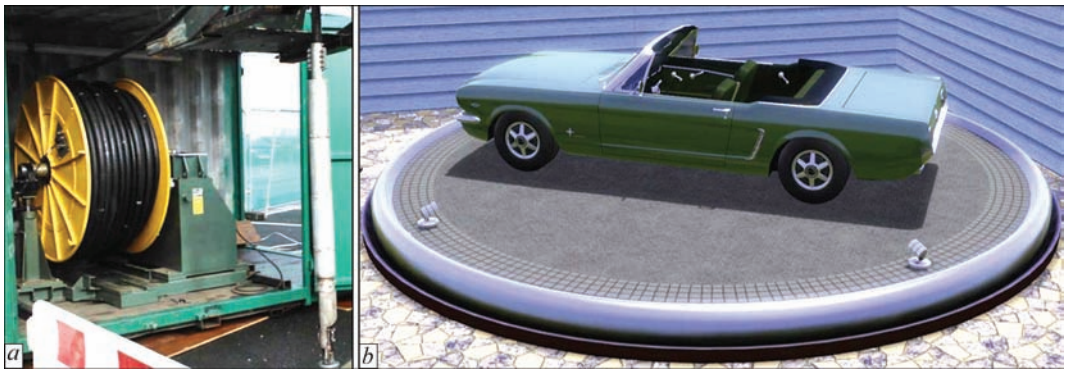

Figure 5. Some other variants for application of MWE: uncoiler for dipping and lifting of welding machine (*a*), demonstration rotating podium (*b*)

The mechanized welding equipment or its separate units and mechanisms can be used also for manufacture of other products. As an example, the development and manufacture of different types of uncoilers (Figure 5, *a*) or demonstration equipment (Figure 5, *b*) can be noted.

A smooth start, providing a stable frequency of spindle and torque rotation over a long period of time, ability of smooth adjustment of the spindle frequency rotation, ability to regulate the speed of gaining the required frequency of its rotation and a high reliability of rotator assemblies were quite appropriate during solution of technical assignment on the development of complex for automatic underwater welding [7] and providing the dipping and lifting of welding machine from the depth of about 200 m, as well as in designing and manufacture of uncoiler for cable assemblies of the deep-water welding complex described in the work [8]. In its turn, the design scheme of vertical rotator is suitable for demonstration rotating podium, which is used, for example, at the automobile exhibitions.

The equipment for new welding and surfacing technologies is developed, in which the oscillation processes are used which allow improving the surfacing process with the increase of its efficiency and obtaining a finely-dispersed structure of the deposited layer [9]. Figure 6 shows installation with controlled oscillations of the product being surfaced, designed and manufactured at the PJSC «IZMSO» according to the technical assignment of the E.O. Paton Electric Welding Institute of the NAS of Ukraine.

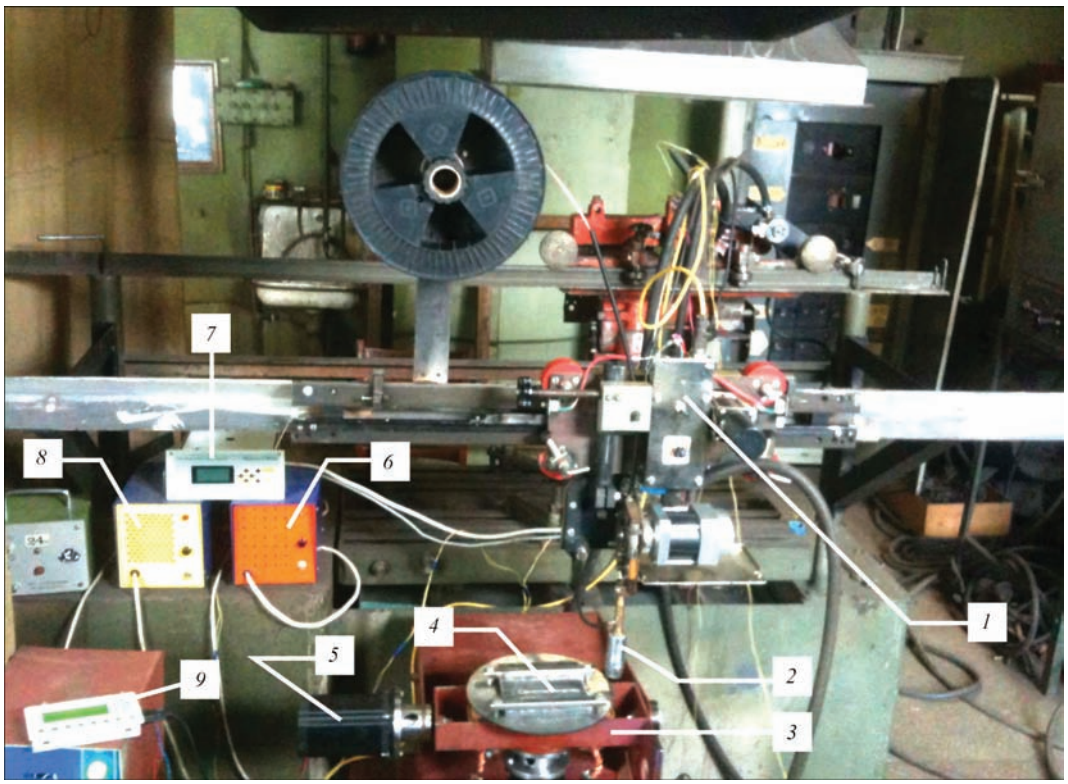

Figure 6. Scheme of installation for surfacing with a movable bed: *1* — control panel for torch moving; *2* — torch; *3* — bed; *4* — part being deposited; *5* — motor, imparting oscillations to the workpiece; *6* — power supply unit of control panel, pos. 1; *7* — indicator of torch speed movement; *8* — power supply unit of motor, pos. 5; *9* — programmable panel for control of motor operation mode, pos. 5

Conclusions

1. As before, MWE remains one of the demanded types of equipment necessary to provide automation and mechanization of welding and related processes, which helps to increase labor efficiency and ensure the specified quality.

2. The application of modern gearless systems for feeding electrode wire on the basis of brushless electric motors with control from computerized regulators provides operation of controlled pulsed electrode wire feed and imparts MWE with new technological capabilities.

3. The use of modern step-type and brushless electric drives, rotation frequency converters of the shaft of asynchronous motors and other electronics greatly facilitates the integration of individual MWE into welding and surfacing complexes, installations and robotic centers under the common control.

4. The modern production of MWE has the opportunity to produce a wide range and model line of serial MWE, and is also ready to develop and manufacture a special MWE taking into account individual wishes of customers.

Authors are thankful to Lendel V.I., the chief designer, and all the staff of PJSC «IZMSO» for the information presented for this article.

1. (1974) *Technology of fusion electric welding of metals and alloys*. Ed. by B.E. Paton. Moscow: Mashinostroenie.
2. Potapievsky, A.G., Saraev, Yu.N., Chinakhov, D.A. (2012) *Consumable electrode shielded-gas welding. Technique and technology of future: Monography*. Tomsk: TPU.
3. Pires, J. Norberto, Loureiro Altino, Bolmsjo Gunnar (2006) *Welding robots. Technology, system issues and application*. Springer-Verlag London.
4. (2011) Arc welding. Ed. by W. Sudnik.
5. (2006) *Industrial robotics: Programming, simulation and application*. Ed. by Low Kin Huat. Pro Literatur Verlag, Germany/ARS, Austria.
6. *GOST 30295–96:* Welding manipulators. Types, main parameters and sizes.
7. Maksimov, S.Yu., Lebedev, V.A., Lendel, I.V. (2015) Sealing of heat exchanger pipes by wet welding at 200 m depth. *Voprosy Materialovedeniya*, **1**, 199–204.
8. Lebedev, V.A. (2015) Mechatronic and other main electrotechnical systems of mechanized equipment for wet underwater welding. *Elektrotechn. i Kompyuternye Sistemy*, **17**, 42–47.
9. Saraev, Yu.N., Lebedev, V.A., Novikov, S.V. (2016) Analysis of existing methods for control of weld metal structure. *Mashinostroenie: setevoy elektronyy nauchnyy zh.*, 4(**1**), 16–26.

Received 26.10.2017

doi.org/10.15407/tpwj2017.05–06.17

APPLICATION OF DIFFERENTIAL-TAYLOR TRANSFORMATION FOR MODELING PROCESSES IN RESONANCE POWER SOURCES

I.V. VERTETSKAYA and **A.E. KOROTYNSKY**
E.O. Paton Electric Welding Institute, NASU
11 Kazimir Malevich Str., 03680, Kiev, Ukraine. E-mail: office@paton.kiev.ua

To model electrical processes in resonance-type arc welding sources, it was proposed to use differential-Taylor transformation, which essentially simplifies computational procedures for analysis of the modes and determination of the main parameters of the secondary circuit. The essence of this method consists in conversion of the time continuous function of the original into the image function from discrete argument, the coefficients of which are called discretes. The accuracy of the derived results is determined by the number of discretes used at the stage of image analysis. 6 Ref., 1 Figure.

Keywords: *original, image, differential-Taylor transformation, DT-model, resonance source*

It is known [1] that differential-Taylor transformation (DTT) proposed and studied by G.E. Pukhov, has become widely accepted in recent years in the problems of mathematical modeling of non-linear electric circuits, which include also arc welding sources. The essence of DTT method consists in conversion of the function of the original of some continuous argument, for instance, time, into the function of the image of discrete argument, the coefficients of which are called discretes. This way transition from differential equations of electric circuits to algebraic ones is performed, that essentially simplifies the processes of modeling and analysis of the derived results.

Here direct and inverse transformation of function $x(t)$ of continuous argument t into discrete function $X(k) = C_k$ of discrete argument $k = 0, 1, 2 – n$ is performed. The above-mentioned pair of transformations is usually presented in the form of the following expressions:

$$X(k) = \frac{H^k}{k!}\left[\frac{d^k x(t)}{dt^k}\right]_{t=0} \leftrightarrow x(t) = \sum_{k=0}^{k=\infty}\left(\frac{1}{H}\right)^k X(k),$$

where direct transformation of $x(t)$ original into $X(t)$ transform is on the left, and inverse transformation of $X(k)$ into $x(t)$ is on the right.

Values of function $X(k)$ at concrete values of argument k are called discretes: ($X(0)$ is the zero discrete; $X(1)$ is the first discrete, etc.).

Using the method of analysis and synthesis of non-linear electric circuits proposed by G.E. Pukhov, we will study operating modes of *LC*-type sources. In the linear approximation their operation is described in sufficient detail in [2, 3]. In the proposed report the task of analysis of operation of these devices, allowing for non-linear nature of reactive and ohmic resistances, forming the secondary circuit, is posed. Figure 1, *a*, shows the simplified schematic image of the considered device, and the equivalent secondary circuit is given in Figure 1, *b*. Here the following designations are used: L_S is the scattered inductance; C is the electric capacitance of the capacitor unit; R_a is the non-linear resistance of the arc gap and voltage drop on these elements, U_L, U_C and U_a, respectively.

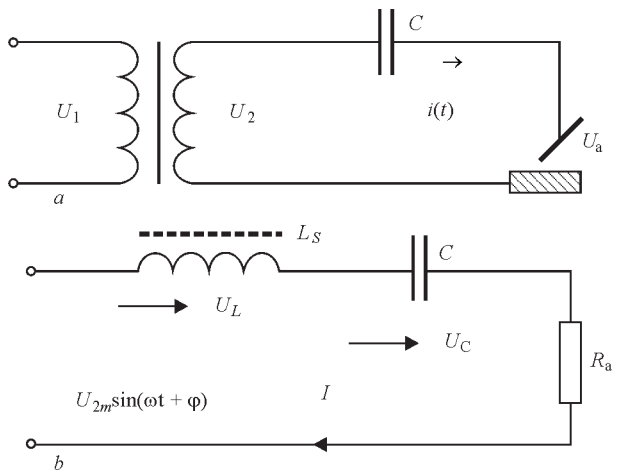

Schematic image of the device (*a*) and equivalent secondary circuit (*b*)

Equation, describing the state of such a circuit, as is known [4], has the following form:

$$U_2(t) = U_L + U_C + U_a, \qquad (1)$$

where

$$U_L = \frac{d\psi}{dt} = L_S(I)\frac{dI}{dt};$$

$$U_C = \frac{1}{C}\left[g_0 + \int_0^t I(t)dt\right], \quad U_a = R_a(I)I(t).$$

If approached strictly, and if in equation (1) all the three terms are considered as non-linear relative to welding current $I(t)$, we obtain the non-linear differential equation in the following representation:

$$\frac{d^2I}{dt^2} + k_1\left(\frac{dI}{dt}\right) + k_2 I = 0, \qquad (2)$$

where

$$k_1 = \frac{R_a}{L_S(I)}, \quad k_2 = \frac{1}{CL_S(I)}.$$

As is known [5], analysis of forced oscillations in such non-linear *RCL*-circuits is performed by the methods of chaotic dynamics. Depending on selection of circuit parameters, manifestations of deterministic chaos are possible here, which, however, is beyond the scope of this report.

Since, as shown by experience, the value of electric capacity C practically does not depend on current in the range of working modes, we will eliminate this non-linearity from further analysis. Therefore, allowing for the fact that initial charge is equal to zero ($g_0 = 0$) by condition, voltage on C is determined by the following expression

$$U_C = x_C I(t) = \frac{I(t)}{314C}.$$

Value of scattered inductance can be obtained experimentally, and it can be assigned in the tabular form, or approximated by a quadratic polynomial

$$L_S(I) = k_0 + k_1 l + k_2 I^2.$$

As regards arc gap resistance, it can also be obtained experimentally for a specific design of the welding source, or from the known relationship $U = U_0 + 0.04$ (GOST 95–77), where $U_0 = 20$ V for manual arc welding. Dividing the right and left part by $I(t)$, we obtain $R_a(I) = U_0/I(t) + 0.04$.

Thus, non-linear equation of welding circuit can be reduced to the following form:

$$\frac{dI}{dt}\left(k_0 + k_1 I + k_2 I^2\right) + I.\left(0.04 + \frac{1}{314C}\right) + U_0 = U_{2m}\sin\left(\omega t + \varphi\right) \qquad (3)$$

We will solve this non-linear differential equation by DTT method [1].

Translation of the equation allowing for the specifics of welding source operation in the region of T-image for time variable t on segment $0 \le t \le H$ gives the following DT-model [1].

$$\frac{k+1}{H} I(k+1)\left(k_0 Ъ(k) + k_1 I(k) + k_2 \sum_{l=0}^{l=k} I(k-l) I(l)\right) + I(k)\left(0.04 + \frac{1}{314C}\right) + U_0 Ъ(k) = \frac{(\omega H)^k}{k!} U_{2m} \times \left(\cos\varphi \sin\frac{\pi k}{2} + \sin\varphi \cos\frac{\pi k}{2}\right), \quad k = 0,1,2,...,\infty,$$

where $Ъ(k)$ is the Taylor unit.

Knowing the initial discrete $I(0) = i(0)$, this formula can be used to successively find discretes $I(1)$, $I(2)$, … , $I(n)$, then present the solution in the form of a finite segment of a power series:

$$i(t) = \sum_{k=0}^{k=n}\left(\frac{t}{H}\right)^2 I(k).$$

The accuracy of the result will depend on the number of counted discretes, on *RLC*-circuit parameters, as well as on the initial phase φ of applied voltage.

It should be noted that G.E. Pukhov table, as well as its refinement, derived in the dissertation work of E.D. Golovin [6], was used at translation of initial equations into the region of images [1].

Thus, the described method can be used at the final stage of circuit design of arc welding resonance sources, when *LC*-circuit elements, providing the requirements of the statement of work, are selected and calculated by the results of circuit analysis. The advantage of the considered method is that it enables welding equipment developer creating algebraic models of the same accuracy, as the initial models-originals.

1. Pukhov, G.E. (1986) *Differential transformations and mathematical modeling of physical processes*. Kiev: Naukova Dumka.
2. Lebedev, V.K., Narushkyavichus, I.R. (1971) Stability of alternating current arc burning in circuit with capacitor. *Avtomatich. Svarka*, **4**, 3–5.
3. Lebedev, V.K., Korotynsky, A.E. (1994) Alternating current arc in circuit with inductance and capacitance connected in-series. *Ibid*., **12**, 47–48.
4. Atabekov, G.I., Kupalyan, S.D., Timofeev, A.B. et al. (1979) *Nonlinear electric circuits*. Moscow: Energiya.
5. Mun, F. (1990) *Chaotic oscillations*. Moscow: Mir.
6. Golovin, E.D. (2004) *Mathematical and numerical modeling of nonlinear devices and devices with alternating parameters*: Syn. of Thesis for Cand. of Techn. Sci. Degree. Tomsk.

Received 26.10.2017

EXHIBITION «WELDING AND CUTTING-2017»

On April 4, 2017 at Football manege in Minsk four exhibitions were opened simultaneously: 17th International Specialized Exhibition «Welding and Cutting-2017», 16th International Specialized Exhibition «Powder metallurgy-2017», as well as exhibitions «Metal Treatment» and «Protection from Corrosion. Coatings». Organizer of the exhitions is CJSC «MinskExpo».

These exhibitions are unique by their topics and participants, among which there were the companies from Belarus, Russia, Ukraine, Lithuania, Turkey, France, Check Republic, Germany and China.

At the exhibitions the participants received a unique opportunity to promote the information about their achievements, the newest developments, to widen the business contacts, to discuss the possibility of joint investigations, to find the potential customers of the scientific-technical products.

Visitors of the exhibition could get familiar with a large exposition of the Ukrainian manufacturers of welding consumables, organized by the International Association «Welding» (Kiev), among which are the companies LLC «Vitapolis», LLC «Sumy-Elektrod» and LLC «TM.Veltek».

LLC «Vitapolis» is manufacturing the welding wires of HORDA trade mark, applying the advanced technologies and equipment. Wires are manufactured for welding of carbon and low-alloy steels, stainless and heat-resistant steels, armored steels. Wires HORDA are delivered in accordance with standards EN, ISO, AWS. Solid wires of 0.8–4.0 mm diameter have a grade CE. They are coiled to reels BS200, BS300, K415 by a precision coiling, and also put to cardboard barrels of 250 and 500 kg weight. Quality Management System corresponds to ISO 9001.

LLC «Sumy-Elektrod», whose history started since 1930, is a manufacturer of special purpose and general purpose welding electrodes. Assortment of manufactured electrodes is 175 grades for welding of different steels and alloys including carbon and alloyed, high-strength and heat-resistant, high-alloyed steels and alloys, nickel alloys, cast iron, as well for surfacing and cutting. The enterprise is equipped with Swiss equipment of a closed technological cycle and advanced laboratory-research base, which allows carrying out a whole complex of investigations and tests in accordance with requirements for the manufacturing products.

Exposition of the Ukrainian manufacturers of welding consumables

LLC «TM.VELTEK» is the largest specialized manufacturer of flux-cored wires for welding, surfacing and spraying in Ukraine and included into three largest manufacturers in CIS. Products of LLC «TM.VELTEK» are certified in system «UkrSepro». Today LLC «TM. VELTEK» realizes regular deliveries of a wide spectrum of products (more than 98 certified grades of wires of 1.2–6.0 mm diameter) to the enterprises of metallurgical and mining industries, ship-, machine- and railway car building, etc. Quality of products and reliability of company are confirmed by numerous awards of the national and international exhibitions and ratings.

Participants and visitors of exhibitions «Welding and Cutting-2017», «Powder Metallurgy-2017», «Metal Treatment» and «Corrosion Protection. Coatings» received additional impetus for realization the most courageous and new projects in future.

Dr. A.T. Zelnichenko

FLEXIBLE PRODUCTION OF WELDED HULLS FROM ENLARGED UNITS FOR LIGHT-ARMORED COMBAT VEHICLES

Nowadays, there is a tendency in the world to increase the operation of light-armored combat vehicles in the regional armed conflicts. At the same time, in Ukraine a centralized production capable to satisfy the need in welded hulls of light-armored wheeled and caterpillar vehicles is still absent, which negatively influences the country defense capability and reduces the attractiveness of Ukraine in the world market of this type of military equipment.

Light-armored wheeled machine

Welded hull of a modern light-armored vehicle is a complex three-dimensional structure weighing up to 5 tons and consisting of more than 2000 parts. The total length of welds is more than 800 m. The serial production of such a workpiece represents a complex technical and production problem. The experience of applying new armored materials produced in Ukraine and other countries for making hulls of domestic light-armored vehicles proves their high service qualities. At the same time, the welding of these steels in real production conditions revealed a number of serious problems requiring comprehensive investigations. The main difficulties encountered in welding of such steels are associated with their tendency to formation of hot and cold cracks. In addition, the technological process of welding (welding consumables, welding modes, preheating conditions of joints and their post-weld heat treatment) should be chosen in such a way that to provide not only high technological strength of welded joints, but also the necessary complex of their subsequent service properties.

Installation for assembly and welding of suspended tanks

According to the existing technology the hull is welded successively, part-by-part in a stationary stand, representing a berth with a large number of auxiliary technological devices, which significantly complicate the work of welders. At the same time 80–85 % of welds have to be produced on steep, vertical and overhead planes. The making of such welds is quite labor-intensive and difficult to produce and can be qualitatively made only by highly-skilled welders. Moreover, the efficiency of one stand is approximately one hull per a month. When it is necessary to produce the hulls of other type, the stands require a complete re-equipment.

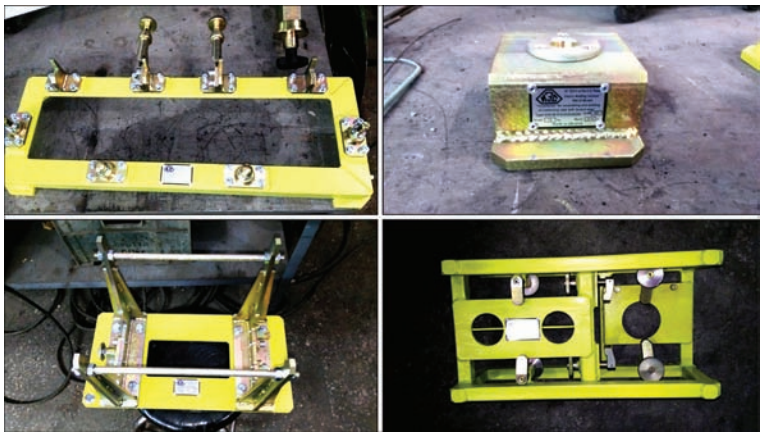

Stands for manufacturing of intermediate composite parts of light-armored wheeled machines

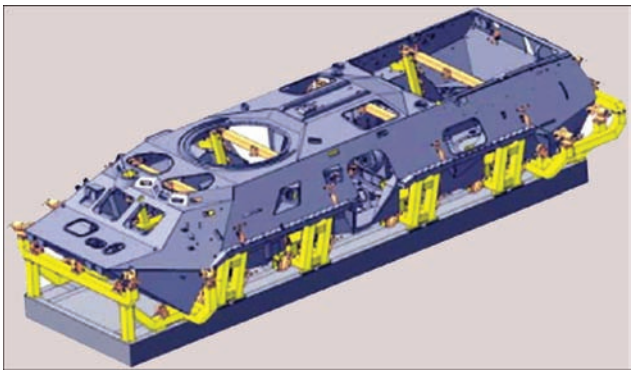

Berth of general assembly and welding of hull of enlarged units

The specialists of the SE «Experimental Design and Technological Bureau of the E.O. Paton Electric Welding Institute» developed a technology which allows designing a versatile, continuous positioning industrial manufacture of welded hulls of light-armored wheeled and caterpillar machines.

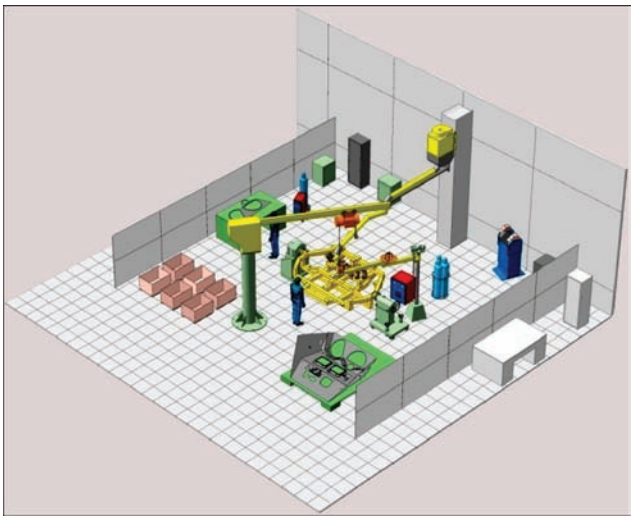

Example of welding site for manufacture of welded hull enlarged unit

The separation of welded hull into separate components (sections) is made taking into account the labor-intensiveness of manufacture of sections, bearing in mind the achievement of balance of this index between the separate sections. The technology of creating the welded hull of enlarged components (sections) which are manufactured at separate production sites allows a more rational use of manufacturing areas, providing a uniform loading of workplaces and operators (welders) and, accordingly, increase in labor efficiency, saving energy resources and welding consumables, as well as rhythmic work of the entire welding production of hulls. The use of this technology allows increasing the production capacity of hulls up to 20 pcs per a month (with a two-shift work), significantly reducing the requirements to qualification of welders and improving the quality of welded joints.

Installation for assembly and welding of motor compartment elements

Also, the proposed technology allows a quick (per a day) change over to the production of hulls of other modification (model). For this purpose, it is necessary to change the assembly and welding devices in special technological equipment, and all the other equipment, the cost of which amounts to 85–90 % of the total cost of production sites, remains unchanged. In addition, depending on the needs of production, the line elements can be manufactured both with the manual as well as with automated control, including the use of robots.

The SE «Experimental Design and Technological Bureau of the E.O. Paton Electric Welding Institute of the NASU» performs works under the contracts with the State Enterprise «Ukrspetsexport» on the development and manufacture of installations for creation of separate components of a light-armored wheeled vehicle using technology developed at the SE «Experimental Design and Technological Bureau of the E.O. Paton Electric Welding Institute». Within the framework of these agreements, the SE «Experimental Design and Technological Bureau of the E.O. Paton Electric Welding Institute of the NASU» jointly with the Pilot Plant of Welding Equipment of the E.O. Paton Electric Welding Institute has developed, manufactured and supplied the Customer with the elements of the continuously positioning line for welding of enlarged units of a light-armored wheeled machine. The creation of installations for these enlarged units is only a small part of capabilities of the developed technology.

G.V. Zhuk, A.V. Semenenko, I. I. Komashnya (Experimental Design and Technological Bureau of the E.O. Paton Electric Welding Institute), A.V. Stepakhno (Pilot Plant of Welding Equipment of the E.O. Paton Electric Welding Institute)